ABSTRACT

Title of Document: OPTIMIZATION OF CARBON MONOXIDE DETECTORS IN A RESIDENTIAL LAYOUT AND ANALYSIS OF DISPERSION CHARACTERISTICS

Derek Engel, Masters of Science, 2012

Directed By: Professor Arnaud Trouvé , Department of Fire Protection Engineering

Current building and life safety standards do not specify the optimal placement of carbon monoxide (CO) detectors in residential structures. Currently, the standards advise to follow manufacturer's instructions, place one centrally on each floor and in each HVAC zone. With the use of computation fluid dynamics (CFD) software FLACS, simulations were run to observe and track CO concentrations, generated from a fire source, throughout a demonstrative box as well as a residential structure under different source and ambient conditions. A MATLAB script was developed to represent CO detector functionality. From this it was possible to evaluate detector placement throughout a structure. The time to detection criterion was analyzed as well as order of alarm in relation to other placements. Final recommendations are presented based upon the dispersion patterns observed.

# OPTIMIZATION OF CARBON MONOXIDE DETECTORS IN A RESIDENTIAL LAYOUT AND ANALYSIS OF DISPERSION CHARACTERISTICS

By

Derek Engel

Thesis submitted to the Faculty of the Graduate School of the
University of Maryland, College Park, in partial fulfillment
of the requirements for the degree of
Master of Science
2012

Advisory Committee:
Professor Arnaud Trouvé, Chair
Professor Stanislav Stoliarov
Professor James Milke

# Acknowledgements

There are several people whom I would to thank for their immeasurable contributions to this project. Without their continued support and guidance this project would have never come to fruition and I owe them a debt of gratitude.

Firstly I would like to thank my advisor, Professor Arnaud Trouvé. Without his knowledge, time and patience this project would not be in the position it is today. His ongoing support and understanding have helped me to stay motivated and complete this lengthy undertaking. I appreciate his accommodation of my schedule as well as his tolerance of my often late night emails.

I would also like to thank Dr. Scott Davis and GexCon US whom have funded my research and allowed me the use of their resources and software. Dr. Davis' guidance and support of my endeavor, while continuing to work full time, has allowed me to complete this project while keeping my sanity. While it was not always easy, and there were several late nights at the office, his support has made this a worthwhile experience.

I would also like to thank my committee members, Professors James Milke and Stanislav Stoliarov for taking time out of their busy schedules to review my work as well as their contributions to my school experience in the classroom.

Lastly I would like to thank my family and my girlfriend, Alissa, whom have put up with the strange hours, “mild” stress-induced panics and unavailability I have had for the past several months. Without them none of what I have produced here would be possible. I also owe Angus, Alissa’s dog, an apology as I haven’t been able to take him on the long walks he loves during the completion of this project. That will change soon. I love you all.

# Table of Contents

# List of Tables

# List of Figures

# 1. Introduction

Carbon monoxide (CO) is a colorless odorless gas than can be a threat to life safety if an individual is exposed for too long. Carbon monoxide takes the place of oxygen in the blood stream forming carboxyhemoglobin (COHb) which deprives vital organs of oxygen. Luckily, however, there are CO detectors that will create an audio or visual alarm when dangerous concentrations of CO are present. Unfortunately, the current recommendation in life safety standards for CO detector placement is not well defined. The current guidance provided by NFPA 720, is to place one on the ceiling in any room which has permanently installed fuel-burning appliances, one centrally located on every habitable floor and one in every HVAC zone of the building, an alternative to this is a performance-based design layout [1]. While NFPA 720 states that CO detectors shall not be used in lieu of fire detection or warning equipment, this study was intended to only look at CO generation and dispersion from representative sources.

Depending upon the style of the CO producing event, the assumptions about dispersion characteristics can vary greatly. Currently, accepted assumptions are that a natural convection style heating system would allow CO to migrate freely from the source. If a HVAC style is forced air, then CO is assumed to be released in a well stirred reactor and distribute evenly throughout the residence. This study looked into optimizing detector placement layout to detect levels of CO from representative fire sources as soon as possible and avoid nuisance alarms as well as studying the characteristics of CO migration as modeled with computational fluid dynamics

(CFD). Suggestions have been made to include carbon monoxide detectors in furnace ducts and in boiler/furnace rooms. This study will look at such placements.

This study used the FLACS CFD software package developed by GexCon to model the gas dispersion scenarios which included various residential structure layouts, heating styles, appliances of CO generation. Carbon monoxide was assumed to be generated at a known source rate. Monitoring points, that represent detector placement location, were placed in various locations throughout the structure. Detectors were placed in positions that represented probable locations that people would be breathing in such as beds and sitting areas as well as possible first detection areas.

The goal for this study was to develop a set of guidelines to most efficiently lay out carbon monoxide detecting equipment depending on the geometry of the residence.

### *1.1. CO Detectors*

Carbon monoxide detectors generally have one of five different detection technologies. All are held to the same UL 2034 standard, and no life safety standard distinguishes between the styles in terms of detector placement. The five styles are: colorimetric reagent, metal oxide semiconductor, electrochemical cell, non-dispersive infrared absorption, and catalytic combustion [2].

The first style, colorimetric reagent, is generally a passive style, such as a badge or sticker that will change color when exposed to CO. These are non-alarming and require that an interested person actually look at them to determine their exposure level. These can be affected by temperature and humidity changes. These are generally not used in residential settings.

A metal oxide semiconductor style sensor is composed of a metal oxide and ceramic mixture. The compounds of the sensor react to a designed species, in this case CO, and change the electrical resistance of the compound. This allows for a high resolution of concentrations; however this style of sensor again susceptible to temperature and humidity, as well as long-term measurement drift and requires high input power.

An electrochemical cell style sensor is a small fuel-cell that oxidizes CO to $CO_2$ which then generates electrical current. This current is measured and coupled to a concentration of CO based on the amperage. There are less draw backs associated with this style as there have been means to overcome the previously mentioned humidity and temperature variances. The downside to this sensor is its dependence upon the fuel-cell type sensing device which can have a maximum useable life.

Infrared absorption based technology uses two light intensity measurement devices and one infrared light source. Based upon the absorption of different wavelengths of light the sensor is able to determine the concentration of various gases present in the

measuring region. This style of detection is independent of temperature and humidity, although other components of the detector may be susceptible to such variations besides the detection equipment itself.

Catalytic combustion sensing mechanisms utilize the heat of combustion of various gases to change an electrical property of a sensing mechanism (resistance, current or voltage). These sensors are generally used to detect methane or other hydrocarbons; however they can be used for CO detection. These are generally temperature and humidity independent however this style is rarely used in residential settings.

As mentioned previously, life safety standards make no mention of differences between the styles of unit. For the purposes of this study, the mode of detection does not matter.

## *1.2. Literature Review*

There have been previous studies to help guide this investigation and provide insight to computational methods and experimental information. While not all of them directly deal with CO, the general flow patterns and observations can be correlated to a release of CO in a similar environment. A review of some relevant literature is provided below.

### 1.2.1. Emissions of CO

Any combustion appliance can be a potential source of CO. Under-ventilated combustion is often the leading source of CO generation. Since the differences of

combustion appliances vary, so too can the style of CO generation. While some natural gas or propane burning appliances, are more cleanly burning and may only produce otherwise unnoticeable products of combustion (colorless, odorless gases and vapors), certain other appliances such as gas powered tools, oil or charcoal burning appliances may produce an irritating smoke to assist in indication to a potentially hazardous condition [3].

According to Beyler et al., CO is not a usual product of combustion under somewhat normal operation of combustion appliances. However, under abnormal conditions, the amount of CO generated by these devices can be significant. These abnormal conditions can be the result of an issue with an exhaust system or with the device itself. Depending upon the appliance or device the range of CO production can vary greatly. To determine the mass of CO generated under non-ideal conditions Beyler presented a correlation to compare the ratio of $CO_2$ to CO in the exhaust. From that, and the energy consumption rate of the appliance, the mass of CO created per unit time can be evaluated. One of Beyler's reviewed reports analyzed CO production from a small gasoline powered generator and the amount of CO generated per kW-hour varied by a factor of two, however when placed under adverse conditions, this value drastically increased and exceeded safe operating conditions [10].

While what Beyler presented was interesting; it is not practical from a modeling perspective. William Pitts has developed a useful engineering algorithm for estimating CO generation in enclosure fires [8]. The provided justification for his

study claims that CO is the predominant life threatening toxin in smoke and that while the number of fire deaths have gone down in recent years, the percentage of fatalities related to CO are increasing.

Prior to Pitts' publication, there were a limited number of options for determining the amount of CO generated in a fire. The first option was to assume a constant amount of CO generated per amount of fuel, the second was to provide a lower and upper yield value based upon whether the fire was well ventilated or under ventilated and a third was based on CO generation rates reported in previous experiments which were material specific and difficult to apply to a real world scenario.

Pitts' proposed solution was the global equivalence ratio (GER) concept. This concept was backed by an analysis of other experimental data, as well as tests including bench scale natural gas combustion and larger scale model fires.

The GER based approach showed the ability to accurately predict CO levels. Under well-ventilated conditions very little CO was generated as one might expect, however as the GER approached and became larger than one (under ventilated conditions) the CO generation rate increased drastically. The main issue reported for this style of prediction, was that the leading edge of the CO and products of combustion plume was non-uniform and found to be much higher than predicted with the algorithm [8].

Pitts has published additional works pertaining to his GER concept [16]. Here he has more specifically narrowed the GER range for CO yield to be near zero for GER less than 0.5 and CO yield plateaus at approximately 0.23 for GER greater than 2.0. These values were concluded through testing performed in reduced scale enclosures. These values were reproduced by Gottuk in the SFPE Handbook [18].

Pitts concludes that at least four mechanisms for CO formation in an enclosure fire. These include quenching or turbulent fire plumes upon entering a rich upper layer, mixing of oxygen directly into a rich upper layer, pyrolysis of wood in high temperature, vitiated (reduced oxygen concentration) environments, and approach to full-equilibrium combustion product concentrations in a rich high temperature upper layer. These formation methods are all dependent upon rich high temperature layers which can be the result of under-ventilated combustion [8].

#### 1.2.2. Dispersion

There have been several studies into the dispersion characteristics of products of combustion within enclosed structures. While only a few of them directly deal with CO, the dispersion of contaminants and other products of combustion should generally be minimally dependent of species type.

Grant et al. has previously presented a discussion on many of the internal and external flow factors than can modify a dispersion pattern within a house [4]. These include: heat transfer, solar radiation, air infiltration, occupants, contaminant source location, furniture, equipment, exhaust, supply air conditions and ambient air flow.

Generally within an indoor environment, there are two classifications of air distribution styles, Grant identifies them as jet and buoyancy driven flows [4]. With a jet flow, a high velocity device is the main air movement mechanism. This is described as similar in style to a force air HVAC system, a source provides airflow, and as the jet loses momentum, buoyancy takes over to disperse the air throughout the room. A buoyancy driven style could best be described to be similar to an HVAC system with a radiator. A point heat source would cause a buoyancy driven flow and would encourage mixing in that manner.

Grant has also focused great attention to the potential impact of contaminant dispersion from HVAC systems [4]. These systems have momentum and thermal contributions making them generally the driving force in an enclosed environment. His study however did not include the effects of breathing, movement of people and door opening have on an air flow pattern.

Experimental evaluations of CO dispersion were performed by the Building Research Establishment (BRE) in the U.K. [5]. Their test facility was within a test house with a floor area of 40 $m^2$ across two floors.

In the BRE study, a controlled CO source was used that would allow for a flow rate and set point temperature to be applied. CO detectors and thermocouples were spread throughout the house. For the base case the CO was released at 100 °C. A total of

90 experiments were performed, generally all of the internal doors were open and all of the windows were closed. Three source locations were used: the kitchen, living room and a bedroom. In most cases as expected, the closing of doors limited the CO migration, and open windows reduced the concentrations. The CO concentrations recorded at the ceiling level were generally the highest. With no mention of an HVAC system, the results presented are somewhat simplistic and follow general buoyancy driven flow [5].

The BRE study showed that if the CO was buoyant as it entered the room, it would remain as such and the upper most alarm location would experience the highest concentrations. When the CO was neutrally buoyant, the study showed that a detector at ¾ height would experience the highest concentrations. The final recommendation based on the experimental data showed that if the CO is expected to be buoyant, the detector should be placed near the ceiling; if the buoyancy is undetermined, it should be placed near breathing level [5].

Beyler et al. has also conducted a review of CO dispersion characteristics. From the papers that were reviewed in his article, the author delves into CO dispersion. He states that generally the CO concentration is higher in the room of origin when there is no mechanical ventilation present. Generally the CO was found to be buoyant; however there were no large observed concentration gradients. After approximately one hour, the CO was found to be well mixed, as this was generally the characteristic mixing time of the structure [10].

Beyler reviews some experimental data collected previously. In two notable tests, CO was found to be stratified in the room of origin however this effect was less noticeable in adjacent rooms. The temperature effect was also similar to this. However the time scales for these tests were generally longer, up to several hours before the well mixed observation is noted. This effect was repeated in a few other tests; however it should be noted all of the experimental results evaluated in this paper were published by the same author [10].

#### 1.2.2.1. CFD Modeling

Indoor air dispersion can be a complicated process. There are many factors which need to be taken into consideration such as airflow pattern, velocity, temperature, humidity and concentration gradients. CFD simulations can be useful to model such flows but can be computationally intensive, zonal models are another option available for larger areas but can lack small scale details [9].

There have been several CFD or computer based analyses of dispersion properties relevant to this study. Grant et al. published a study focused on the CFD implications of contaminant dispersion within indoor structures [4]. Bukowski [6], as part of a larger study, analyzed a CFD based approach. Jayaraman, Mora, Chow and Duci [7],[9],[13],[14], have all also performed some type of numerical CFD modeling, be it finely meshed CFD or a zonal based approach.

Bukowski's conclusions were that the data obtained from his CFD model was inadequate and required too much computational power to be effective, however based on the date of publication (1999) his abandonment of a finely meshed CFD model is no longer justified. Bukowski also performed a zonal approach with the conclusion being that locations of detectors should be close to source appliances as the concentrations are generally higher [6].

Jayaraman el al. presented the development of a combined zone and CFD model for the analysis of dispersion throughout a building. The benefits of their zone model allow for fast solutions and permeability of walls easily, however these models assume uniform conditions (well-mixed) and instantaneous air movement. CFD models can resolve the issue of instantaneous transport, however with large scale applications become too cumbersome to work with. This program was being developed to simultaneously manage a COMIS multi-zone model with a STAR-CD CFD model [7].

Jayarman's solution to the requirements of a CFD model was to development his new model which would allow for a specification of "CFD-zones" (CFD modeled) and "simple zones" (well-mixed zone areas). This would allow for the user to modify the parameters to provide more detail in large areas such as living spaces while not using resources for areas in which the zone approach would be satisfactory [7].

Beyler et al. covered several models such as CONTAM and COMIS as well as their comparisons with experimental data. As these zonal models assume well mixed environments the results correlated well with smaller scale rooms and long time-scales. Multiple other variations of these zonal models (including novel approaches dealing with smoke layers and inclusion of solar radiation) are presented and their results are generally agreeable with the limited experimental data presented in terms of temperature and total air movement [9].

Beyler's discussion also covered CFD models that were able to capture more detail. The turbulence models used in the CFD tools, such as k-ε, resolve more detail about specific airflow patterns that were lacking from the zonal models, such as recirculation in a room around a center point. When velocity is the focus of the analysis the zonal models were only able to capture broad trends of average velocity and often missed relatively small time scale events such as high velocity peaks. With respect to a grid sensitivity, as the number of cells went up the represented detail also went up, however the more coarse grids were deemed to be still in an acceptable range for simplified analyses [9].

CONTAM combined with AIRNET and ASCOS is used to predict the carbon monoxide levels in enclosed parking garages in a study performed by Chow. For the most part, the OSHA requirements on CO exposure levels are very low, allowing only 25 PPM over an eight hour period. Since motor vehicles are a constant source of CO this must be exhausted from an enclosed garage regularly. After modeling 10

representative parking garages, Chow found that both the CFD-Zone model used and a well-mixed assumption were identical for the maximum CO exposure levels. For a large volume such as the ones presented (1,000$m^3$ to 35,000$m^3$) with the designed mixing provided by the ventilation system and ambient (car) movement, this was not unexpected. This was however only a peak value. When the concentrations were compared in a transient manner against the simulations, discrepancies arose. The actual movement of cars cannot be predicted and therefore resulted in non-reproducible variations in the data [13].

Again a parking structure analysis was performed by Duci et al. on parking structures. Since CO is a significant component of motor vehicle exhaust, it can make long term exposure in enclosed spaces hazardous [14]. To compare a numerical solution, experimental data was collected at six parking garages in the city of Athens, Greece. Measurements were taken during the day-time during weekdays (when CO concentrations would likely be the highest) [14].

Rather than use a commercially available product, Duci and his colleagues expanded on other papers' development of a CFD based code. With this, after programming the appropriate conservation and boundary equations, produced results comparable to a coarse grid simulation in today's CFD packages. The illustrations show general air movement, however lack the detail to develop recirculation zones and details of a smaller nature [14].

A tool such as Jayarman's would be useful in the style of calculations provided in this report. An HVAC system could be modeled as a single zone while allowing the open habitable space to be analyzed with a CFD level of detail. At the time of the report this model was still being developed however it shows promise to be available in the future and the philosophy could be optimized for analysis to CO and other toxin dispersions which can occur over long (real world and simulation) time scales [7].

Generally the discussion indicates that it is possible to model reasonably well CO dispersion with CFD or numerical based solvers. The experimental data compared relatively well with numerical models, indicating it is a worthwhile endeavor.

#### 1.2.3. Detection

Dispersion and emissions are both paramount factors in the discussion of detector placement; however there can be effects of detections that will enable a sensor to respond more quickly in one location or another. As such the means of detection was investigated. Bukowski, Beyler et al. and Ryan et al. [6], [10], [11], have all published literature pertaining to this.

Bukowski's report focused on fire tests with an analysis of the smoke production and migration [6]. The report was geared towards mobile homes. While this did not explicitly analyze CO, other products of combustion will likely follow a similar pattern and thus it provides a worthwhile discussion.

At the time of Bukowski's report, there was limited data presented for smoke detector placement in mobile homes, his study sought to expand on that knowledge base by performing tests in summer and winter conditions, as well as different HVAC operation modes. This study also evaluated the effect of closing doors on detector performance [6]. The requirements for a smoke detector in such structures are designed to protect the sleeping areas. There is a requirement for one ceiling-mounted smoke detector in each zone in which sleeping areas are located. This means that if two bedrooms are adjacent only one detector is needed. Previously reported data had shown that the best place for detector placement was nearer the common areas as these were more likely places of origin [6].

The general test procedure for Bukowski's investigation was to equip an array of detectors of both photoelectric and ionization type around the structure. There were then 25 tests performed encompassing both winter and summer conditions and different fire source types (smoldering, flaming, kitchen (oil fire) and living space (furniture fire)) [6].

From Bukowski's tests it was concluded that all of the detectors activated in a reasonable amount of time which would have resulted in notification before incapacitation. There were differences between the styles of detector however not significant enough to affect life safety. The data shows that there was no noticeable difference between an exterior wall mounted position and interior wall mounted

position, however the detector closest to the source always had a shorted time to alarm as one might expect [6].

Perhaps the most interesting conclusion regarding the topic Bukowski's report is that while previous studies published by Bukowski and Harpe for the NBS had shown the HVAC system had a noticeable effect on detection time, those values were reported for a multi-level home, in a single level home the differences become less noticeable. The time to detection was relatively unchanged with the HVAC system in operation; however the amount of exposure to the smoke was changed. The effect of the HVAC system was coupled with the open or closed position of the doors. When doors were closed and a HVAC system was operational, exposure in bedrooms went up significantly. In these cases the products of combustion were transported through the HVAC duct work [6].

A paper published by Ryan et al. was directed more towards specific CO detectors. His study analyzed the functionality characteristics of detectors in use in subject's homes. While there is a "push to test" button on most detectors, he noted, this only ensures that power and alarm functionality are working, not whether CO is adequately detected [11].

In order for Ryan et al. to test the functionality of common detectors in service, a call was placed to members of a community whom temporarily donated their detectors for evaluation. A test rig was created which could supply a known concentration of CO

along with regulated purified breathing air. Each detector was placed in exposure to a 70 ppm concentration as required as part of the UL 2034 standard. If a detector passed this test, it was evaluated at higher concentrations (150 then 400 ppm). It was deemed malfunctioning if it failed at any one of the set concentrations. From the results, it was determined that the overall failure rate for the 30 detectors evaluated was 57%. Detectors older than 10 years made up 40% of the detectors evaluated yet had a 66% failure rate [11].

Based on the other information collected with the detectors by Ryan, it was found that 40% of homes were not protected by their CO alarms. 17% of detectors alarmed early, while not as serious, this was also deemed a failure as it would lead to otherwise unwarranted response such as calling a local fire department or evacuation. A large number of the failures were related to the age of the device. It was noted that UL 2034 only requires units function for 3000 hours, or about 1 heating season. Beyond that most detector manufactures recommend replacing the alarm every 5-7 years. Another interesting note is that when the community members donated their CO alarms, a new loaner unit was provided to them. An analysis of the brand new loaner units revealed a failure rate of 25% [11].

Final assessments of detector siting were presented by Beyler. Generally it was the opinion of the author, as well as his reviewed documents, that detectors should be placed near the ceiling. Beyond that, there was some gray area. One study recommended 1-3 meters from a combustion appliance, however if there is no

appliance in the room or area of protection, it should be placed near breathing level [10]. With Ryan's findings that there is a significant change that an individual CO alarm would not be functioning properly, more than one detector should be recommended.

### 1.2.4. Human Response

As mentioned previously, CO is a colorless, odorless and poisonous gas that can result from incomplete combustion. The severity of the health effects of CO exposure is directly related to the concentration and duration of exposure. CO is dangerous as the absorption of CO is approximately 250 times stronger for CO than for oxygen, thus it gets replaced in the blood stream and deprives the body of oxygen. Carboxyhemoglobin levels less than 10% are not considered to be dangerous for the average healthy person, escalating from there; the effects can include headache, fatigue, nausea, loss of consciousness, coma and death. Since the earlier symptoms of CO poisoning can mimic symptoms of other diseases or activities (such as colds or consuming alcohol), they can go unnoticed [3]. Hnatov, Beyler, Yoon and Peterson, [3], [10], [12], [15], have all commented on the effect of CO on a human being. An analysis of the trends of the style of CO generation related deaths reveals that since 1999, the number of deaths related to heating equipment and other potential CO sources has remained relatively constant, while the number of deaths with the CO source being a generator has steadily risen and has increased by approximately an order of magnitude [3]. For the period from 2001 to 2003, approximately 500 non-fire related deaths resulted from CO poisoning each year and approximately 15,000

individuals were treated for high levels of exposure. The sources of the CO were almost always combustion powered appliances [10].

Hnatov reports that during 2007, there were an estimated 183 CO exposure related deaths reported to the Consumer Product Safety Commission (CPSC). Hnatov's report is biased towards deaths from heating related equipment. The focus of the study was on consumer products; as such the distribution of fatalities will not be applicable to other categories of CO generation equipment such as generators and engine-driven tools [3].

Hnatov further breaks down the 183 CO related deaths reporting that 38% were associated with a heating appliance. Of that 38%, 87% were gas fired systems. Focusing on the gas fired appliances 43% were methane fueled, 40% propane, 13% kerosene or oil, and the remaining 4% were the result of an unspecified fuel type. The paper further breaks down the fuel type numbers into style of appliance. All of which were the result of an installed furnace operating incorrectly [3]. The other large source of CO poising statistics was that an additional 38% of deaths were from engine-driven tools (including generators, mowers, tractors, snow blowers etc.). Generator related deaths were the highest contribution with 93% of all "tool" related fatalities. The remaining deaths comprise of a few (less than 5) fatalities in each category, some of which include, charcoal grills, ranges or ovens, water heaters and fireplaces. It is also revealed that in 85% of all CO exposure incidents only one person was affected [3].

Further analysis into the data show that the number of CO related exposure deaths is higher in the winter months, as would be expected, due to the increased usage of combustion appliances. Another interesting finding was that people over the age of 45 had a disproportionally higher number of deaths, and that the number of deaths in males was also disproportionally high. Race and country of origin were also investigated and not shown to have any statistically significant results [3].

Through several studies performed for various areas and states around the country, it was found that warmer climates generally had lower CO poisoning incidents. Beyond that, the source of the CO was generally a heating or cooking appliance with men having a significantly higher ratio of poisoning to women (2.5:1 or greater) [10].

The number of lives that could be saved with CO detectors has not been analyzed and was the undertaking of Yoon et al. Their study evaluated the deaths reported to the New Mexico Office of the Medical Investigator (OMI) and assessed whether they could have been prevented through the use of a detector [12].

The source data was reported to the OMI and for the purposes of Yoon's study, only deaths that were listed as "unintentional inhalation" were considered. Of these, based on other details reported, Yoon assessed whether they were likely asleep at the time as well as other factors such as being under the influence of alcohol as this would impair any potential response [12].

Based on the results Yoon determined that for the time period analyzed, CO poisoning accounted for approximately 1% of all deaths reported to OMI. Of those, approximately 20% were listed as unintentional inhalation. Further analysis showed the heavy male bias previously mentioned in previous papers. Eighty two percent of people judged to have been in vehicles at the time of poisoning were deemed to be awake compared with 51% having been located at a residence and awake. An elevated blood alcohol level was found in 41% of the cases [12].

Yoon points out that there should be an audible alarm developed for placement in motor vehicles. Also any alarm, placed in a residence or otherwise should be able to awaken an inebriated person who has fallen asleep. It was determined that, with such a significant portion of the data indicating that a person was awake at the time of incapacitation or onset of CO poisoning, a fatality should have been able to be prevented [12].

It was a goal of Peterson et al. to study CO absorption into the body. CO is an ideal gas to analyze in that respect, as it is inert and not utilized by bodily tissues. Any CO obtained through inhalation, is expelled through the lungs. As a baseline the Coburn, Forster and Kane (CFK) equation was evaluated. This equation proved to be useful for the limited set of people tested (sedentary, Caucasian males). In order to expand this beyond the scope of the original equation, several other correction factors were analyzed. These additional factors included the differences in partial pressures of

oxygen in the lungs, the diffusivity in the lungs, total blood volume and ventilation rate of the alveoli in the lungs [15].

For each of the corrections mentioned, Peterson conducted an analysis on the effect of a range of exposures. They found that the average partial pressure of oxygen in the lungs does not follow a linear correlation as the term in the CFK equation as presented. The diffusivity of the love and blood volume also varied wildly with the subject and their individual lifestyles [15].

The various parameters were then experimentally validated. Volunteers were placed in an enclosure and exposed to a known concentration of CO for a set period. Blood samples were taken throughout the test and the COHb was measured. Some additional parameters were varied, such as the amount of activity they performed while in the chamber. From the results it was determined that the CFK equation was able to adequately match the CO uptake in each of the test subjects. There were minor discrepancies as female subjects tended to absorb CO more readily than the male counterparts. The addition of the exercise variable changed the alveolar ventilation rate by a factor of approximately two and a half. Another interesting note was that non-continuous exposure was able to be accurately predicted [15].

From Purser in the SFPE handbook [20], the effects of toxic exposure are directly related to two factors. The first factor is the time of exposure to a toxic substance. The second factor is the concentration of the toxic material to which a subject is

exposed. While there are variations depending upon length of exposure (shorter exposure follow more linear trends of absorption, while longer exposures experience a curved pattern), both are critical to assess overall hazard and exposure levels. As such, both time of exposure and exposed concentration should be actively monitored.

There is a plethora of relevant data to the uptake of CO to the body as well as studies of death rates and their potential CO source. In each of these there is a relevant conclusion that there are significant numbers of avoidable deaths that result from CO poisoning each year. The update methods are well defined however; people do not recognize their effects nor are adequately protected against them.

# 2. Numerical Setup

This section will describe in more detail some of the input parameters and mathematical tools that were used to help in this investigation.

## *2.1. CO Correlations*

For the CO source term in this study, the CO was assumed to be generated at a known rate and concentration. This would fix the CO concentrations and allow the focus of the study to be independent of combustion chemistry at the source which as described in several of the previously review papers can be very difficult. For the CFD model the CO was assumed to be generated at the end of the intermittent region of a "waste basket" sized fire. Figure 1 shows a mock-up of a fire scenario. The reddish-purple area above the fire source was assumed to be the location of the CO source in the CFD simulations. As is illustrated, the combustion chemistry is avoided, and the hot CO along with entrained air is modeled as the source.

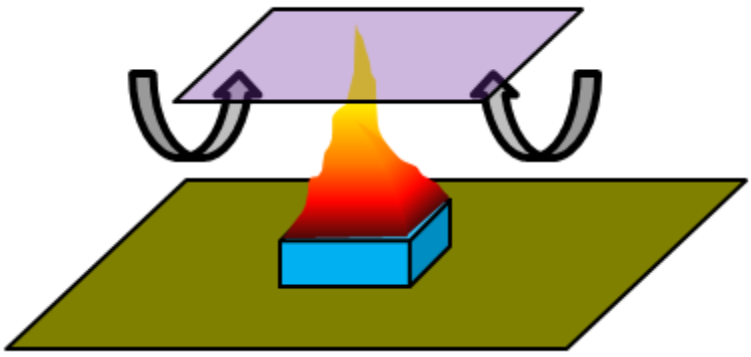

**Figure 1: Illustration of CO source term.**

2.1.1.Plume Temperature Evaluation

From the McCaffrey Plume correlation, the centerline temperature at a given height for the flame region can be expressed as Equation 1, found from the SFPE handbook and from Karlsson and Quintiere's Enclosure Fire Dynamics [19].

**Equation 1:** $$T_o = 22.3\left(\frac{\dot{Q}^{2/5}}{z}\right)^{5/3} + T_\infty$$

Where T is the centerline temperature, $\dot{Q}$is the convective heat release rate and Z is the height above the fuel region. To model the temperature at the end of the transition region, the height of the flame was assumed to be Equation 2.

**Equation 2:** $$z = 0.2\,\dot{Q}^{2/5}$$

Substituting the flame height at the end of the transient region, for the height at which the plume formation begins, yields Equation 3.

**Equation 3:** $$(T_o - T_\infty) = 22.3\left(\frac{1}{0.2}\right)^{5/3}$$

All of the values in Equation 3 are constants; therefore a constant temperature source at 326 °C has been obtained. This assumption works, as long as the CFD modeled source is positioned at the end of the intermittent flame region; however for this investigation, the flame height is not important, only the transport of the products of combustion. Therefore the temperature of the CO source can be fixed as at constant temperature for this study.

2.1.2.CO Yield

Using the McCaffrey plume entrainment correlation, the mass flow of the products of combustion can be assumed to be Equation 4. In the McCaffrey correlation, there is no dependence upon source fuel type. The only necessary information is the fire size.

**Equation 4:** $$\dot{m} = 0.026\dot{Q}\left(\frac{z_f}{\dot{Q}^{2/5}}\right)^{0.909}$$

From the previous assumption that the source term would be taken at the end of the intermittent region; Equation 2 and Equation 4 can be combined to yield a result only dependent upon fire size.

**Equation 5:** $$\dot{m} = 0.026\,\dot{Q}\,(0.2)^{0.909} \text{ or } \dot{m} = 6.020(10^{-3})\dot{Q}$$

This results in products of combustion mass flow rates of 0.060 kg/s for a 10 kW fire and 0.60 kg/s for a 100 kW source fire.

From Quintiere's, Fundamentals of Fire Phenomena, the range of CO yield for common elements, including polymers is 0.001 to 0.116 g/g [21].

Determining the CO yield can be found from Equation 6.

**Equation 6:** $\dot{m}_{co,s} = y_{co} \frac{\dot{Q}}{\Delta H_f}$

Using a range of typical fire sizes for a typical "waste basket" size fire is assumed to be between 10 and 100 kW. With our range of fire sizes, it was assumed that the heat of combustion was constant at 15 MJ/kg, a representative value for paper in a waste basket. This would result in a typical mass loss rate of our fuel of between 0.66 and 6.66 g/s. Applying the range of CO yields found in Quintiere, the maximum and minimum CO mass flow rates through the fire plume can be assumed to be between $6.67 \times 10^{-7}$ and $7.73 \times 10^{-4}$ kg/s. For simplicity, this study will focus on the following CO release rates: $6.67 \times 10^{-7}$, $6.67 \times 10^{-6}$, $6.67 \times 10^{-5}$ and $6.67 \times 10^{-4}$ kg/s.

### *2.2. FLACS CFD Solver*

All of the simulations performed in this analysis have been done so with use of the CFD software tool FLACS. FLACS has been developed and maintained through GexCon AS based out of Norway since 1980. This software was originally developed to support the needs of the chemical process industry, however has evolved to be a well-rounded tool for the analysis of gas dispersions, gas explosions and dust explosions. GexCon is also developing a fire model for FLACS which will be released in the near future.

The commercially released FLACS v9.1 solver utilizes the compressible Reynolds Averaged Navier-Stokes (RANS) equations over a 3d Cartesian grid. The next version of the software will allow use of an incompressible solver to be commercially released in the future. For this report, the use of the unreleased version of the

incompressible solver has been approved. This model is validated against experimental data and has been proven to be reliable. The reasoning for using this model is that it allows the computer simulations to be performed in a much shorter real-world time span.

Rather than mesh around obstacles and resolving the surface interactions, FLACS uses a distributed porosity concept. This technique involves, quantifying the amount of blockage and turbulence that would be generated in each grid cell and assigning an equivalent blockage. With this, the fluid will interact with the assigned porosity of the cell and not directly with the objects present. This technique allows for the efficient handling of geometries with very complex features [22].

The turbulence model used by FLACS is the k-ε model. Since this study is only tracking the movement of CO around a structure, and not more complex phenomena such as flame folding around obstacles the sub-grid model used in FLACS is not relevant.

#### 2.2.1. FLACS Validation

FLACS has been extensively validated over the course of its development. From the GexCon website, there have been several studies in which the FLACS CFD model has been compared to experimental results. Some of the notable tests, focusing on those applicable to gas dispersion are [24]:

- 1994-1998 Ventilation studies vs. wind measurements at various oil platforms (e.g. Oseberg-C, Beryl-B, Nelson)

- 1997-1999 MOGELEG, GexCon lab scale experiments on the effect of nitrogen and $CO_2$ dilution (JIP report 1998)

- 1996-1999 SMEDIS, EU project on evaluation of dispersion modeling (JIP report 1999)

- 2004-2009 Various HySafe hydrogen dispersion and explosion studies (Several papers by Hansen & Middha)

Beyond that GexCon has used FLACS to participate in several blind studies. This type of evaluation requires the modeled results to be produced before the test results are released. When the test results are known ahead of time, it can allow for the modification of the model or input parameters to better match the results. With a blind study, the usefulness of the model is truly evaluated. The FLACS solver generally produced the most accurately matching results to that of the test. Some highlights from the GexCon website include [25]:

- H2 dispersion INERIS 6C

- Helium dispersion CEA Garage test

- Shell H2 refueling station

- Dispersion scenarios at Manhattan

### *2.3. MATLAB CO Alarm Script*

As FLACS does not inherently have a way to model CO detector functionality, a script was generated to model the alarm times for CO detection. Since the UL standard does not have a requirement for variable CO concentrations and the alarm activation criteria for commercially available CO detectors was not found, one was developed. It was based on the UL 2034 requirements and recommendations seen in Figure 2 and Figure 3. Please note that the following requirements and equations were designed for an "average" healthy individual and may underestimate response for someone with sensitivity to such exposure. This derivation was based on information available at the time of this report.

Table 38.1
Carbon monoxide concentration versus time for alarm test points based on 10 percent Carboxyhemoglobin (COHb)

Table 38.1 revised November 14, 2001

| A. Carbon monoxide concentration and response time | |
|---|---|
| Concentration, ppm | Response time, minutes |
| 70 ±5 | 60 – 240 |
| 150 ±5 | 10 – 50 |
| 400 ±10 | 4 – 15 |
| B. False alarm – carbon monoxide concentration resistance specifications | |
| Concentration, ppm | Exposure time, (no alarm) |
| 30 ±3 | 30 days |
| 70 ±5 | 60 minutes |

**Figure 2: UL test alarm criteria [27].**

Figure 38.1
Carbon monoxide concentration (ppm CO) versus time (minutes)
Figure 38.1 revised October 15, 1997

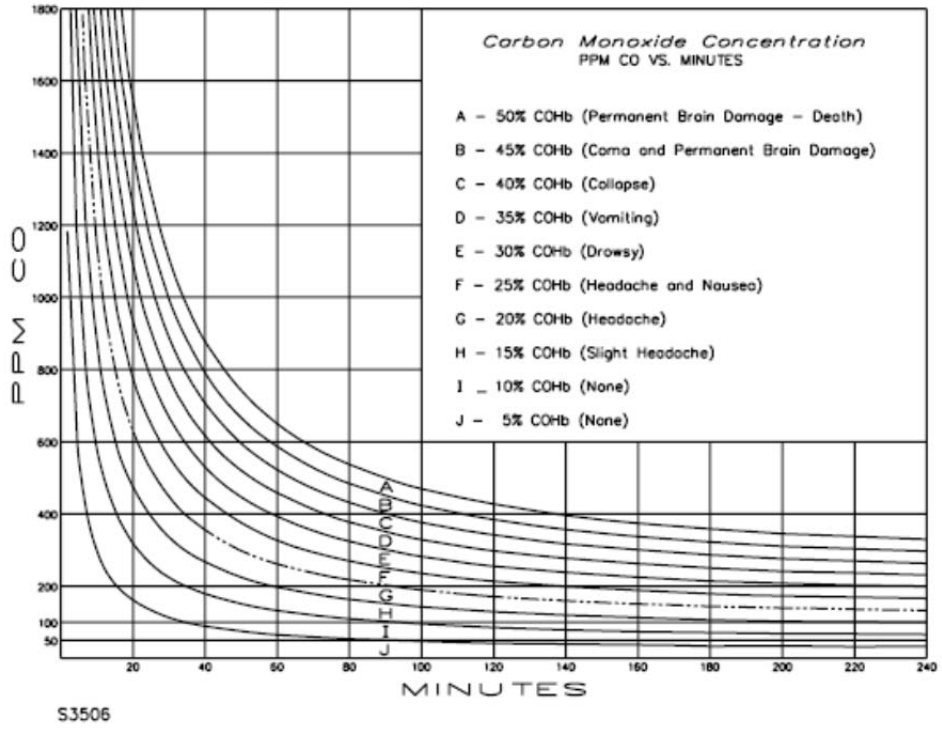


Equation For determining estimated percent COHb in blood[a]

$$\%COHb_t = \%COHb_0[e^{-(t/2398B)}] + 218[1-e^{-(t/2398B)}]\,[0.0003 + (ppm\ CO/1316)]$$

*in which:*

*$\%COHb_t$ is the percentage of COHb at time t,*

*$\%COHb_0$ is the percentage of COHb in the blood at time 0,*

*t is the time in minutes, and*

*B is 0.0404 (heavy work effort).*

[a] A proposal for evaluating human exposure to carbon monoxide contamination in military vehicles, Steinberg, Nielson, March 1977, AMCMS Code 672716.H700011; Coburn, R.F., Forster, R.E., & Kane, P.G. Considerations for the physiological variables that determine the blood carboxyhemoglobin concentration in man. Journal of Clinical Investigation, 1965, 44 1899-1910.

**Figure 3: CFK equation for COHb% as described by UL 2034 [27].**

**Equation 7:**

$$\%\boldsymbol{COHb_t} = \%\boldsymbol{COHb_0}\left[e^{(-t/2398 \cdot B)}\right] + \mathbf{218}\left[\mathbf{1} - e^{(-t/2398 \cdot B)}\right]\left[\mathbf{0.0003} + \left(\boldsymbol{ppm\ CO}/\mathbf{1316}\right)\right]$$

Equation 7 is the reproduced CFK equation represented in UL 2034 (Figure 3), where $COHb_t$ is the concentration of carboxyhemoglobin at time t, $COHb_0$ is the percentage

of COHb at time zero, t is the time in minutes and B is a constant at 0.0404 (a conservative scaling factor for heavy work effort).

Using this equation, an iterative approach was programed using the MATLAB software package. Since the Coburn equation is only useful for exposure to a constant concentration of CO it is not ideal for this application. However, rather than abandon this approach, the Coburn equation was able to be modified to allow for use with a variable CO concentration profile.

By taking the derivative of Equation 7, Equation 8 is obtained.

**Equation 8:**

$$\frac{d}{dt}\%COHb_t = \frac{\%COHb_0 e^{-t/(2398 \cdot B)}}{-2398 \cdot B} + 218\left[1 - e^{-t/(2398 \cdot B)}\right] \frac{\frac{dCO}{dt}}{1316} + \\ + \left(0.0003 + \left(\frac{ppm\ CO}{1316}\right)\right)\left(\frac{218 e^{-t/(2398 \cdot B)}}{2398 \cdot B}\right)$$

The time-concentration output for each of the monitor points used in the FLACS solver is imported into MATLAB as a matrix. A preliminary programing loop was carried out to get the time rate-of-change of CO for each monitor point at each time step. Next, for each of the monitor points, an iterative process was run using Equation 8 for each CFD output time. As the logged time progresses, previous data is recorded and used as a basis for the next iteration. The time concentration profile is the last step, and a simple evaluation records the time at which target COHb concentration is reached. The final output is then the time it takes to achieve a set

concentration in the bloodstream. From Figure 2 the target concentration was set to be 10% as per the UL standard.

A preliminary evaluation was done to evaluate the dependence upon sampling time. Both one second and one minute sampling times were evaluated. The results for each were compared against the exact solution or the UL provided 10% COHb concentration curve. The results are presented in Table 1 for the 70, 150 and 400 PPM concentrations. The results for the one second sampling rate were within 0.2% of the exact solution, while the results for the one minute sampling were greater than 5% for the 400 PPM concentrations. In addition, various time dependent CO profiles of known concentration were evaluated and compared to the exact solutions. The determination was made that the one-second sampling interval would provide the most accurate results and will be reported in the current study.

**Table 1: Comparison of Script with Exact Solution.**

| CO PPM | Exact Solution | 1 Sec Sampling | 1 Min Sampling |
|---|---|---|---|
| | Time (min) | Time (min) | Time (min) |
| **70** | 188.79 | 188.82 | 190 |
| **150** | 49.71 | 49.73 | 51 |
| **400** | 15.83 | 15.85 | 17 |

The script was able to obtain the matching curves in Figure 4. This profile is an illustration of the time for an average person to reach a 10% COHb blood concentration with exposure to various concentrations of ambient CO.

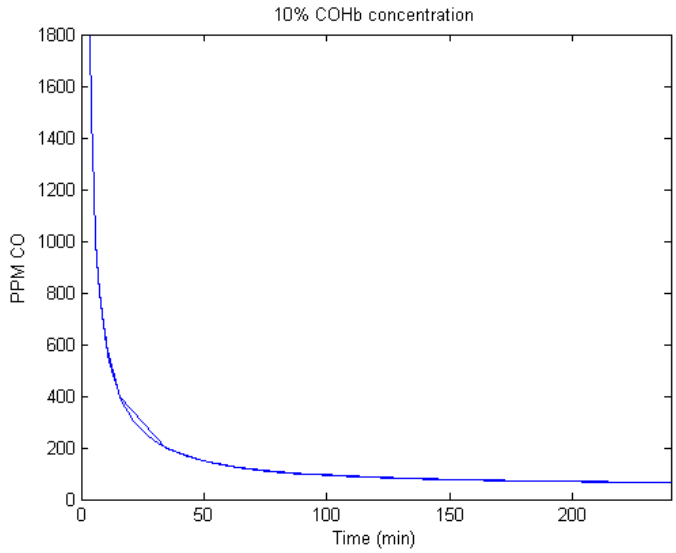


**Figure 4: Generated script and exact solution of UL COHb formula.**

In order to test the script's usefulness on varying CO exposure concentrations, several test profiles were evaluated and compared with an exact integral solution. The test profiles and results can be found in Figure 5 and Table 2 respectively.

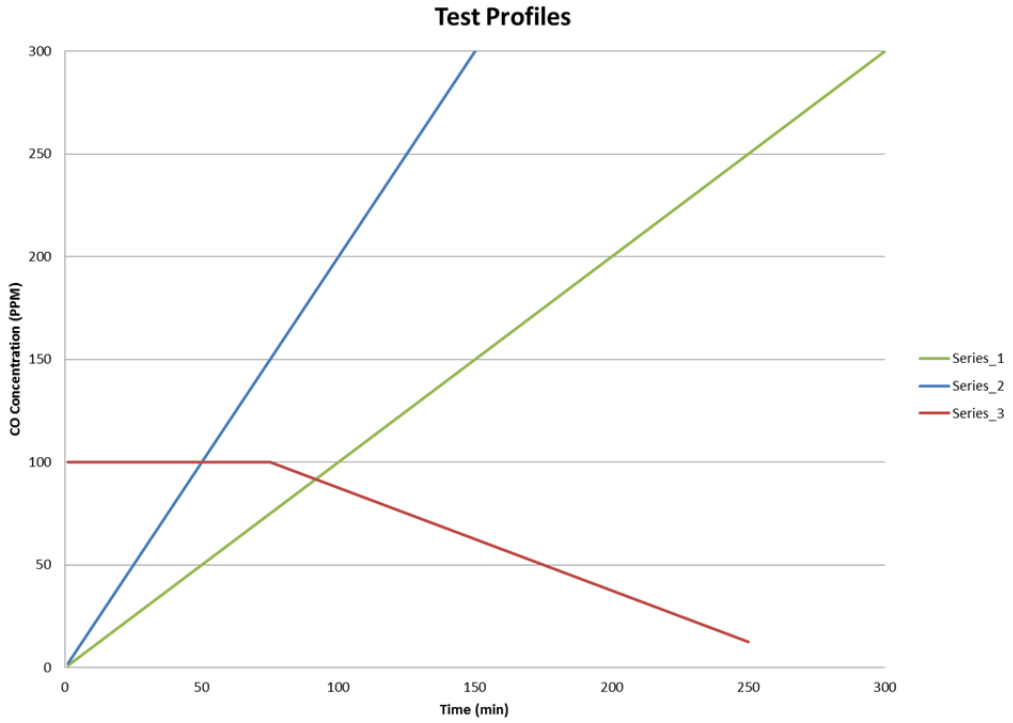


**Figure 5: Profiles used for evaluation of CO script.**

**Table 2: Results from script.**

| Profile | Time to Detection (min) |
|---|---|
| **1** | 97 |
| **2** | 64 |
| **3** | n/a |

MathCAD was used as a tool to check the known profile results, they can be found below in Figure 6. This shows that for each of the profiles, the time to detection was appropriate. The first two concentration profiles are linearly increasing and the COHb outputs were as expected. For profile number three there was no time to alarm detected so it was necessary to check the output of the script to verify that at no point was the COHB% calculated to be above the set 10% threshold.

$$\alpha := 2398 \cdot 0.0404$$

PPM = t

$$\int_0^{97} \frac{218}{1316}\left(1 - \exp\left(\frac{-t}{\alpha}\right)\right) + \left(0.0003 + \frac{t}{1316}\right)\cdot\left(\frac{218}{\alpha}\cdot\exp\left(\frac{-t}{\alpha}\right)\right) dt = 10.206$$

PPM = 2*t

$$\int_0^{64} \frac{218}{1316}\left(1 - \exp\left(\frac{-t}{\alpha}\right)\right)\cdot 2 + \left[0.0003 + \frac{(2\cdot t)}{1316}\right]\cdot\left(\frac{218}{\alpha}\cdot\exp\left(\frac{-t}{\alpha}\right)\right) dt = 10.283$$

PPM = -0.5*t+137.5

$$\int_0^{75} \left(0.0003 + \frac{100}{1316}\right)\cdot\left(\frac{218}{\alpha}\cdot\exp\left(\frac{-t}{\alpha}\right)\right) dt + \int_{75}^{250} \frac{218}{1316}\left(1 - \exp\left(\frac{-t}{\alpha}\right)\right)\cdot -0.5 + \left[0.0003 + \frac{(-0.5\cdot t + 137.5)}{1316}\right]\cdot\left(\frac{218}{\alpha}\cdot\exp\left(\frac{-t}{\alpha}\right)\right) dt = 1.974$$

**Figure 6: MathCAD proof.**

The third calculation was broken into two parts, the constant exposure for the first 75 minutes and the decaying profile for the next 175 minutes. The first integral calculates the COHb for a constant exposure then then this is used as at initial condition for the second part of the profile. It was concluded that, in fact, with profile number three no alarm condition was detected and the concentration of COHb at 250 minutes was 1.9%.

This style of iterative approach has been previously recommended in the literature. In a report submitted to the Gas Research Institute (GRI) entitled Evaluating the Performance of Residential CO Alarms [28] the author recommends an integration algorithm based on the UL-cited Coburn equation. The author points out several flaws in the UL standard. They include: no specific citation to the Coburn equation in the text, it does not apply to varying CO concentrations and it assumes an unrealistic baseline for COHb levels all of which have been previously noted here.

This GRI reference applies the same principles as the MATLAB equation presented here. It is based on the time rate of change of CO and its effects on the COHb levels of an individual.

While this script is useful in analyzing carbon monoxide exposure response in humans, it may not accurately represent a time to exposure that a commercially available CO detector would alarm at. This being said, the CO detection algorithm presented here is perhaps better described as a human response to CO algorithm as it

would likely be adequate to predict a 10% COHb level in an average healthy person but may not mimic a delay or other functionality that would be present in a CO detector. In order to more accurately model CO uptake, a return to the CFK equation derivation from their original publication [26] would be a worthwhile endeavor and a revision of this script would then become necessary.

A full copy of the MATLAB code can be found in the appendix.

# 3. Representative Box

Before simulations were performed on a large scale geometry and realistic setup, a determination had to be made whether a CFD model was practical and how much variation in CO concentration as well as alarm time would be observed. It was determined that a simplistic cube shaped geometry with a few key fixed parameters was a useful starting place.

## *3.1. FLACS Simulation Setup*

The goal of this section is to illustrate the horizontal stratification concept with a simplified geometry. A test box case has been performed with four prior mentioned source rates (6.6e-7, 6.6e-6, 6.6e-5, 6.6e-4 kg/s) based on the results found from the CO yield analysis performed previously. The box is cubical with sides of 3m. Four different vent configurations (passive opening high and low, and air source high and low), two different fire source terms (10 and 100 kW) and three ventilation rates (0, 5 and 10 ACH) have been modeled to assess the effect of the ventilation conditions on the distribution of CO concentration.

The general configuration is illustrated in Figure 7. The details are as follows: a clean air source from one of either the top or bottom locations (indicated by yellow boxes (right) and a passive opening, located in one of either the top or bottom opening (in red, left). The arrow in the lower left is the source fire location, kept constant throughout all simulations.

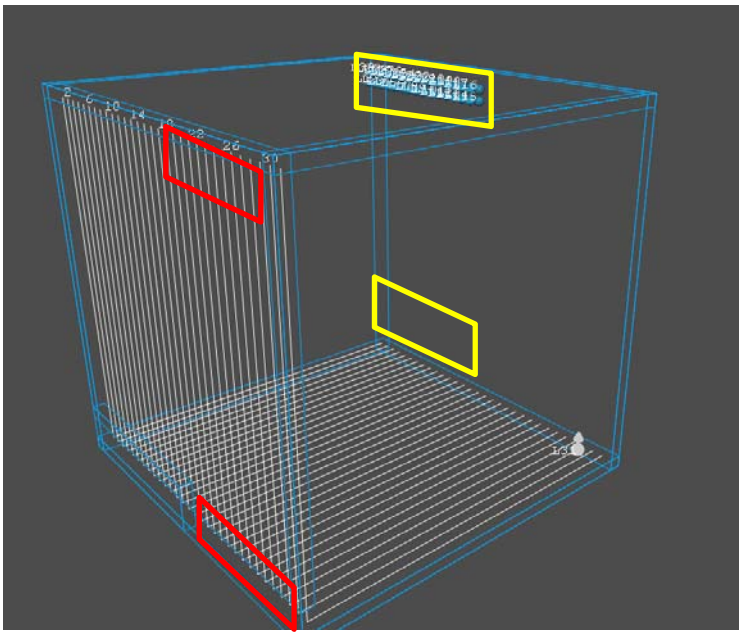

**Figure 7: Representative Box Geometry, Grid, and Source Fire Location.**

To minimize the local effects of only having one high velocity ventilation (air) source, an area was chosen of 1.5m by 0.2m (0.3 $m^2$ area) to represent the outlet of a ventilation system. In the setup described here, the ventilation system is open. This means that fresh air is introduced into the domain, and allowed to naturally leave through an equally sized passive opening in the geometry. The air source and passive vent openings were chosen to not be directly across from each other, so that would ensure there would be interaction between the CO source and the ventilation patterns.

There were a total of 27 monitor points in each of these scenarios. The first level is illustrated in Figure 8. There were three levels of nine points each. The lowest level had numbers 1-9, the middle layer (at the center) had numbers 11-19, and the uppermost (near the ceiling) had numbers 21-29. An overview of their locations can be found in Figure 8.

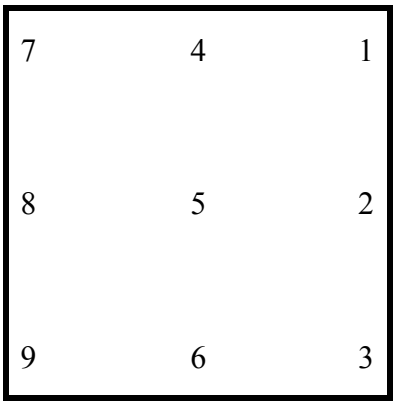


**Figure 8: Monitor point/detector layout.**

The fire source was located near monitor point 1, and where applicable, the passive opening was located near point 3 and the ventilation source was proved in the same corner as point 7.

### 3.1.1. FLACS CO Source Term

For the CO source in FLACS, the leak (fire source) type was specified as "Jet". The leak type selection means that the source contains fuel and has momentum. The parameters to be used in a jet leak are as follows: area, mass flow (or velocity), relative turbulence intensity, turbulence length scale and temperature. The temperature was specified to the set value of 326 °C as determined previously. The mass flow was specified as 0.60 kg/s for 100kW source and 0.060 kg/s for 10kW source, also as was determined previously. This mass flow was chosen to represent the entire mass flow of smoke that would originate from the "source fire". The turbulence intensity was chosen as 20% and the turbulence length scale was chosen as 10% of the grid cell size per FLACS recommendations and common practice. The source area was chosen to be similar to the area of a wastebasket opening and the mass flow rate was evenly distributed across nine grid cell faces. For these

simulations the total source area was 0.09 $m^2$. This is a somewhat arbitrary source, but is reasonable for the estimation of a small, high CO yield source fire.

The definition of a CO source in FLACS was not as straight forward as the other parameters in this instance. FLACS was developed to model flammable gas cloud dispersion, and as such treats leaks (sources) as flammable gas sources. For this type of dispersion CO was chosen to be the source "fuel". The reason that the fuel designation is relevant is that rather than specify a diluted source mixture by mass or volume percentage, it is done by equivalence ratio. Thus to match the desired range of CO yield, the equivalence ratio of the source leak was modified. The equivalence ratio of CO is based on the flammability range in the FLACS model, specified to be the mole fraction range of 0.222 to 0.740.

As a check to assess the accuracy of the calculations, the mass flow rate was checked in the output of the FLACS simulations. Over the first few iterations of the calculation, the mass of "fuel" (CO) was measured. The results found in Table 3 summarize the results over the beginning of the vented box with the passive opening in the high position simulations. This was chosen so that there would be minimal interference with mixing and CO could build up in the upper section of the box.

**Table 3: Mass flow rate checks.**

| Target | Time 1 | | Time 2 | | Calculated Mass Flow Rate |
|---|---|---|---|---|---|
| | Time (s) | CO Mass (kg) | Time (s) | CO Mass (kg) | |
| 6.0E-07 | 51.1 | 8.98E-07 | 110.1 | 3.64E-05 | 6.02E-07 |
| 6.0E-06 | 51.1 | 8.97E-06 | 92.2 | 2.57E-04 | 6.03E-06 |
| 6.0E-05 | 51.1 | 8.96E-05 | 90.2 | 2.45E-03 | 6.04E-05 |
| 6.0E-04 | 50.3 | 1.50E-04 | 69.0 | 1.15E-02 | 6.05E-04 |

### *3.2. Results*

The following are the results from the scenario with 5 ACH and both vent and opening in the "high" position. This vertical cut plane illustrates stratification across the width of the room, highlighting the dependence of detector placement on time for detection. The following images are of CO concentration at a given time, the units are in volumetric ratios (multiply the scales by $10^6$ to get ppm).

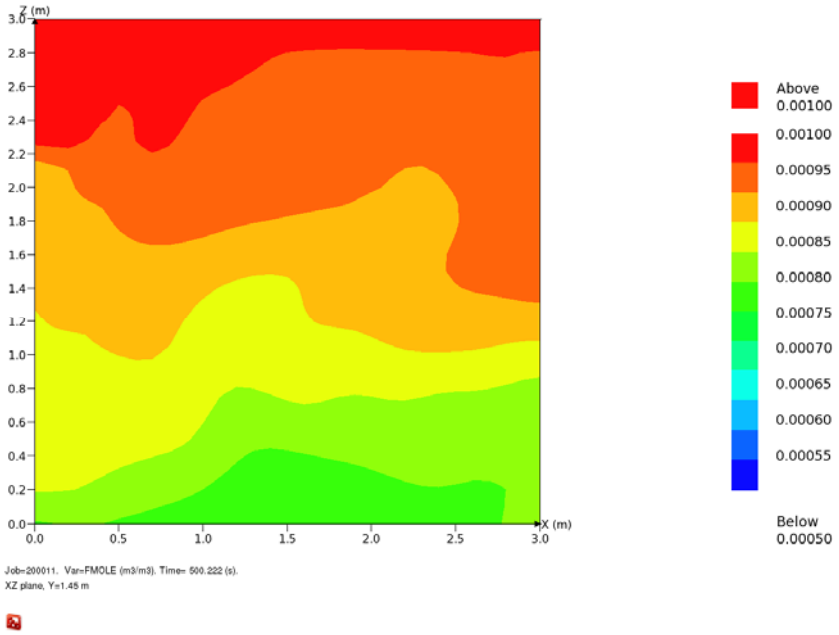


**Figure 9: Vertical stratification with release of 6.67e-5 kg/s with vent and passive opening in "low" position.**

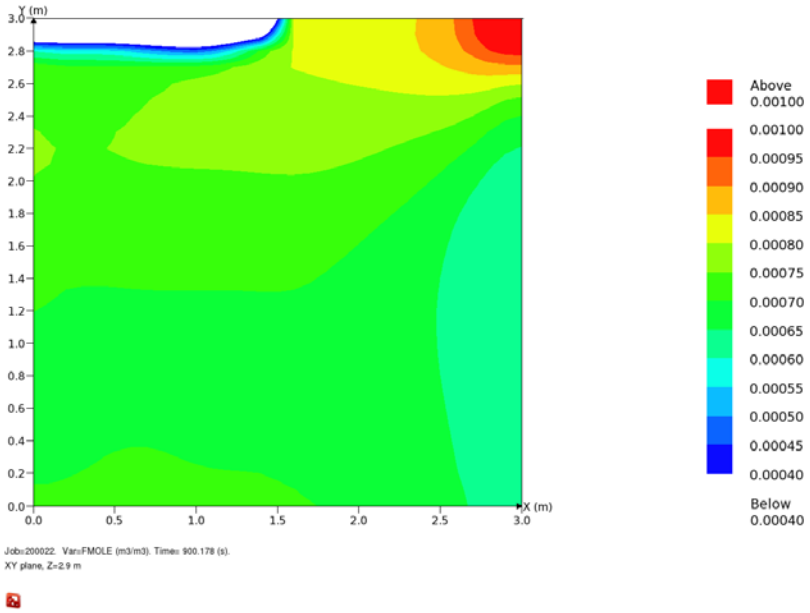


**Figure 10: Top level (XY) for 5 ACH, 6.67 e-5 kg/s CO generation rate, passive and inlet openings in the "high" position.**

Figure 9 is a vertical cut plane near the fire source. This plot shows us that the concentrations of CO are much higher near the top of the representative box. This is due to both the source velocity of the CO origin, and the inherent buoyancy of the elevated temperature source. Figure 10 shows a cut plane across the top-most plane of the box. In this scenario, there is clean air being brought in from the upper left and there is an exhaust in the lower right. This illustration shows that the concentration across the flow pattern can vary by a factor of two.

The following Figure 11 through Figure 14 illustrate the concentration levels found at the top of the simplified box scenario. Monitor point 25 (dark blue) is located at the center near the top of the box. The other four points, 26 through 29, are located at the top level of the box near corners (refer to Figure 8). These figures provide a visual reference to the differences in concentration that a detector could experience at steady state conditions. A description of each scenario can be found in the captions. The

CO source term (release rate and mass flow rate of products) was held constant through these four scenarios. For each of these a different HVAC style was used both the passive opening (exhaust) and clean air source in the high and low positions.

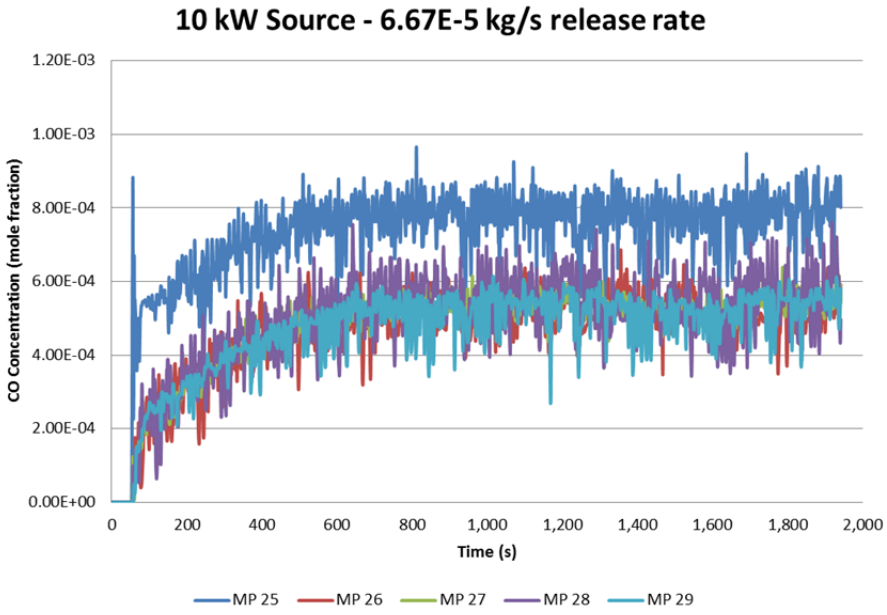


**Figure 11: Top level monitoring points for 10 ACH, 6.6e-5 kg/s CO generation rate, passive opening high and air source low. MP25 is in the center, the other four are in the corners.**

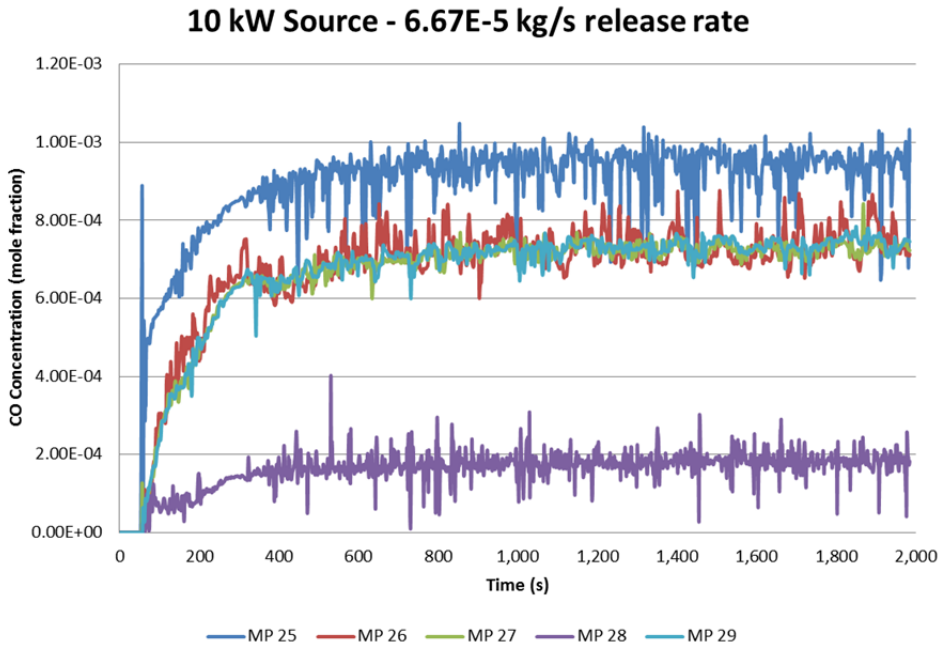


**Figure 12: Top level monitoring point results for 10 ACH, 6.6e-5 kg/s CO generation rate, passive opening low and air source high. MP25 is in the center, the other four are in the corners.**

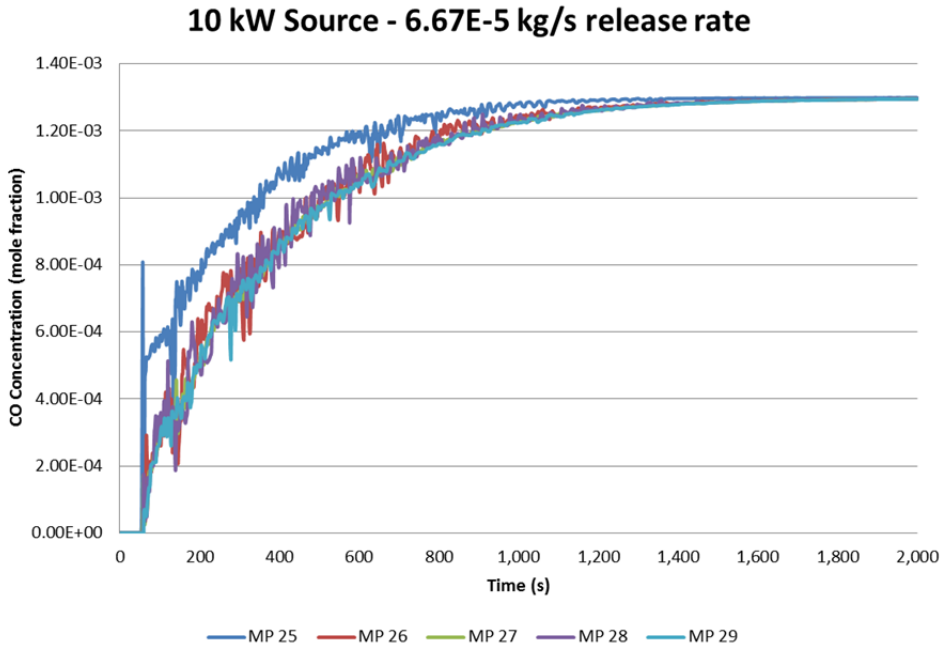


**Figure 13: Top level monitoring points for 0 ACH, 6.6e-5 kg/s CO generation rate, passive opening low. MP25 is in the center, the other four are in the corners.**

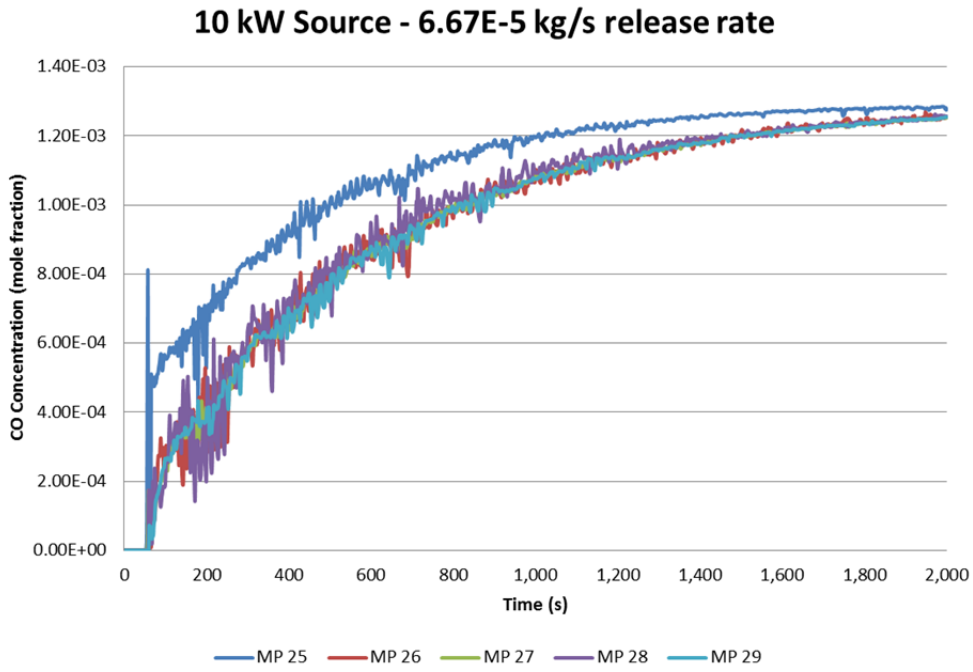


**Figure 14: Top level monitoring points for 0 ACH, 6.6e-5 kg/s CO generation rate, passive opening high. MP25 is in the center, the other four are in the corners.**

From the previous illustrations, it is clear that HVAC styles can have a great impact on the total concentration of CO at various points, as well as the time to reach steady state conditions. The time to steady state varies by up to an order of magnitude, from approximately 200s to almost 2000s and the CO concentration ranges from 500 to almost 1200 PPM.

### *3.3. 0 ACH Flow*

Specific scenarios were evaluated next. In this first part, the box scenarios were run without any external ventilation conditions. Any movement of the CO in this case was due to natural buoyancy. In each of the 0 ACH scenarios, there was a passive opening to eliminate pressure build up.

#### 3.3.1. 10kW Source

The 10kW source was the first evaluated. For this source condition, eight scenarios were evaluated. A complete table of time to detection results can be found in the appendix for each of these scenarios. The data is captured graphically for each of the significant CO source rates in Figure 15 through Figure 17. A 0 value indicates that there was no alarm criteria found and an alarm event was not triggered. For these cases there was no monitor point number 10 or 20.

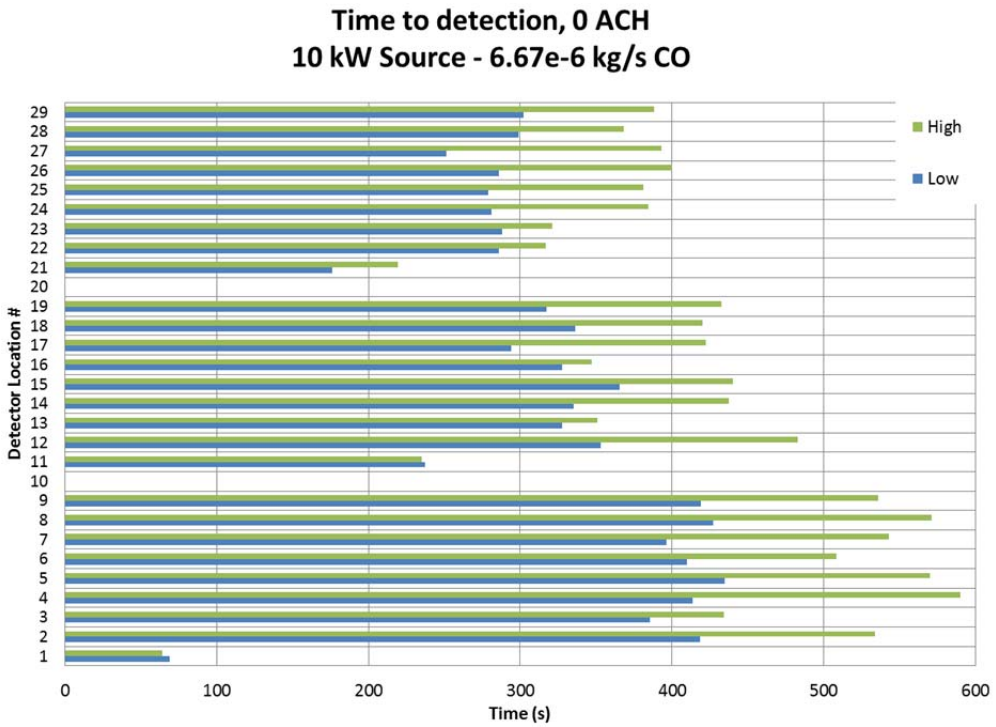


**Figure 15: Time to detection for each monitor point, passive ventilation for a CO generation rate of 6.67e-6 kg/s, 10kW source term.**

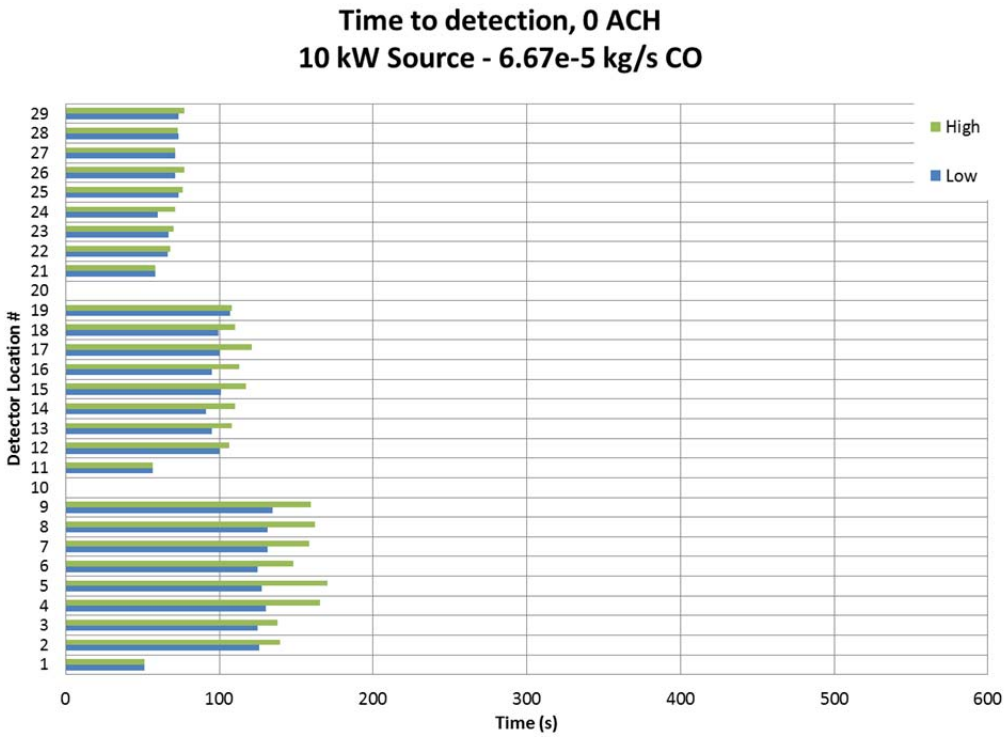


**Figure 16: Time to detection for each monitor point, passive ventilation for a CO generation rate of 6.67e-5 kg/s, 10kW source term.**

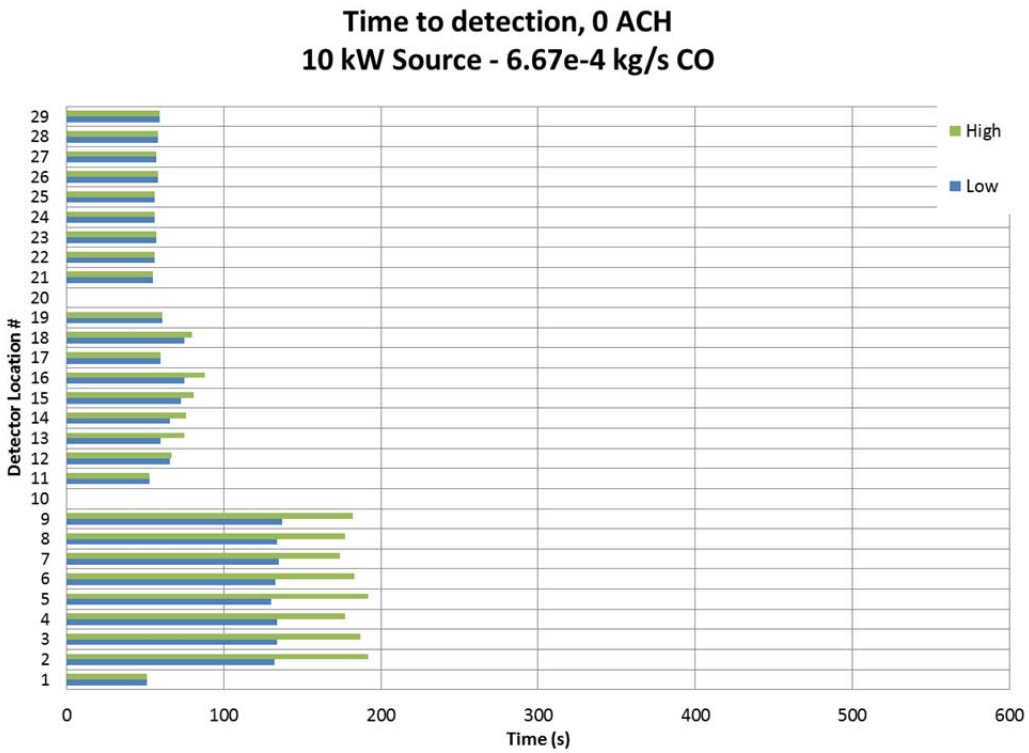


**Figure 17: Time to detection for each monitor point, passive ventilation for a CO generation rate of 6.67e-4 kg/s, 10kW source term.**

After reviewing the results, the 6e-7 kg/s generation rate does not ever produce CO concentrations that would qualify for alarm criteria. Beyond that, generally the time to detection was the shortest for the location directly above the source near the top of the box. The longest time to detection was generally on the opposite corner from the source, near the floor level. This illustrates that generally the CO remains buoyant and detectors should be placed near ceiling level, as close to the source as possible.

A further look shows, generally the time to detection is shorter when the buoyant CO is captured and not allowed to escape when the vent in lower position. When the vent is located at the bottom it forces CO to accumulate in the box, and build to higher concentrations, thus reducing the detection time.

### 3.3.2. 100kW Source

After the10 kW source was evaluated, the 100kW style source was evaluated. As was for the previous case, eight scenarios were evaluated. Again, a complete set of tabulated results can be found in the appendix for each of these scenarios. The data is captured graphically for each of the significant generation rates in Figure 18 and Figure 19. In the following results a 0 value indicates that there was no alarm criteria found and an alarm event was not triggered.

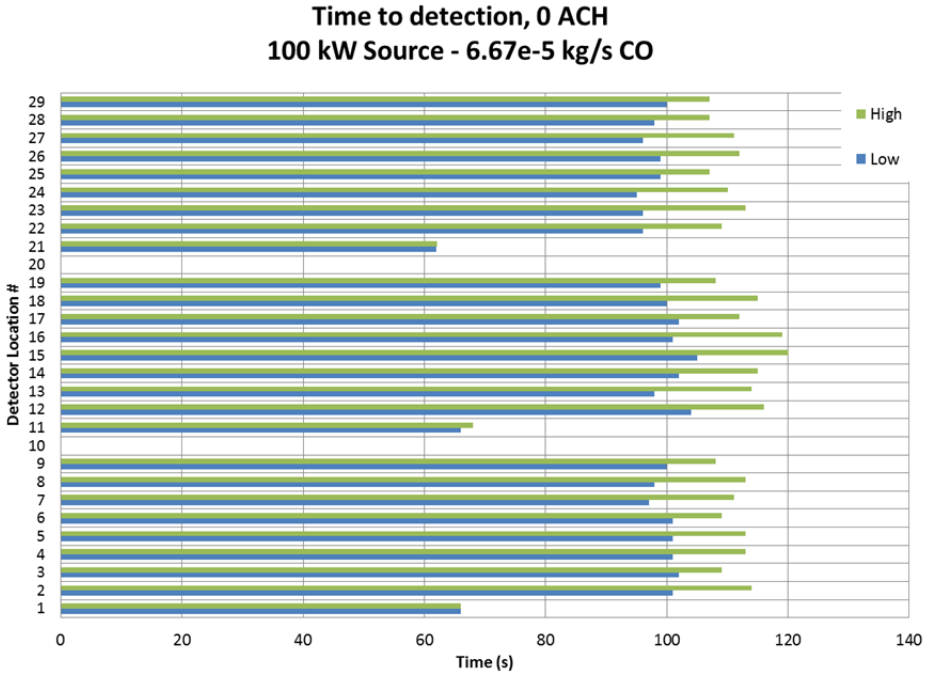


**Figure 18: Time to detection for each monitor point, passive ventilation for a generation rate of 6.67e-5 kg/s, 100kW source term.**

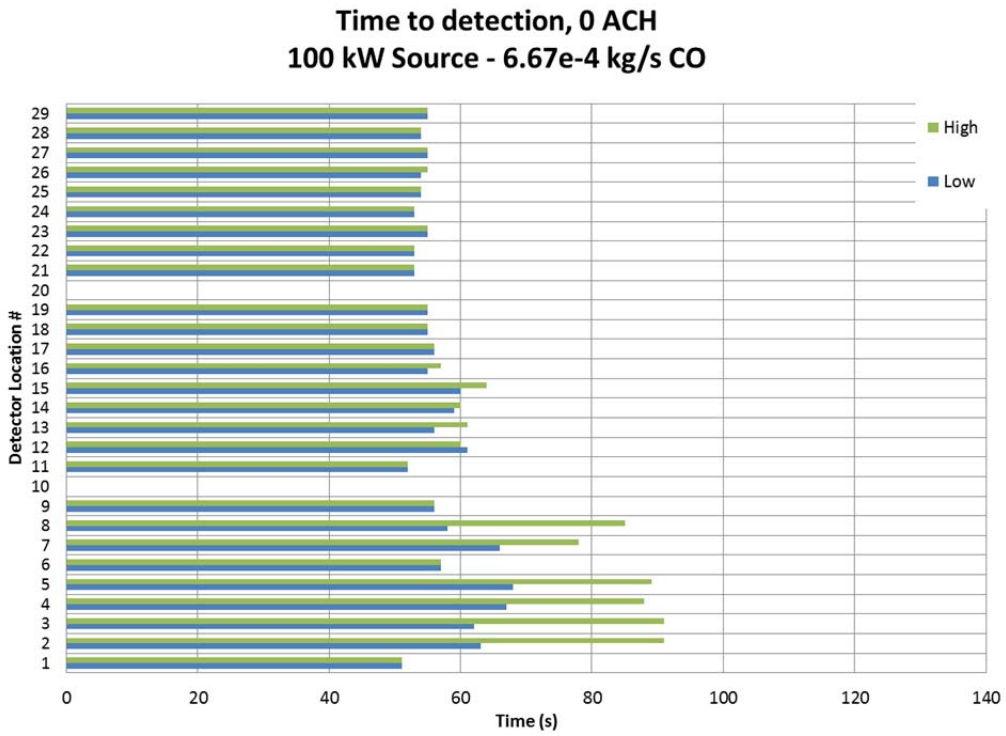


**Figure 19: Time to detection for each monitor point, passive ventilation for a generation rate of 6.67e-4 kg/s, 100kW source term.**

With the increased mass flow rate, and increased mixing, the CO alarm times have been delayed significantly. As such, now the 6e-6 as well as the 6e-7 kg/s source flow rate do not produce criteria which would trigger an alarm.

With the higher heat release rate fire, the CO is generally well mixed. This is evident from the times to alarm being very consistent across locations, and heights. From Figure 18 there is a slight variation in time to detection for the highest level, the time to detection is slightly shorter, beyond that there is no clear correlation between height or detector location.

### *3.4. 5 and 10 ACH Ventilation Conditions*

With the addition of a 5 or 10 ACH outside ventilation condition to the CO fire source term, things become significantly more complicated. Not only does the air source introduce another variable, the source air flow was placed in two locations at two velocities. The results of this investigation are found below.

#### 3.4.1. 10kW Source

Results from all scenarios are found tabulated in the appendix. The data may be more easily understood graphically in Figure 20 through Figure 23. These figures only capture the two largest CO generation rates. Since the lowest release rate does not produce an alarm, and the second lowest release rate has wide variation in detection times, they were not useful. In the following tables a 0 value indicates that there was no alarm criteria found and an alarm event was not triggered. There is also no data available for monitor point numbers 10 and 20 as they did not exist.

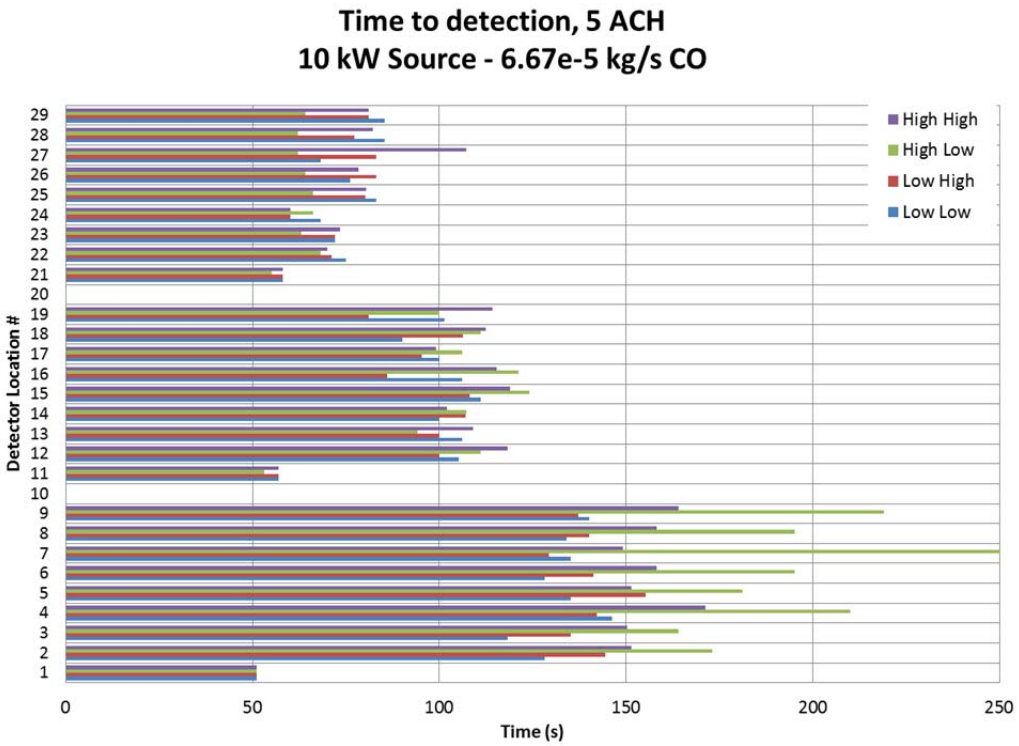


**Figure 20: Time to detection for 10kW source, 6.67e-5 kg/s release and 5 ACH ventilation.**

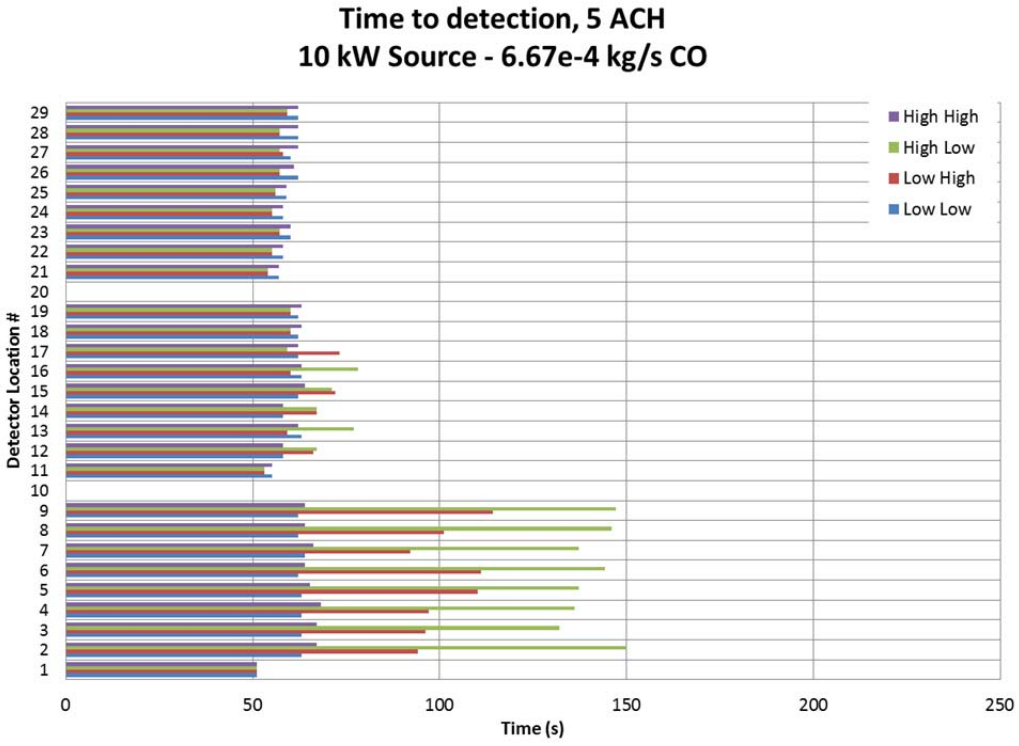


**Figure 21: Time to detection for 10kW source, 6.67e-4 kg/s release and 5 ACH ventilation.**

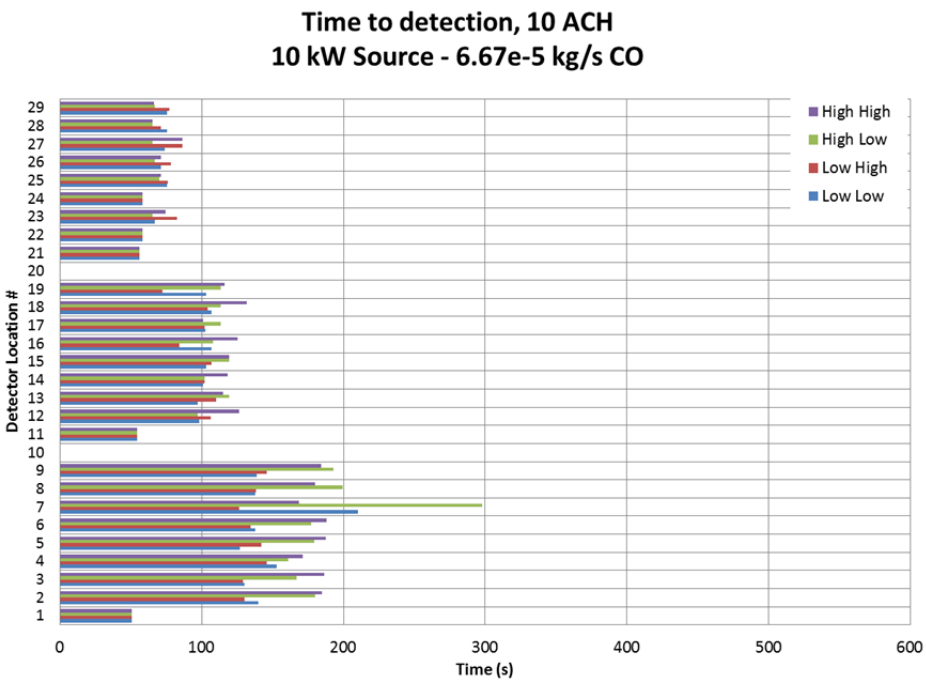


**Figure 22: Time to detection for 10kW source, 6.67e-5 kg/s release and 10 ACH ventilation.**

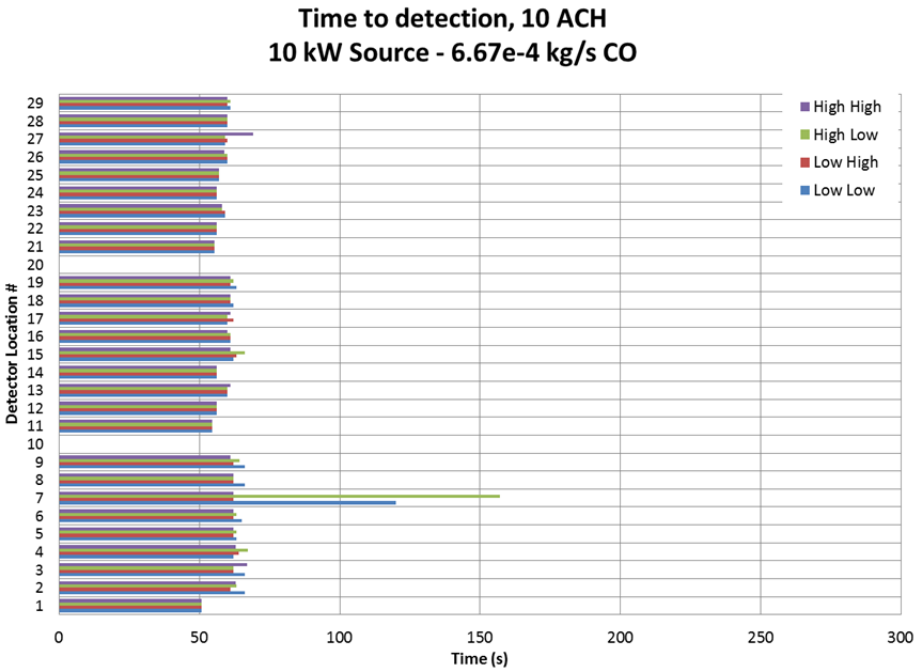


**Figure 23: Time to detection for 10kW source, 6.67e-4 kg/s release and 10 ACH ventilation.**

With the ventilation on, a more extreme difference in between the upper most and lower most detection levels is observed. The buoyancy driven flow is not as pronounced in these cases as evident from the relative similarities between the upper

and middle levels. A glance at the differences in detection times across the same level show some interesting results. In the higher ACH box, the HVAC provides more mixing and the difference in time to detection is minimal, however with the 5 ACH criteria, there can be some places where the time to detection is twice as high. This variation by a factor of two could be significant in a real world scenario and illustrates that more guidance in needed on detector placement.

### 3.4.2. 100kW Source

The results for all scenarios performed with the 100kW source term are found tabulated in the appendix and graphically in Figure 24 through Figure 27. The same stipulations as the previous sections hold true here again: 0 value indicates no alarm and monitor points 10 and 20 did not exist.

The results for this higher heat release rate fire are similar to the no ventilation condition, in that there are no alarm-able concentrations found in the two lowest (6.67e-6 and -7) CO generation rates in the time frame modeled in FLACS. The higher mixing induced by the greater mass flow rate of the source dilutes the CO products and allows it to escape more evenly out of the passive vent.

Generally what can be observed from these results is that with high heat release rate sources and source velocities, the system moves to a more well mixed state. In Figure 25 for example, nearly all the detector points alarm at the same time. This indicates an equal exposure in both time and concentration to the CO. As such it can

be determined that there is some threshold where the ventilation rate no longer matters and the only relevant mixing term is the CO source.

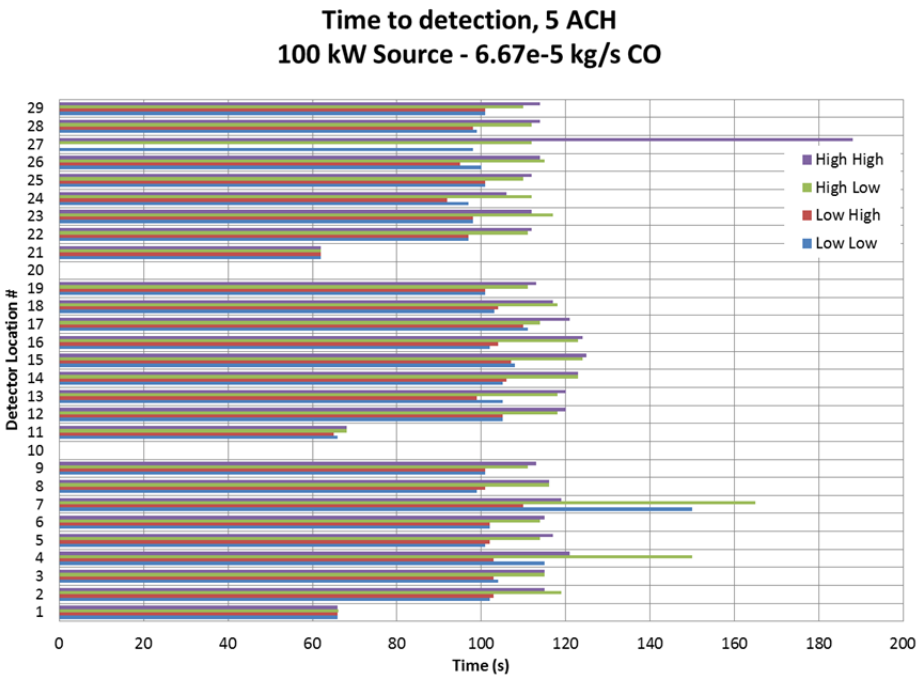


**Figure 24: Time to detection for 100kW source, 6.67e-5 kg/s release and 5 ACH ventilation.**

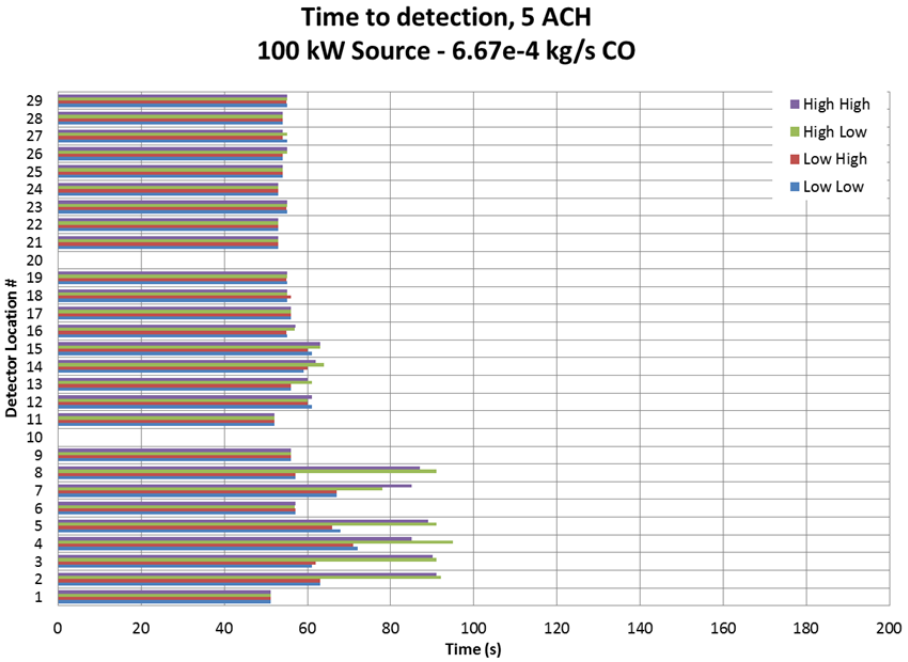


**Figure 25: Time to detection for 100kW source, 6.67e-4 kg/s release and 5 ACH ventilation.**

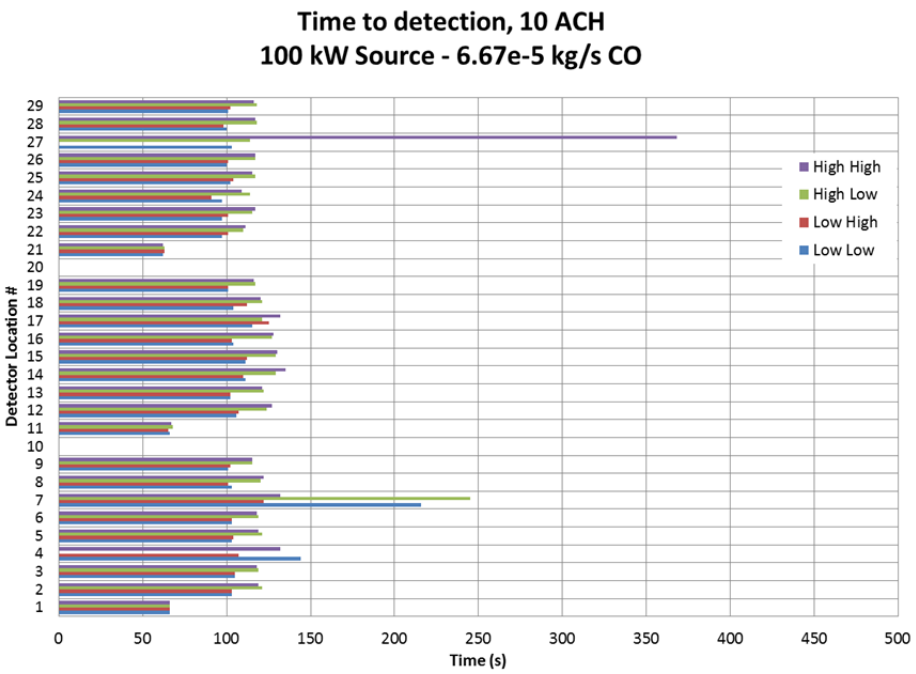


**Figure 26: Time to detection for 100kW source, 6.67e-5 kg/s release and 10 ACH ventilation.**

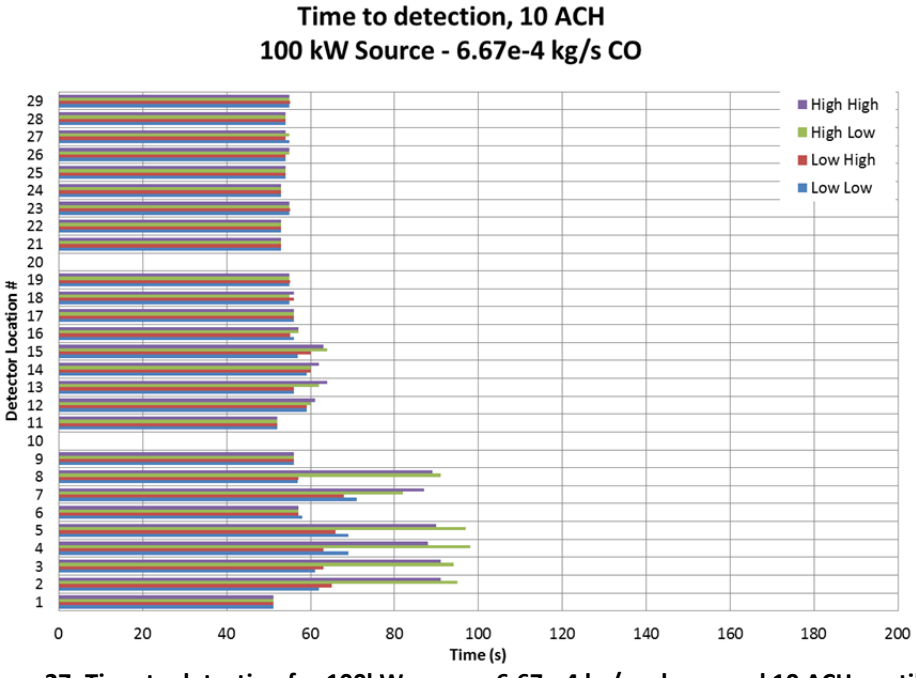


**Figure 27: Time to detection for 100kW source, 6.67e-4 kg/s release and 10 ACH ventilation.**

### *3.5. Buoyancy versus velocity*

A supplemental study was performed on the source velocity as compared to the flow induced from the HVAC system. The results are presented in the following sections. For each of the cases, the velocity was measured in meters per second at 10, 50, 100, 150, 200 and 250 cm above the fire source.

#### 3.5.1. No Ventilation

For the representative box case, only the source fire condition was assumed to be present for both geometry configurations (vent high and low). The results for the 10kW case are presented in Table 4 and 100kW in Table 5.

**Table 4: 10kW source velocity measurements.**

| 10 kW Source (m/s) | | Height Above Source (cm) | | | | | |
|---|---|---|---|---|---|---|---|
| **Passive Opening** | **Vent Source** | **10** | **50** | **100** | **150** | **200** | **250** |
| Low | None | 1.17 | 1.30 | 1.40 | 1.39 | 1.32 | 1.21 |
| High | None | 1.20 | 1.63 | 1.92 | 1.96 | 1.89 | 1.78 |

**Table 5: 100kW source velocity measurements.**

| 100 kW Source (m/s) | | Height Above Source (cm) | | | | | |
|---|---|---|---|---|---|---|---|
| **Passive Opening** | **Vent Source** | **10** | **50** | **100** | **150** | **200** | **250** |
| Low | None | 11.57 | 11.71 | 11.79 | 11.68 | 11.31 | 9.76 |
| High | None | 11.60 | 12.15 | 13.05 | 13.37 | 12.15 | 8.26 |

These results show that as the size of the source fire increases, the velocity increases. Since the mass flow rates of the products increases by an order of magnitude, and the representative area remains the same, the change in velocity in expected. While the extreme velocities presented near the source may not be totally representative of a

true source fire, the intention was observe the migration of the CO on a larger scale. Thus, this result is reasonable.

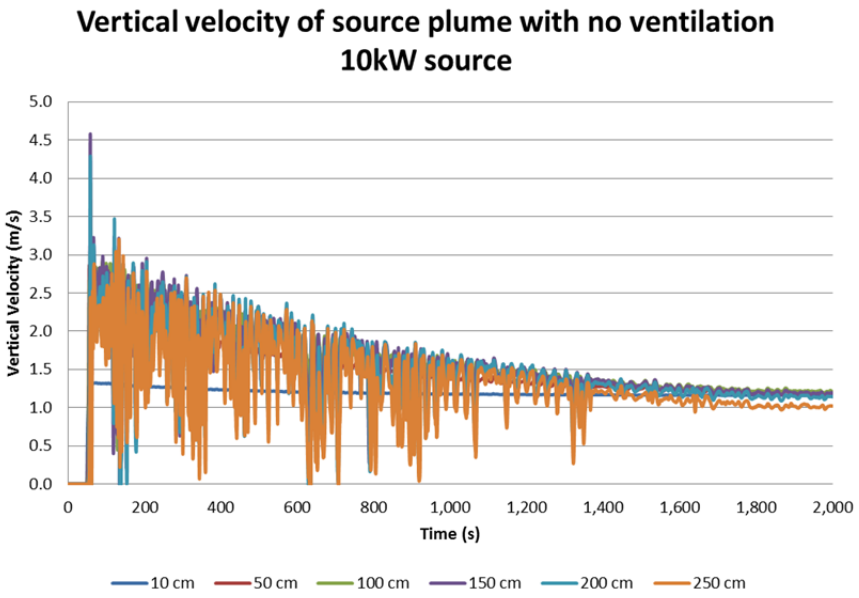


**Figure 28: Vertical velocity at various heights above source term, for 10kW source term, passive opening low.**

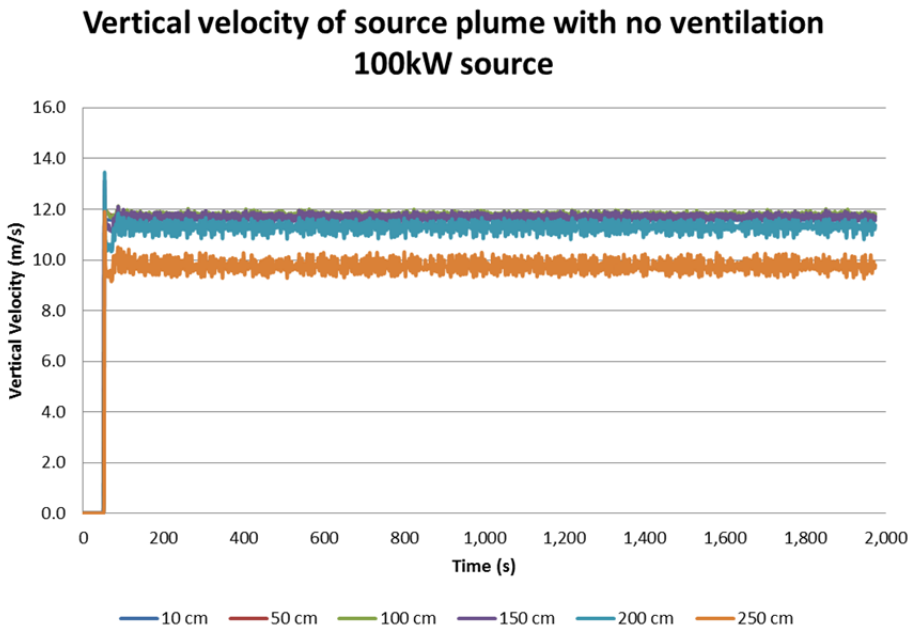


**Figure 29: Vertical velocity at various heights above source term, for 100kW source term, passive opening low.**

### 3.5.2. Ventilated Box

The cases were repeated with only the ventilation sources present (i.e. no fire source term). The results are presented in Table 6 for 5 ACH and Table 7 for 10 ACH.

**Table 6: 5 ACH box velocities.**

| 5 ACH (m/s) | | Height Above Source (cm) | | | | | |
|---|---|---|---|---|---|---|---|
| **Passive Opening** | **Vent Source** | **10** | **50** | **100** | **150** | **200** | **250** |
| Low | Low | -0.02 | -0.06 | -0.06 | -0.06 | -0.05 | -0.03 |
| Low | High | 0.02 | 0.04 | 0.04 | 0.05 | 0.04 | 0.02 |
| High | Low | 1.29 | -0.03 | -0.05 | -0.05 | -0.05 | -0.03 |
| High | High | 0.04 | 0.03 | 0.05 | 0.06 | 0.06 | 0.03 |

**Table 7: 10 ACH box velocities.**

| 10 ACH (m/s) | | Height Above Source (cm) | | | | | |
|---|---|---|---|---|---|---|---|
| **Passive Opening** | **Vent Source** | **10** | **50** | **100** | **150** | **200** | **250** |
| Low | Low | -0.04 | -0.11 | -0.13 | -0.13 | -0.10 | -0.05 |
| Low | High | 0.02 | 0.07 | 0.09 | 0.10 | 0.08 | 0.04 |
| High | Low | -0.01 | -0.05 | -0.09 | -0.11 | -0.10 | -0.06 |
| High | High | 0.09 | 0.06 | 0.11 | 0.13 | 0.13 | 0.10 |

Comparing the results of the HVAC only induced flow and the CO source fire induced flow, it is evident that the majority of the dispersion flow patterns are dominated CO source and the buoyancy driven flow. The HVAC system merely provides background movement designed to encourage mixing, as it would in a real-world application. A comparison between the 5 and 10 ACH values would indicate a good linear correlation between the two ventilation rates. As the ventilation rate doubles, so too does the ambient velocity.

### *3.6. Representative Box Simulations General Conclusions*

From the box simulations there are a few observable trends in the data. As the strength of the source increases, the time to detection decreases. This is a consequence of the higher concentration of CO decreasing the time to alarm. This is somewhat obvious due to the nature of the CO detection algorithm however is useful to point out.

As the strength of the source increases, the effect of detector placement becomes less pronounced. In general, the stronger CO source would yield more uniform alarm times, visible when comparing Figure 15 and Figure 16, and also Figure 20 and Figure 21. The weaker CO source showed more variation in concentration with respect to position.

Also the stronger the source, the more uniform the dispersion of CO was. The larger 100kW source provided more mixing. This was specified, as the source area was kept the same and the mass flow rate of the exhaust increased by an order of magnitude, thus increasing the ambient velocity by an order of magnitude. When the 10kW source was observed, the variation among detection times could vary by up to approximately 20%, while when the 100kW source was analyzed the variation in time was on the order of 5-10%.

From the 5 and 10 ACH simulations, it was also observed that there are some key points in which detector placement should be avoided. Namely any position which could be directly influenced by an inlet or outlet. An example of this occurs in Figure

26 where a corner point is in the direct path of a clean air inlet and its detection time is greater than 3 times longer than its surrounding points.

There was very little variation on average between 5 and 10 ACH in the box. This is also supported by the analysis in to the velocities of the sources, which tended to dominate the mixing as opposed to the HVAC system.

From the results, it is evident that CO detectors are best placed on the ceiling, away from any interference with a potentially diluted or clean air source.

# 4. Real World Geometry

In order for this study to be applicable to read world applications, a real world model was developed. A "typical" house was modeled loosely off a house used in a full scale house fire experiment reported to NIST [29].

## *4.1. Statistical Analysis of Residential Structure Layout and HVAC Styles*

In order for this house to be representative of a broad range of installations, it was necessary to analyze trends in current homes.

### 4.1.1. Geometry Analysis

As part of this investigation, geometry considerations were investigated, and in order to make this more useful to the field, an analysis was done to find the percentage of residences that this would affect. The following tables are from the American Housing Survey (AHS), as part of the U.S. Census Bureau [17]. Table 8 shows the number of stories in owner occupied units broken down by region. Table 9 has similar data, the number of bedrooms per residence in owner occupied residences.

**Table 8: Number of stories in owner occupied structures.**

| Stories in Structure | Northeast | Midwest |
|---|---|---|
| 1 | 6.6% | 16.8% |
| 2 | 32.6% | 44.3% |
| 3 | 49.6% | 35.0% |
| 4 to 6 | 9.3% | 3.5% |
| 7 or more | 1.9% | 0.4% |

**Table 9: Number of bedrooms in owner occupied structures.**

| Bedrooms | Northeast | Midwest |
|---|---|---|
| None | 0.3% | 0.0% |
| 1 | 3.8% | 2.0% |
| 2 | 18.9% | 18.6% |
| 3 | 47.7% | 51.3% |
| 4 or more | 29.4% | 28.0% |

This data was meant to focus the scope of this investigation to the most common geometric layouts. From the previously presented tables, the predominant number of stories in the Northeast and Midwest regions is two or three, and the number of bedrooms is generally greater than three. The data from the AHS was included for all regions of the country, however the southern regions were omitted from presentation here, due to their relatively low heating requirements and CO related injuries.

#### 4.1.2. HVAC Style Analysis

Also from the AHS [17], a survey was conducted of the type of heating appliance in each owner-occupied home. This was also broken down into fuel type used for their heating equipment. The data presented in Table 10 and Table 11 is broken down by percentages of each region's responses.

**Table 10: Heating equipment used in different housing regions.**

| Main Heating Equipment | Northeast | Midwest |
|---|---|---|
| Warm-air furnace | 49.0% | 85.9% |
| Steam or hot water system | 40.7% | 5.8% |
| Electric heat pump | 2.2% | 3.2% |
| Built-in electric units | 4.3% | 2.2% |
| Floor, wall, or other built-in hot-air units without ducts | 1.3% | 1.0% |
| Room heaters with flue | 0.5% | 0.4% |
| Room heaters without flue | 0.1% | 0.2% |
| Portable electric heaters | 0.0% | 0.2% |
| Stoves | 1.4% | 0.7% |
| Fireplaces with inserts | 0.1% | 0.2% |
| Fireplaces without inserts | 0.0% | 0.0% |
| Cooking stove | 0.0% | 0.0% |
| Other | 0.3% | 0.1% |
| None | 0.0% | 0.0% |

**Table 11: Heating fuel used in different housing regions.**

| Main House Heating Fuel | Northeast | Midwest |
|---|---|---|
| Electricity | 9.0% | 12.1% |
| Piped gas | 49.1% | 73.6% |
| Bottled gas | 4.4% | 9.5% |
| Fuel oil | 32.5% | 2.2% |
| Kerosene or other liquid fuel | 1.2% | 0.1% |
| Coal or coke | 0.3% | 0.1% |
| Wood | 3.1% | 2.2% |
| Solar energy | 0.0% | 0.0% |
| Other | 0.3% | 0.3% |

From the data presented, there is a significant portion of each of these regions that rely on forced hot-air or steam/hot water radiator. These are the types or heating style that will be studied in this report. Both the piped gas and fuel oil are the predominant fuel types, again facilitating the creation of CO.

### *4.2. Geometry Layout*

A representative house has been modeled in FLACS to include a realistic ventilation scheme. The following are images of the house.

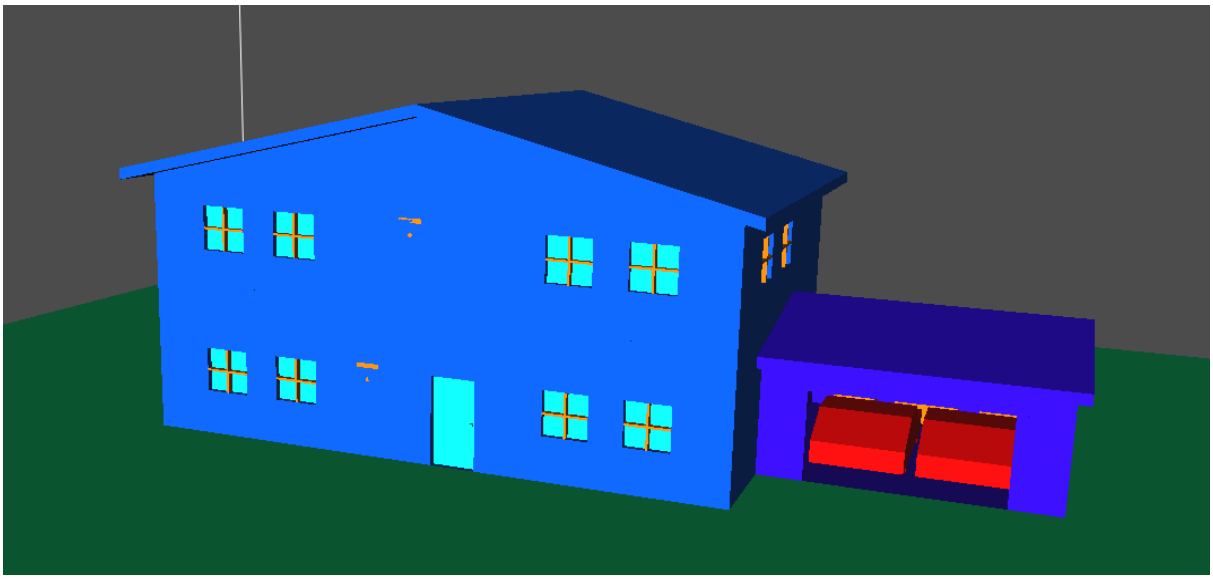

**Figure 30: Exterior of house.**

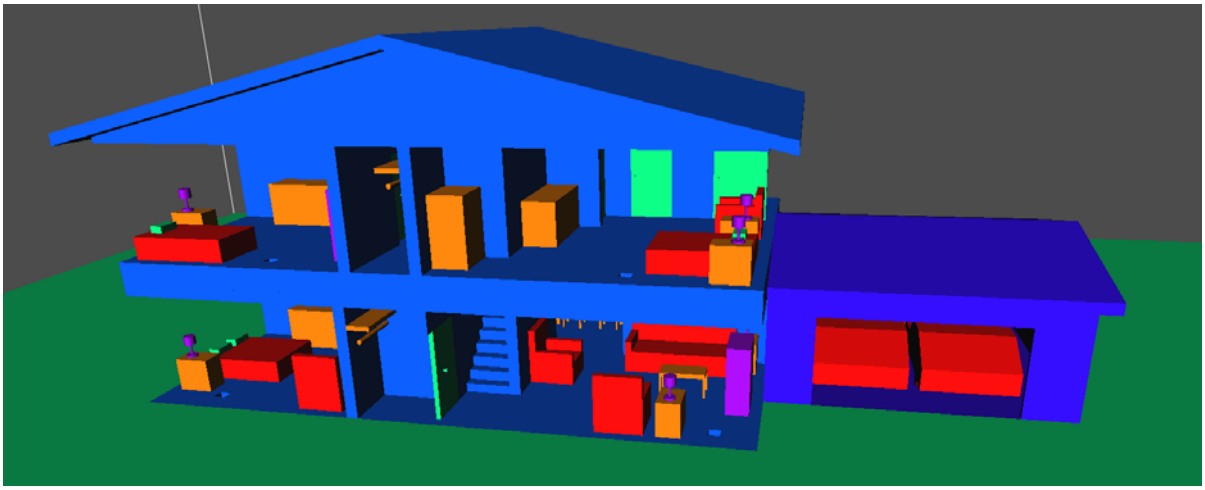

**Figure 31: Exterior view with exterior walls removed, front view.**

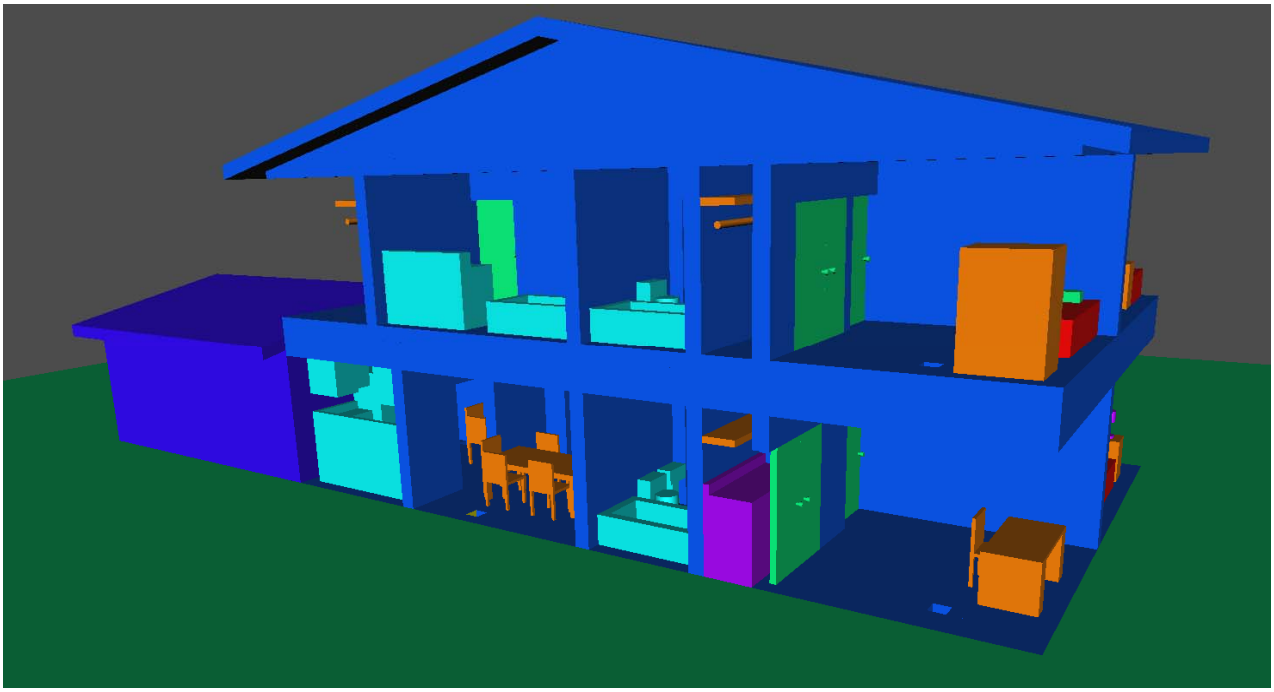

**Figure 32: Exterior view with exterior walls removed, rear view.**

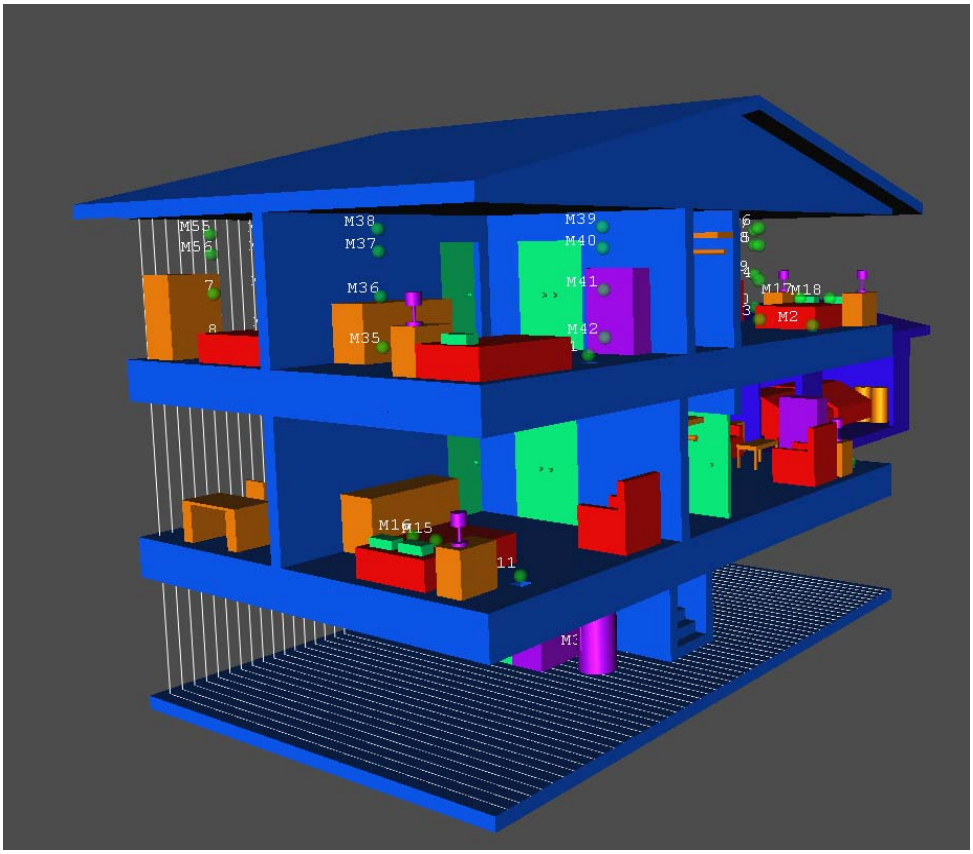


**Figure 33: Walls removed and ground plane removed. Illustration of grid and monitor point (detector) locations.**

The house is a three level detached home with four bedrooms and an office. It also has an open living space, dining room, kitchen and attached garage. The basement is generally open with a staircase located centrally in the structure. The area of each of the floors is approximately 105 square meters for a total of 315 square meters including the basement area. There is a passive opening into the attached garage from the kitchen to allow for pressure relief from the CO/fire source.

One variable considered in this study was the effect of closed doors on the CO dispersion. Closed doors as modeled in FLACS would result in no communication between the different sides. Since FLACS deals with the distributed porosity geometry, doors were allowed to have a 5% opening along the bottom row of cells which would approximately mimic the amount of communication between two sides of a closed door in an actual setting. The key difference here being a real world installation may allow for CO migration at the ceiling level, a room in the model would have to have a CO concentration near floor level to communicate with adjacent spaces.

The following Figure 34 and Figure 35 show the 2d layout of each of the main living floors and their descriptions.


**Figure 34: Second (upper) floor layout.**

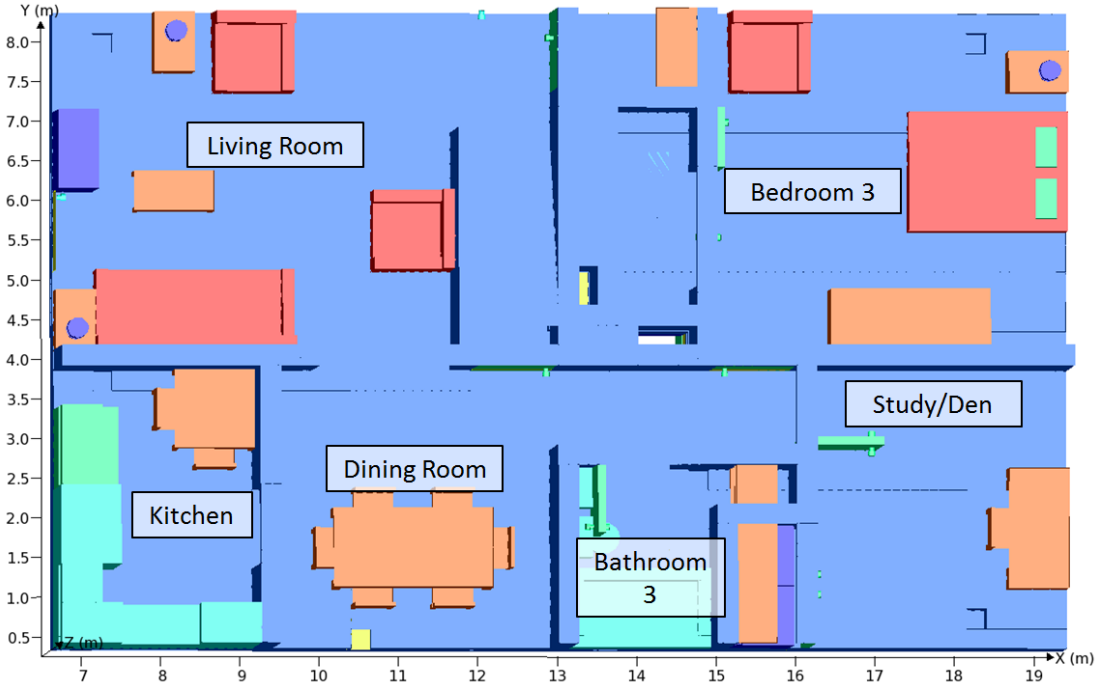


**Figure 35: First (main) floor layout.**

### *4.3. HVAC System Design*

Within the geometry, there is a mixing air distribution system built into the walls and floors. The ductwork pathways run to each room in the structure, and depending upon the area of the room, have either one or two ASHRAE Group B supply outlets (discharge air vertically in a non-spreading jet) [31]. Each of the vents is located on the floor near the exterior of the structure.

The general layout of the HVAC system has two air intakes, one centrally located on each above grade level, near the center of the structure, next to the staircase (yellow hashed arrows in the following figures). On the first floor there are six air supplies each located near the exterior walls of the house (red and white checkered circles). There is one in each of the bedroom style rooms, one in the kitchen, one in the living room area, one in the dining room and one in a bathroom. Figure 36 shows an overview of the first floor. The red and white hashed circles are HVAC outlets (supplying conditioned air) blowing vertically, out of the page, and the yellow hashed arrow points to an HVAC inlet (removing air from the surrounding) taking in air from the –Y (horizontal) direction.

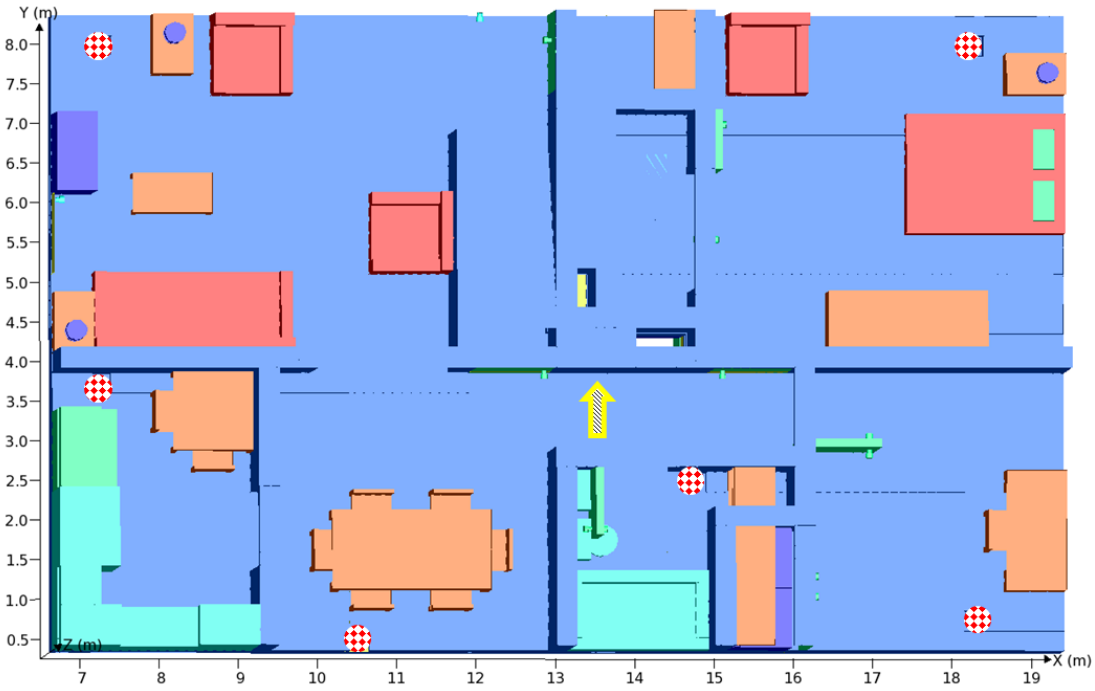


**Figure 36: First floor HVAC layout and overview.**

On the second floor there are also six outlets, also located near the exterior walls of the structure. There is one in each of the bedroom style rooms, two in the master bedroom and one in each of the bathrooms, the style of supplying or removing air is the same for each of the elements. Figure 37 shows an overview.

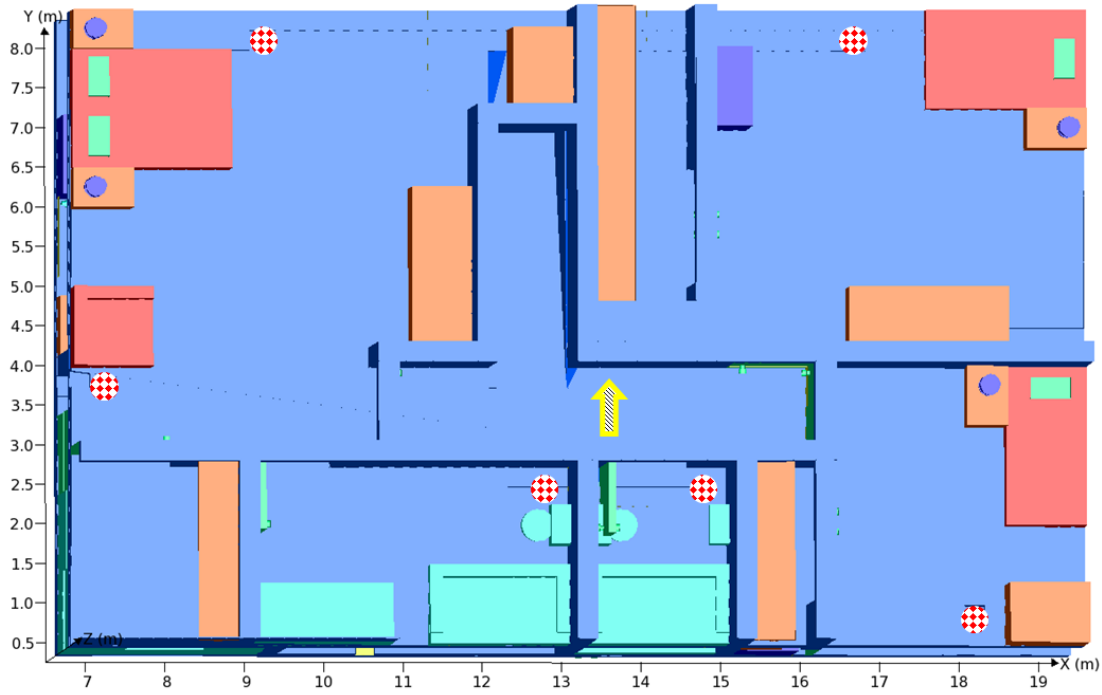


**Figure 37: Second floor HVAC layout and overview.**

In a residential application, duct work sizes are varied to create an even flow throughout the system. As a result of the optimization of grid, and the Cartesian based grid of FLACS it was more efficient to optimize the air flow through the vents by maintaining the duct size constant, and adding a porous plate which would vary the flow resistance and allow for an individual control over the supply side vents. Figure 38 shows the HVAC duct work system of the second floor. The red arrow indicates the source of the conditioned air. This then flows up and follows any of the white arrows around the structure. These paths are cut out of the floor elements to allow for air flow. In a separate ducting element the ambient air is returned to the furnace by way of the yellow arrow. The flow resistance plates are not pictured here, they were modeled as zero-thickness elements and do not appear in the visualizations.

There is one plate for each outlet register to model flow resistance and turbulence generation.

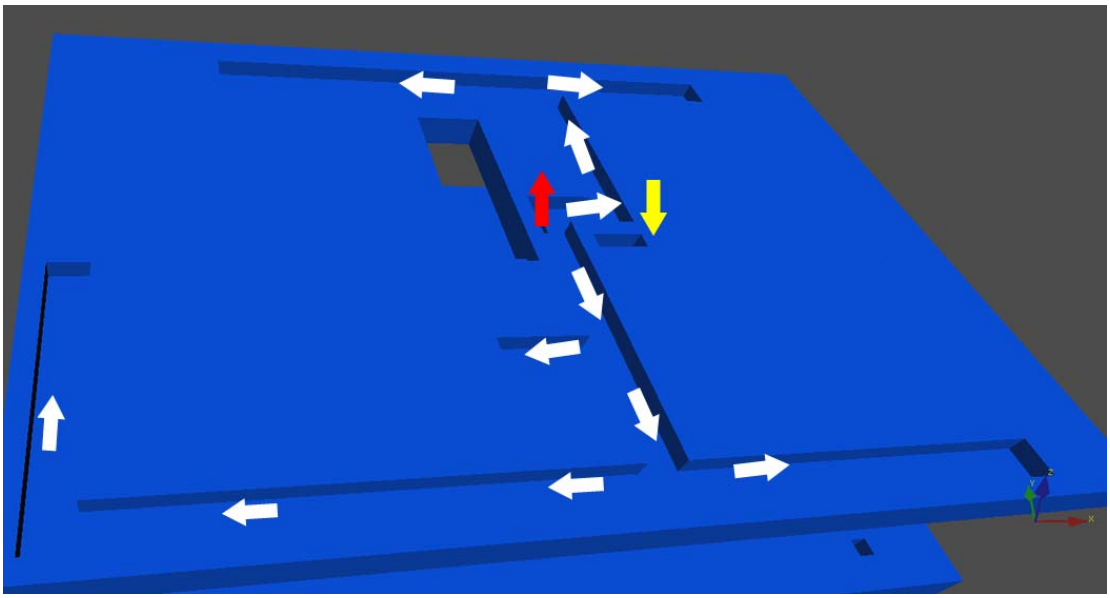

**Figure 38: HVAC system description.**

All of the ductwork modeled in FLACS had a cross section of 0.5 by 0.5m. While this is larger than what a typical ductwork might be in a residential application, this was necessary to allow for two grid cells in each horizontal and vertical direction to model the flow. The actual openings for the HVAC system into the open areas were 0.25 by 0.25m.

The model of the forced hot air furnace system is in the basement where there are five CFD fan elements within the semi-closed ductwork system. There are two based on the suction side of the fan system and three on the air supply side. These elements are in the ductwork that runs to each floor. The elements are specified as "FAN" in FLACS. They were assigned an area and velocity, however due to the logic in FLACS this is converted into a mass flow rate in the solver. This will have a

negligible impact on the effects of the fans as the density of CO is similar to that of air, had this been the study of a hydrogen release, a corrective term should have been included. Each of the elements has been set to a specified heating value of 25 °C; this will mimic the functionality of a HVAC system operating in a heating mode.

According to ASHRAE 62.2, for a house of this area, with 4-5 bedrooms, the minimum fresh air volume to be introduced to the structure by external means is 75cfm, which corresponds to approximately 0.2 volumes of external air per hour. The mechanical mixing system provided 5 to 8 air turn-overs (no clean air brought in) per hour. For the time scales that were dealt with in this investigation, the volume of clean air intake was determined to be insignificant.

From Principles of Smoke Management [30], the equivalent area for air infiltration for this dwelling is $0.05m^2$, assuming "loose" construction and that only the main and upper floors contribute. This equivalent area is approximately equal to the equivalent area open to the outside surroundings through the garage in the computer model. While this open area is not distributed around the structure evenly, there is no pressure gradient from wind or external factors to cause mixing in the CFD model. As such the point opening was deemed to be acceptable.

The HVAC system was not designed to communicate with the outside air as it would in fact do in an actual application. Each of the specified ACH rates would likely be better described as an "air-turnover" or "air-movement" rate than a true air-change

rate. What this means is that when a 5 ACH rate is specified, the HVAC system moves 5 volumes of air throughout the house in an hour; it does not bring in 5 volumes of fresh air every hour. This is also partially compensated by the CO source term in FLACS. The specification of a fuel-lean jet as the source element allows for the introduction of both CO and fresh air. From the specified mass flow rates discussed earlier, this will allow approximately 0.4 or 4 fresh volumes of air to be brought in every hour depending upon the fire source term used in the scenario.

The furnace system was also designed to allow some infiltration and allow CO to disperse through the HVAC ducting. The side wall of the furnace system was assumed to be partially porous. This assumption was justified by assuming that the furnace system would use the surrounding air as the combustion supply air and not intake the air from outside the residence. A specific value for infiltration was not obtained, however an approximation was made based on exemplar furnaces.

### *4.4. Detector and monitor point locations*

The following images capture the array of monitor points used in the FLACS simulation to represent CO detector placements. In total there were 114 detector placement locations evaluated. This included four placements in a "tree" style pattern (same X and Y coordinate, varying height) in each room, placement over each air outlet, one placed on each level of the HVAC system, one at each of the air inlets, and various places where people would like be sleeping or spending time (such as beds or couches).

Figure 39 through Figure 41 show the places where detector trees were located. These included four detector heights located at 0.35, 1.15, 1.85 and 2.2 m above the floor.

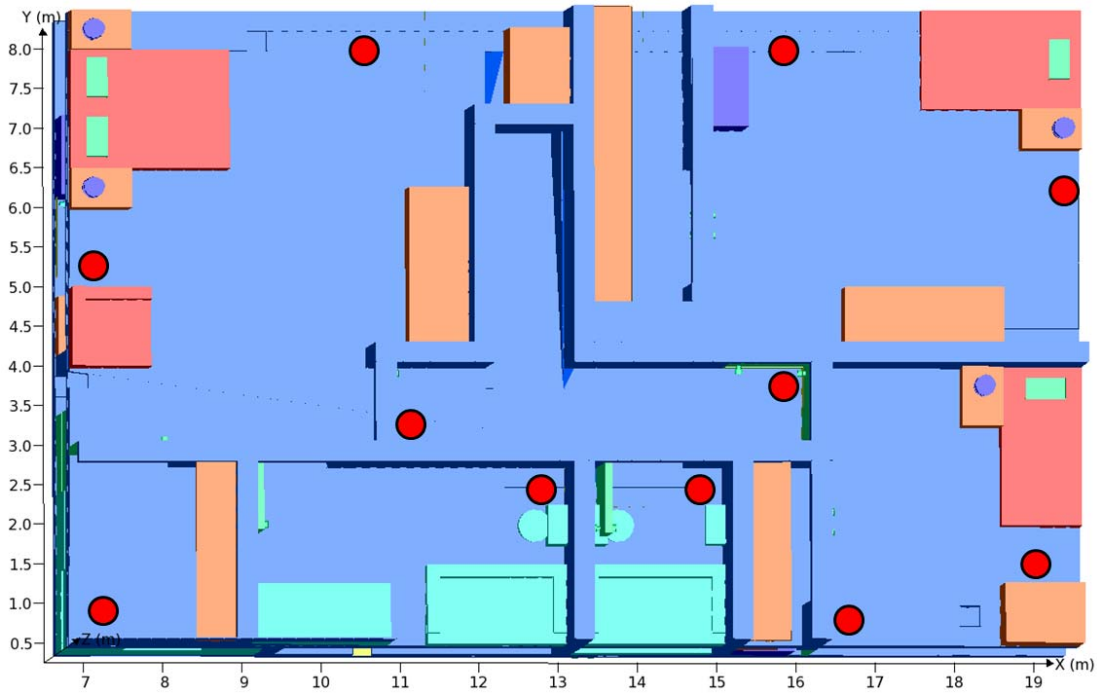


**Figure 39: Monitor point (detector) locations for the upper floor.**

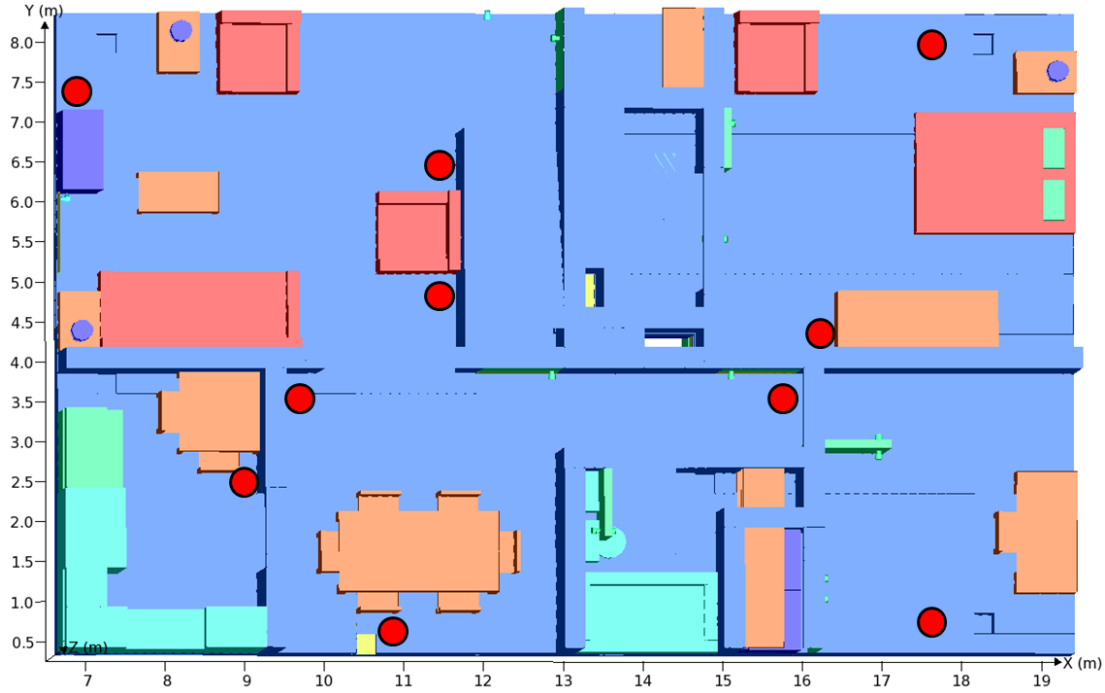


**Figure 40: Monitor point (detector) locations for the first (main) floor.**

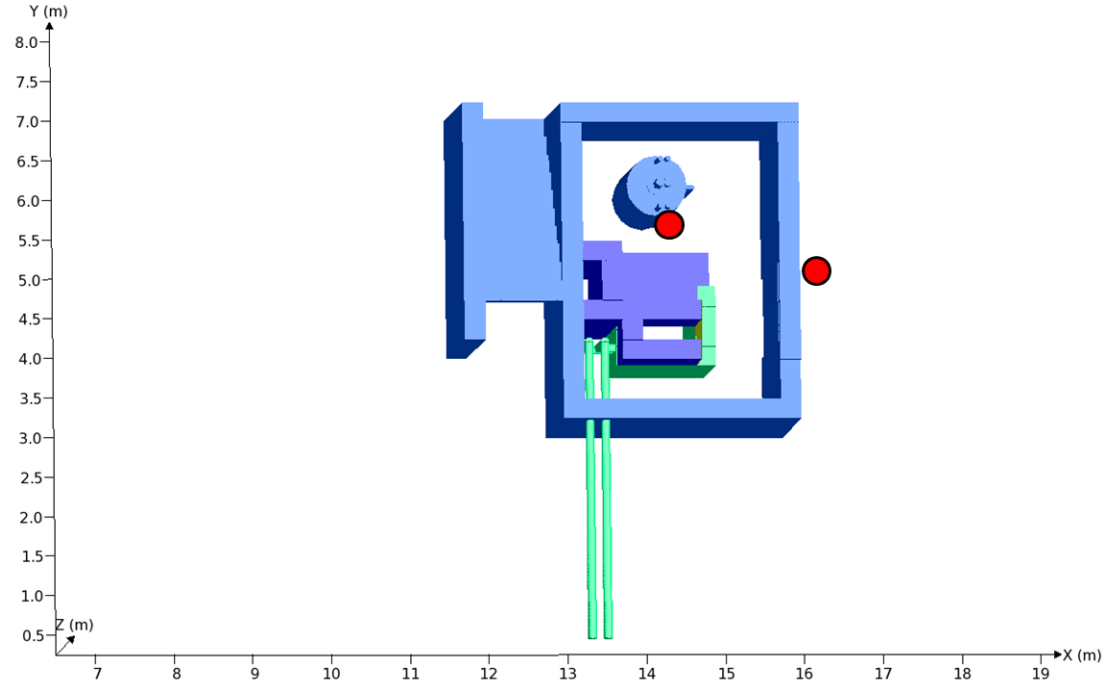


**Figure 41: Monitor point (detector) locations for the basement.**

## *4.5. Description of Scenarios*

### 4.5.1. FLACS Input parameters

For these scenarios, a 0.25 m grid resolution was used. While not necessary for FLACS simulations, this grid was kept uniform in all directions. The 0.25 m grid was within FLACS recommended guidelines to resolve CO and air transport within the ductwork, yet coarse enough to allow simulations to complete in a reasonable amount of time. A 0.125m grid was analyzed, and the average time to detection difference was found to have an average difference of less than 5%. The RANS method of CFD solvers are less dependent upon grid cell size than an LES method used in other packages (i.e. FDS). Based on the testing and guidelines, the grid cell size was determined to be adequate. The boundary conditions were set as NOZZLE to allow free exchange between the house and the passive opening near the garage. The simulations were allowed to run to a maximum of 10,000 seconds.

### 4.5.2. Ambient Conditions

After evaluating the previously discussed report on the non-fire related CO deaths reported to the CPSC in 2007 [3], 84% of CO poisoning cases were found to have occurred in either "cold" or "transition" months (September through April). These months are generally when a heating system would likely be in use. As such, it was determined that focusing on a system in a heating configuration would be most worthwhile. For this the HVAC system was assumed to be operational, and where applicable, providing conditioned air at 25 °C, 5 °C above ambient. It was also decided to use 0, 5 and 8 ACH based on the recommendations of the ASHRAE

reference. It was decided that unlike the previously studied vented box simulation, that 10 ventilation or turnover rates would likely be excessive for a residence, as such 8 was decided to be realistically the upper end of the range.

From the box evaluation preliminary study, it was found that the two lowest CO generation rates (6.67e-7 and 6.67e-6 kg/s) would likely not produce concentrations that would trigger an alarm in a reasonable amount of time (both real-world and simulation time). As such, the 6.67e-5 and -4 kg/s generation rates were studied.

Similar to the vented box, a 10kW and 100kW waste-basket size fire was determined to be the source of the CO providing 0.06 and 0.6 kg/s of products of combustion respectively.

#### 4.5.3. Source Locations

Two source locations were determined to be most representative of a CO generation source. The kitchen, near a gas fired oven, and basement, near a water heater and furnace system. An overview of the source locations can be found in Figure 42 and Figure 43.

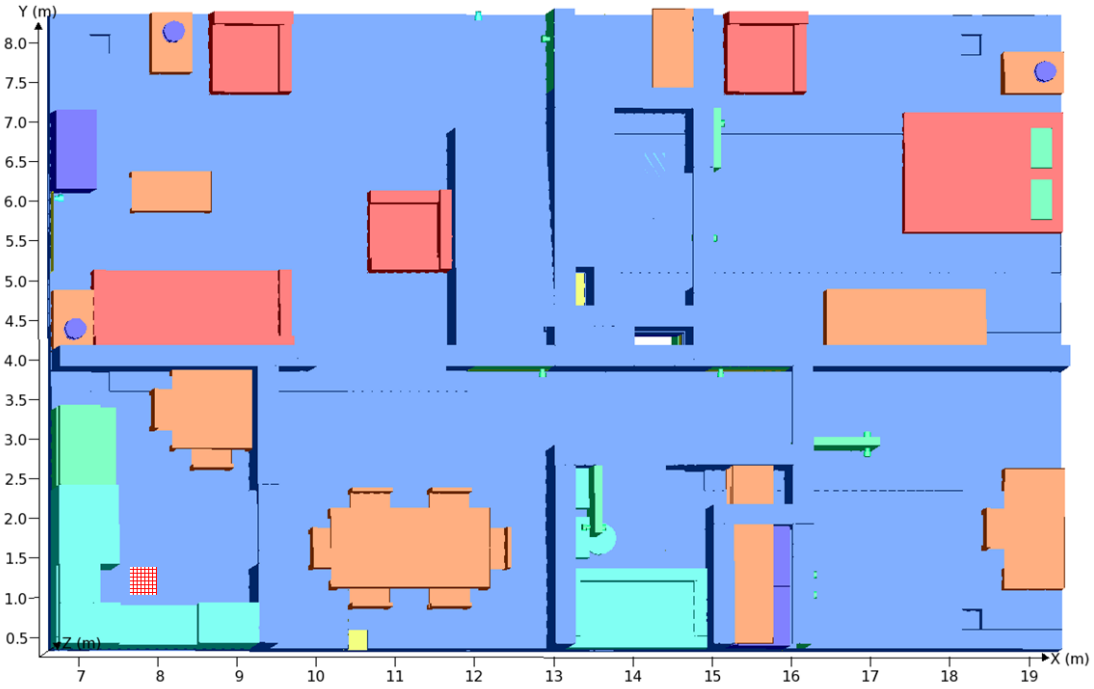


**Figure 42: Kitchen source location (red hashed area in lower left).**

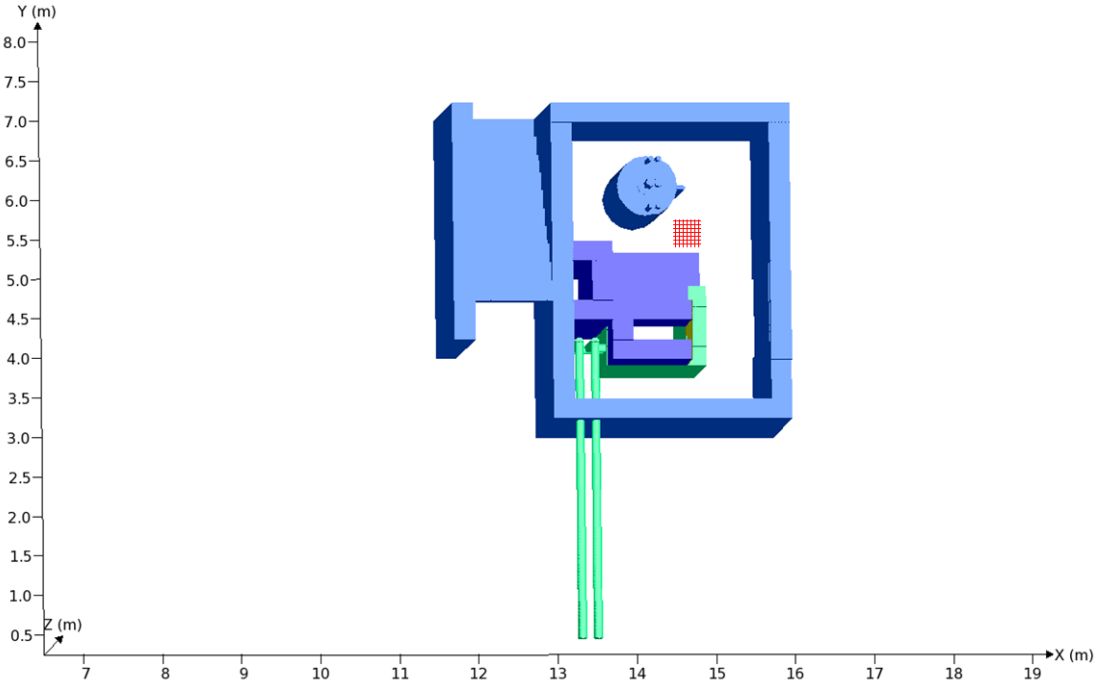


**Figure 43: Furnace room source location (red hashed area in center).**

*4.6. Results*

To begin, a few general observations about the results have been observed. For all the scenarios performed, as one might expect the shortest time to alarm position was located in the same room of origin, near the ceiling. The following tables provide the average rank, as well as the minimum and maximum order of detection. The rank is defined as the numbered sequence of alarm conditions (i.e., rank 1 alarmed first and rank 2 alarmed second, however the actual time difference was not taken into consideration). The "lowest" heading indicates the latest the position alarmed in any scenario, while the "highest" indicates the soonest the position alarmed in any scenario.

**Table 12: Ranks for all scenarios with CO generation in basement and doors open for select locations.**

| Average | Lowest | Highest | Description |
|---|---|---|---|
| 1 | 1 | 1 | Heat Appliances Room 2.2m |
| 2 | 2 | 1 | Heat Appliances Room 1.85m |
| 17 | 31 | 6 | Upstairs Hallway Tree -X side 2.2m |
| 20 | 34 | 6 | Upstairs Hallway Tree -X side 1.85m |

**Table 13: Ranks for all scenarios with CO generation in kitchen and doors open for select locations.**

| Average | Lowest | Highest | Description |
|---|---|---|---|
| 1 | 2 | 1 | Kitchen 2.2m |
| 2 | 3 | 1 | Kitchen 1.85m |
| 4 | 9 | 1 | Kitchen 1.85m |
| 5 | 7 | 3 | Dining Room 2.2m |
| 5 | 8 | 4 | Dining Room 1.85m |

There is a simple message than can be taken away for this that covers all of the subsequent scenarios performed. For the shortest time to detection, the CO detector

should be placed near the CO source, near the ceiling. From the results provided in Table 12 and Table 13, the first detection always occurred in one of these locations.

The subsequent sections will separate out several of the criteria tested for further analysis. All of the raw time to detection data has been provided in the appendix. Also data for all monitor points will be for the highest (2.2m) location unless otherwise noted.

#### 4.6.1. Kitchen Fire Source

A fire source in the kitchen will be the first analyzed. This is the more simplistic release location for reasons to be elaborated upon later in Section 4.6.2. Generally, the CO has only one pathway to migrate throughout the house regardless of the HVAC condition or source term. The kitchen door is open to the surrounding areas and CO is allows minimal flow resistance or direction.

A general dispersion pattern from the kitchen source location can be found in Figure 44 and Figure 45. These images from top left to bottom center, capture the CO migration from 300 s after source start to 750 s after source start.

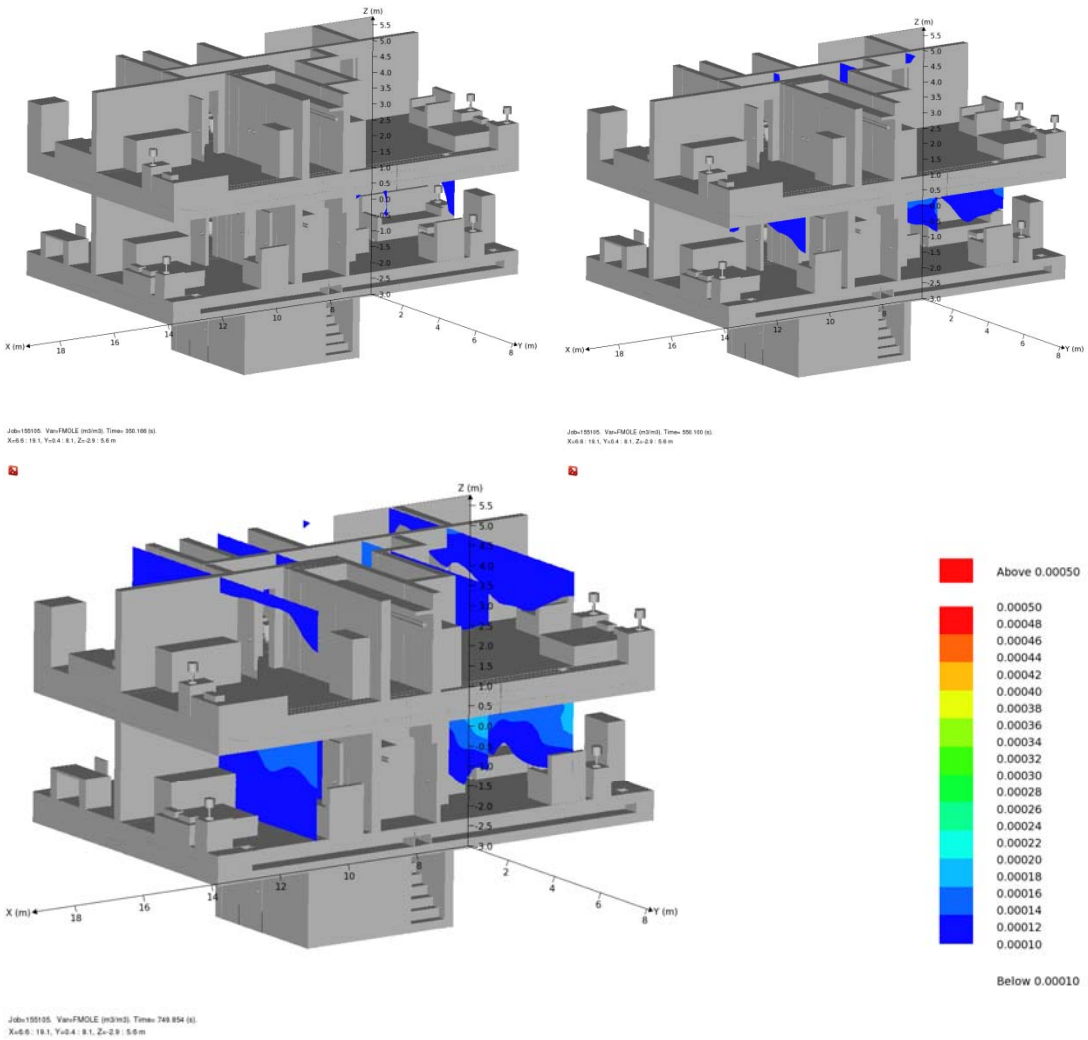


**Figure 44: General CO dispersion pattern 3d cut plane plots from kitchen, at 300s (top left), 500s (top right) and 700s (bottom) after source start. 0 ACH, 10kW Source, 6e-5 kg/s CO release rate.**

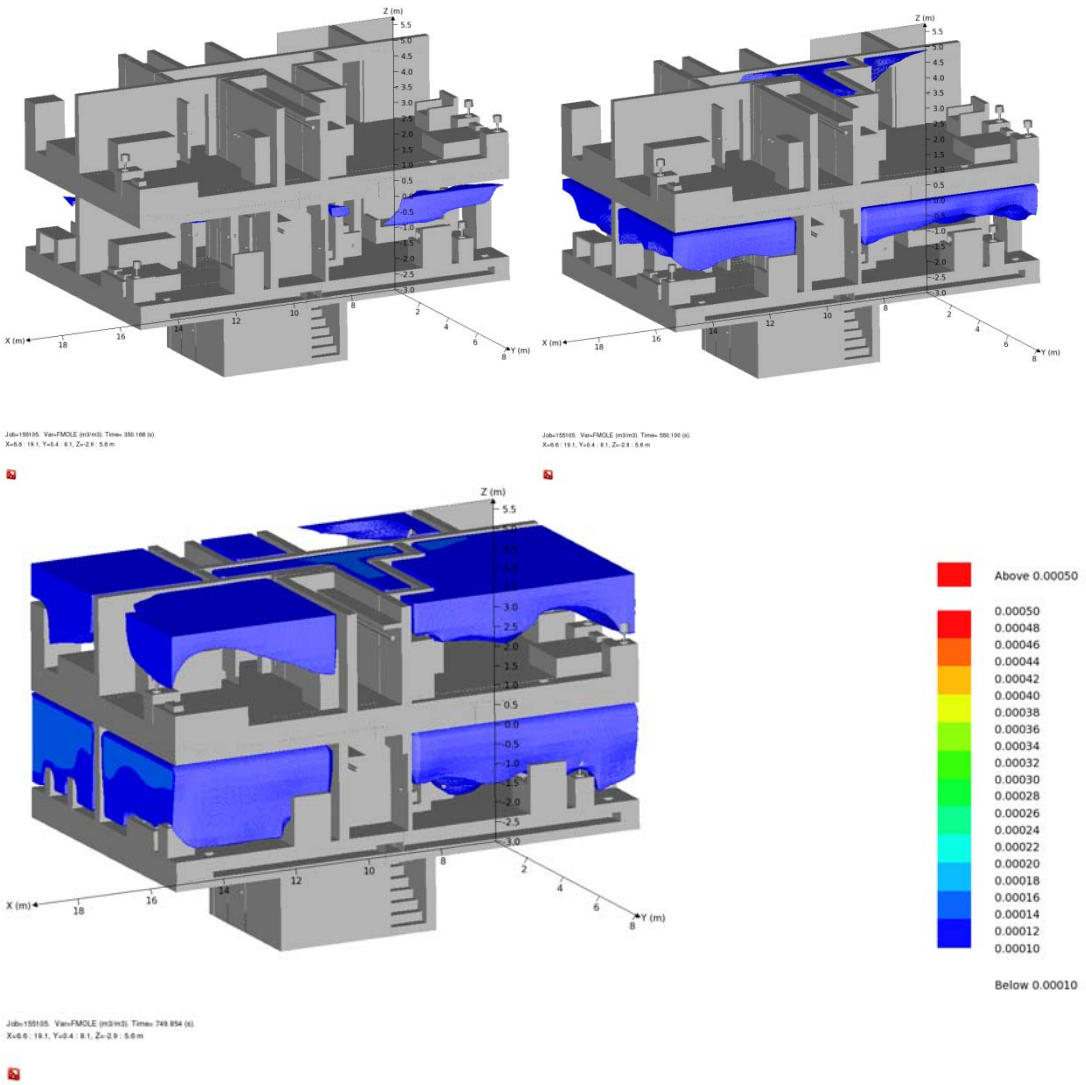


**Figure 45: General CO dispersion pattern volume plots from kitchen, at 300s (top left), 500s (top right) and 700s (bottom) after source start. 0 ACH, 10kW Source, 6e-5 kg/s CO release rate.**

From these image sequences it can be seen that the buoyant CO rise to the ceiling of the kitchen, fill the small space above the door frame and then migrate freely out to the surrounding rooms and up the stairs to the second floor. This sequence is not complicated and could have been easily predicted without the use of CFD. However as the analysis of detection time criteria begins things become more interesting. The following Table 14 ranks the top ten detector placement locations. As described previously, the rank is defined as the numbered sequence of alarm conditions (i.e.,

rank 1 alarmed first and rank 2 alarmed second, however the actual time difference was not taken into consideration). The "lowest" heading indicates the latest the position alarmed in any scenario, while the "highest" indicates the soonest the position alarmed in any scenario.

**Table 14: Top ten ranked CO detector alarm placements for kitchen source scenarios with doors open.**

| Average | Lowest | Highest | Description |
|---|---|---|---|
| 1 | 2 | 1 | Kitchen 2.2m |
| 2 | 3 | 1 | Kitchen 1.85m |
| 4 | 9 | 1 | Kitchen 1.15m |
| 5 | 7 | 3 | Dining Room –X Side 2.2m |
| 5 | 8 | 4 | Dining Room –X Side 1.85m |
| 6 | 8 | 4 | First Floor Hallway Tree 2.2m |
| 6 | 8 | 4 | First Floor Hallway Tree 1.85m |
| 7 | 9 | 4 | Dining Room +X Side 2.2m |
| 8 | 12 | 5 | Dining Room +X Side 1.85m |
| 10 | 11 | 9 | Living room, interior wall 2.2m |

From Table 14 the order of average alarm time is about what would be expected. The CO migrates from the kitchen, to the dining room and out into the common space.

With the doors closed, the time to detection for the first ten average rank detector placement remains relatively unchanged. Since all of the detector placements for the top ten ranks are in common areas, the closing of doors does nothing but decrease the amount of open volume for the CO to fill.

**Table 15: Top ten ranked CO detector alarm placements for kitchen source scenarios with doors closed.**

| Average | Maximum | Minimum | Description |
|---|---|---|---|
| **1** | 1 | 1 | Kitchen 2.2m |
| **2** | 2 | 2 | Kitchen 1.85m |
| **4** | 4 | 3 | Dining Room –X Side 2.2m |
| **4** | 4 | 4 | Dining Room –X Side 1.85m |
| **5** | 7 | 2 | Kitchen 1.15 |
| **6** | 8 | 4 | Dining Room +X Side 2.2m |
| **7** | 8 | 5 | First Floor Hallway Tree 2.2m |
| **7** | 8 | 5 | First Floor Hallway Tree 1.85m |
| **8** | 9 | 7 | Dining Room +X Side 1.85m |
| **11** | 11 | 10 | Living room, interior wall 2.2m |

A look at the dispersion plot for a release with 8 ACH (compared with 0 ACH seen previously in Figure 44 Figure 45) shows that the pattern for CO dispersion has not drastically changed. Figure 46 and Figure 47 present the flow path with 8 ACH.

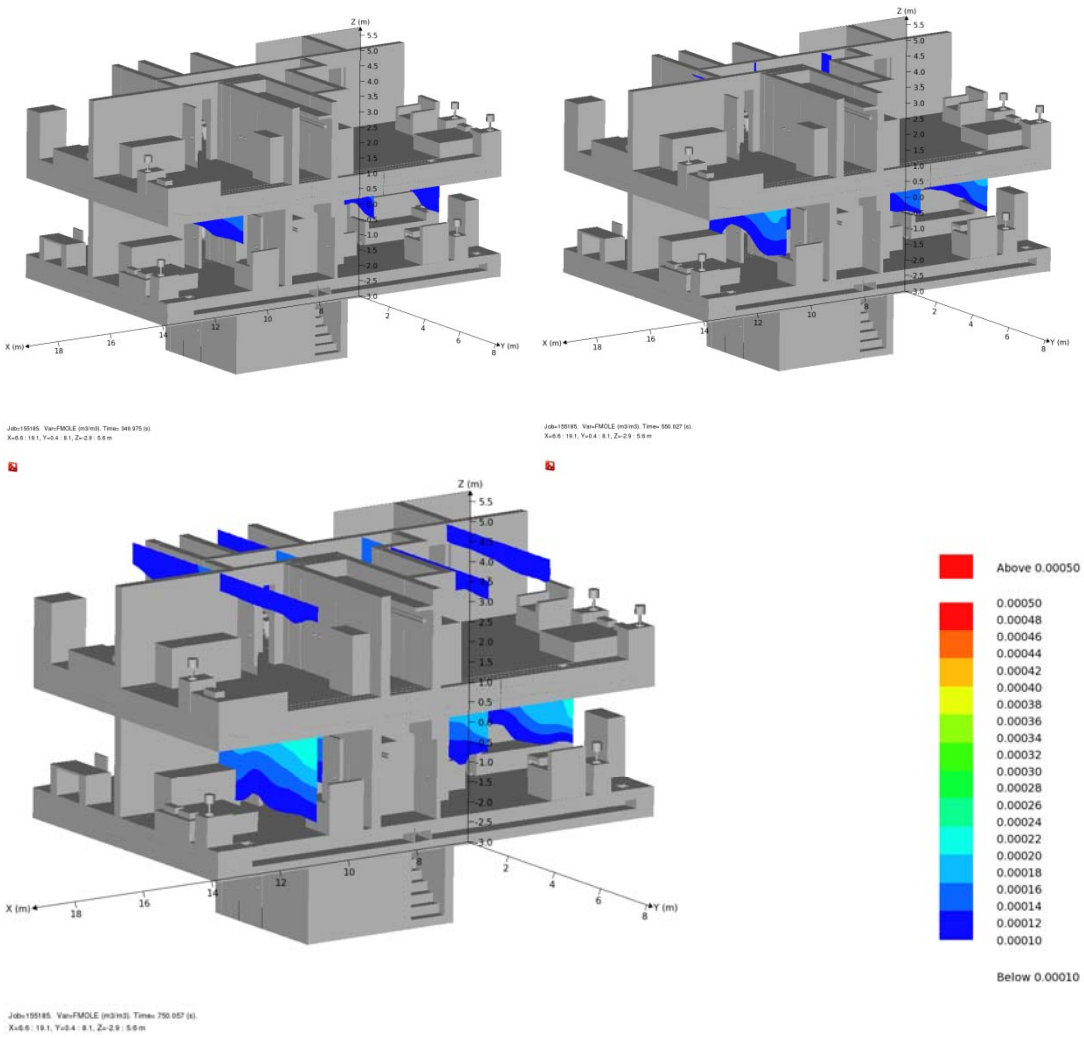


**Figure 46: General CO dispersion pattern 3d cut plane plots from kitchen, at 300s (top left), 500s (top right) and 700s (bottom) after source start. 8 ACH, 10kW Source, 6e-5 kg/s CO release rate.**

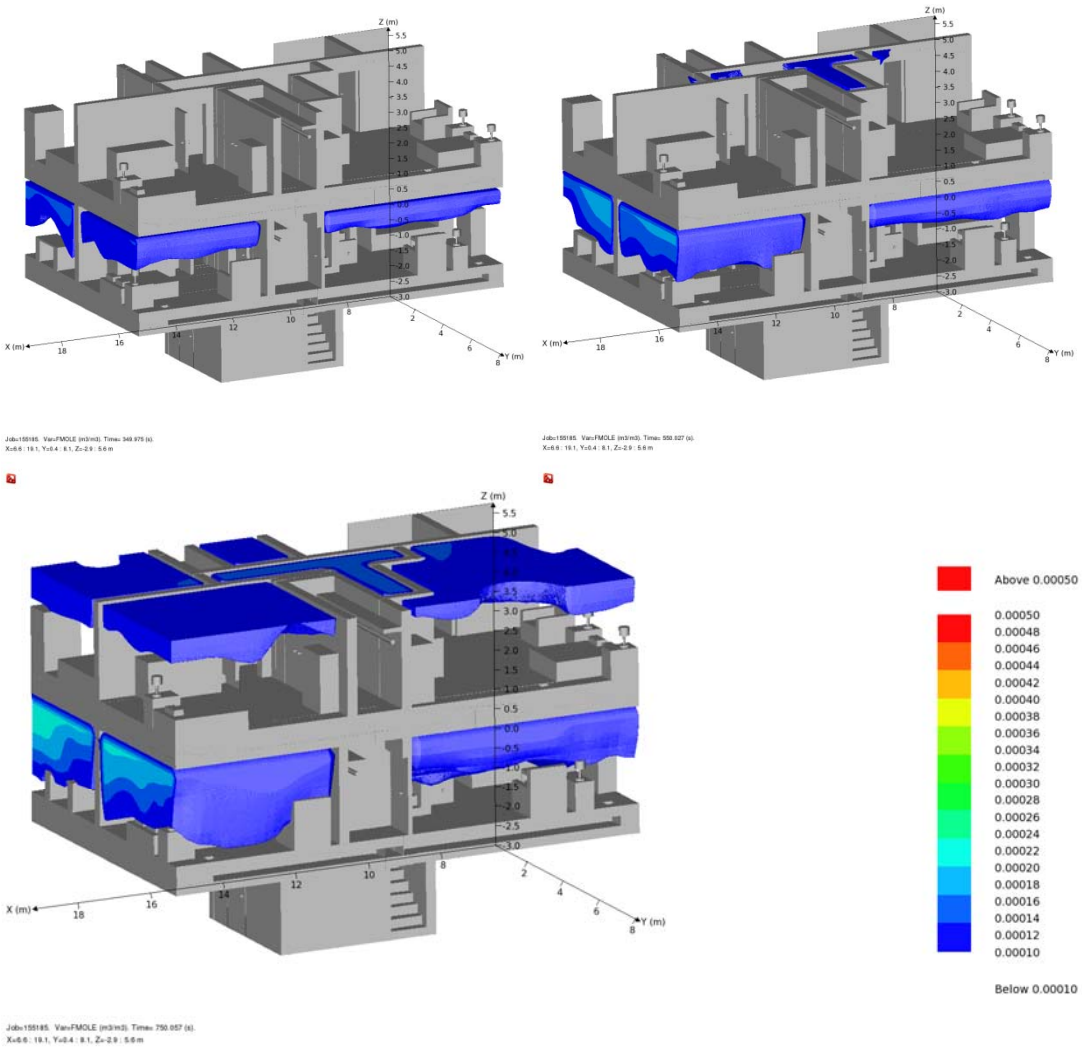


**Figure 47: General CO dispersion pattern volume plots from kitchen, at 300s (top left), 500s (top right) and 700s (bottom) after source start. 8 ACH, 10kW Source, 6e-5 kg/s CO release rate.**

For the most part, the CO filling time scale and direction remains the same. The areas of high and low concentration vary slightly, as evidence by the bottom frame in both scenarios.

To analyze this beyond a qualitative visual evaluation, the CO time profiles for several key monitor points throughout the residence are found below in Figure 48.

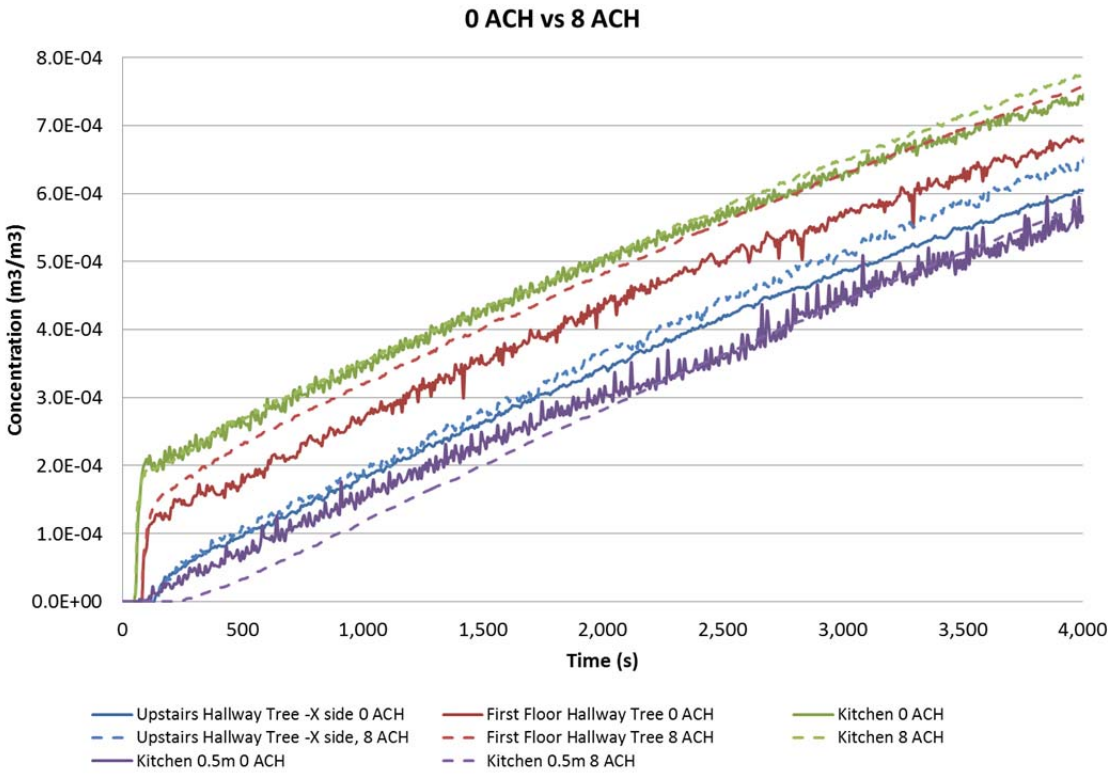


**Figure 48: Concentration at CO at various points through house, 0 ACH (solid lines) vs. 8 ACH (dotted lines).**

Figure 48 shows the CO concentrations throughout the duration of the simulations. Generally the patterns are unchanged. It is unlikely that a difference in ambient conditions will greatly affect the CO dispersion patterns, and thus it is easier for the CO detector placement to have recommended location. The 8 ACH final values are likely higher near the end of the simulation due to a more evenly mixed environment, with 0 ACH there is a time delay in dispersion and the higher concentrations will generally take longer to achieve steady state. In the 10,000s for which the CFD simulations were run, this was likely not achieved yet, however all of the detectors which were in position to trigger an alarm had done so, hence the simulations were stopped.

#### 4.6.1.1. General Conclusions from Kitchen Fire Source

With this type of CO dispersion, the requirements set forth by NFPA 720 are likely adequate. With three detectors to place, the results recommended from the results of this study would be to place a detector in the kitchen, in the common area near the kitchen on the first floor and one at the top of the stairs on the second floor. Since the main path for CO migration from the kitchen to the second floor was the stairwell, it would be this author's recommendation to dictate CO detector placement relative to the stairwell rather than "centrally located". If this geometry had been modified such that the stairwell was off center, located near one end of the house, CO would have been allowed to migrate past several bedrooms before encountering a likely detector placement. By attaching a position requirement to the stairwell, CO is more likely to be observed in higher concentrations in the migration path, rather than centrally located on the upper floor.

### 4.6.2. Basement Fire Source

The basement CO fire source provided unique challenges. Since the CO was released in a semi confined room containing the furnace and water heating equipment, there were two main paths for the CO to travel. The first, under 0 ACH conditions, was able migrate through the unused HVAC system directly to the second floor since there was no flow check valve or pressure gradient to stop "backwards" flow. As the concentration fills the upper floors the CO begins to fill from the top down penetrating all open areas through the open doors. The sequence of images in Figure 49 and Figure 50 illustrate the migration. While this phenomenon is likely an artifact

of the manner in which the geometry and HVAC system was designed in the model, it is a potentially realistic scenario as the HVAC return pathway will likely be the shortest. Within an enclosed room when the HVAC system is not operational CO could disperse in this manner.

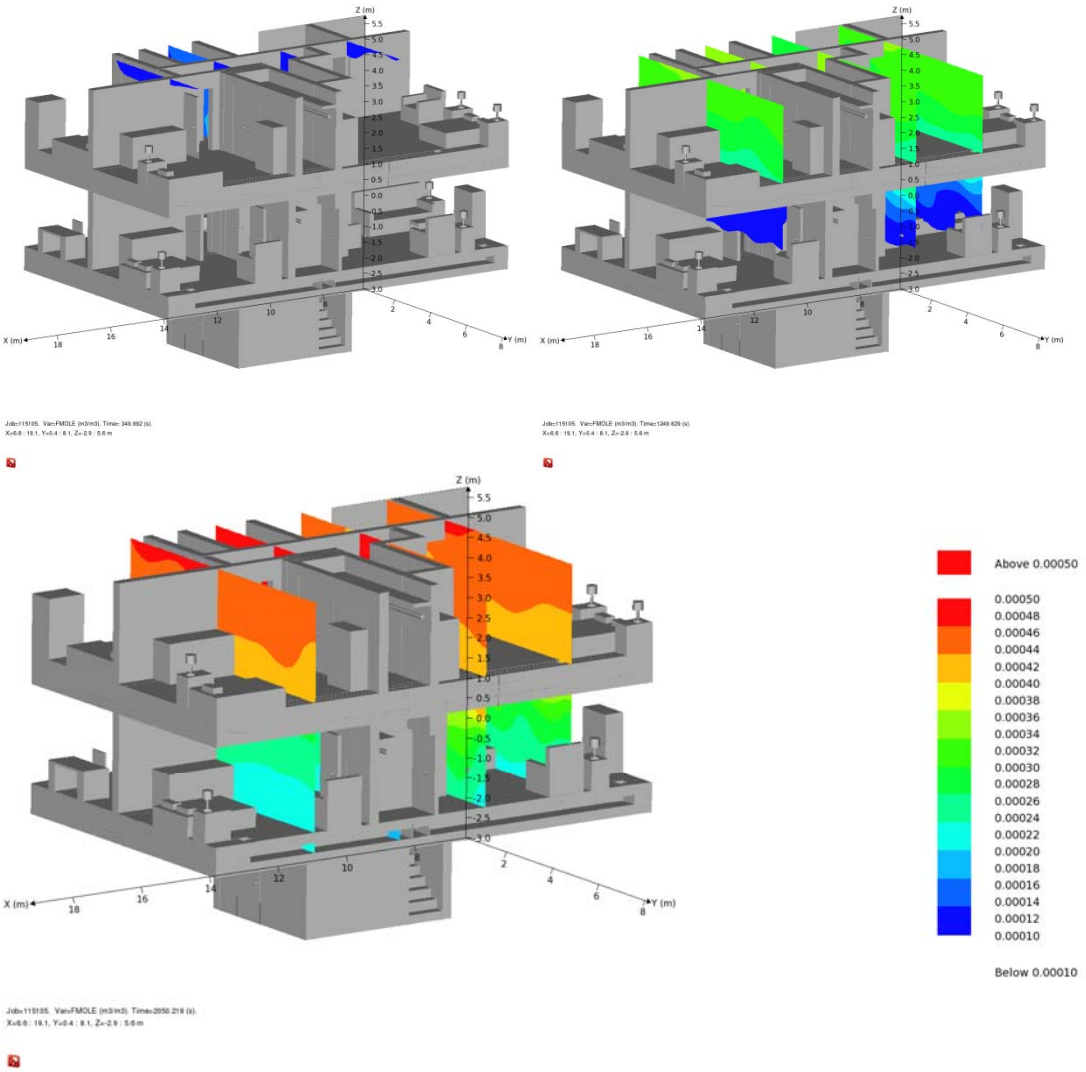


**Figure 49: General CO dispersion pattern 3d cut plane plots from basement, at 300s (top left), 1200s (top right) and 2000s (bottom) after source start. 0 ACH, 10kW Source, 6e-5 kg/s CO release rate.**

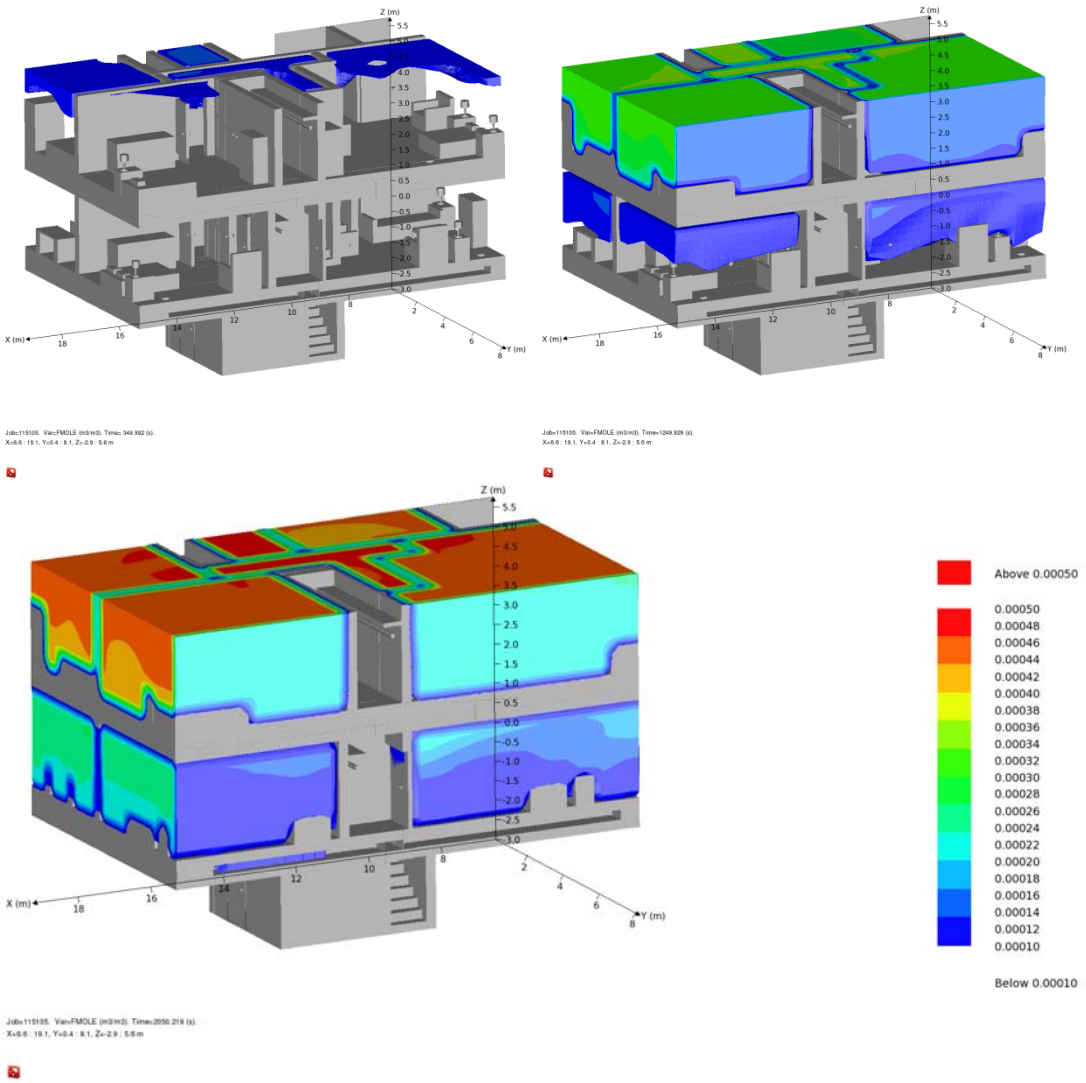


**Figure 50: General CO dispersion pattern volume plots from basement, at 300s (top left), 1200s (top right) and 2000s (bottom) after source start. 0 ACH, 10kW Source, 6e-5 kg/s CO release rate.**

The second pathway, under the 5 and 8 ACH conditions, was to infiltrate the HVAC system and disperse with the conditioned air. The sequence of images in Figure 51 and Figure 52 illustrate this phenomenon.

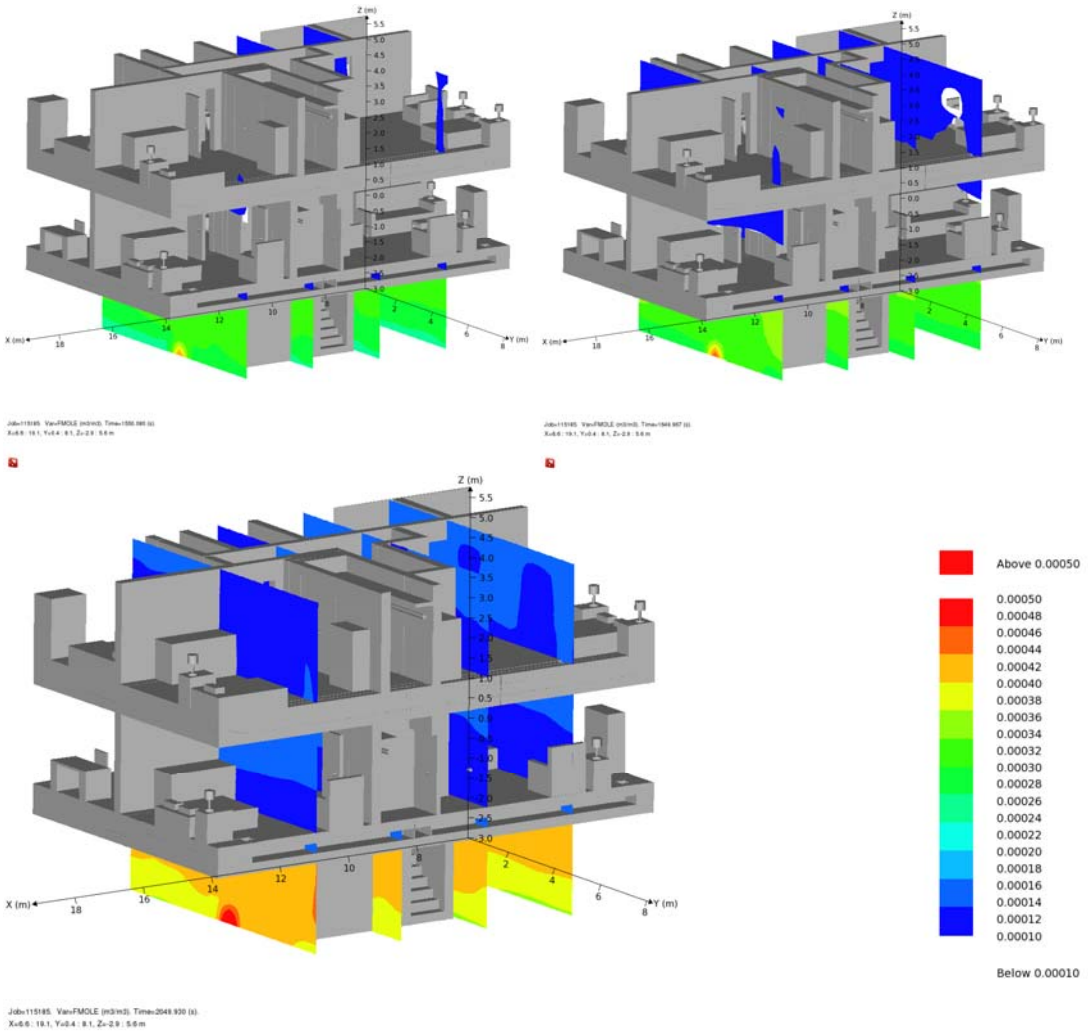


**Figure 51: General CO dispersion pattern 3d cut plane plots from basement, at 1500s (top left), 1600s (top right) and 2000s (bottom) after source start. 8 ACH, 10kW Source, 6e-5 kg/s CO release rate.**

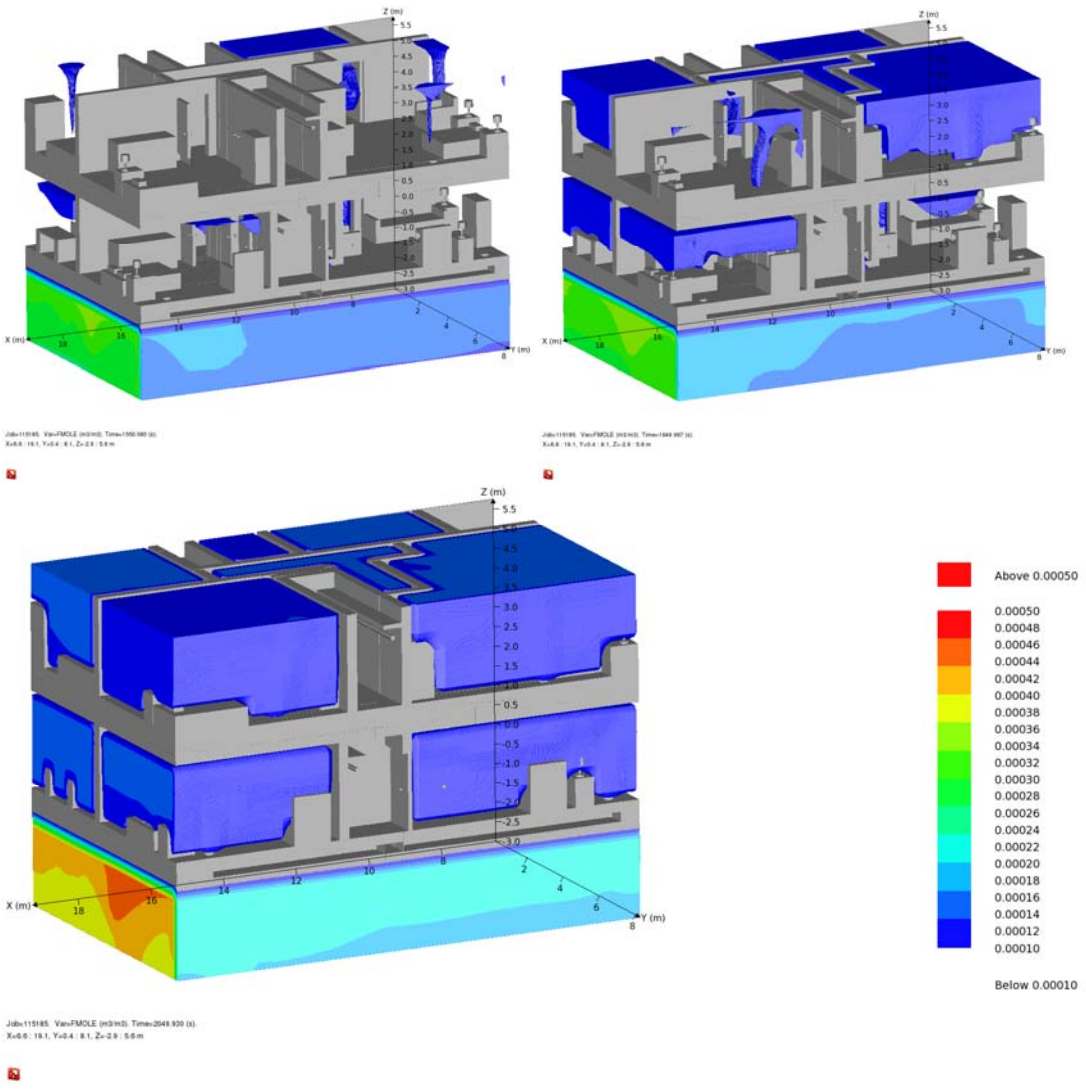


**Figure 52: General CO dispersion pattern volume plots from basement, at 1500s (top left), 1600s (top right) and 2000s (bottom) after source start. 8 ACH, 10kW Source, 6e-5 kg/s CO release rate.**

Since there are now two distinct pathways, which do have not have much overlap there was much more variation in the results and CO concentration time profiles. As such there is no easy all-encompassing recommendation that can be formed as with the releases from the kitchen area.

If the first ten detectors to alarm for a case with 0 ACH and with 5 ACH are analyzed for the closed door geometry there is an observable difference. Table 16 displays the first ten alarm locations for releases in the basement under the specified conditions.

**Table 16: First ten detector placement locations for 10kW, 6e-5 kg/s, closed door geometry from the basement.**

| 0 ACH | | 5 ACH | |
|---|---|---|---|
| **Rank** | **Description** | **Rank** | **Description** |
| 1 | Heat Appliances Room 2.2m | 1 | Heat Appliances Room 2.2m |
| 2 | Heat Appliances Room 1.85m | 2 | Heat Appliances Room 1.85m |
| 3 | Return Outlet Second Floor | 3 | Outlet of Heating Appliance 2.2m Room |
| 4 (tie) | Upstairs Hallway Tree -X side 2.2m | 4 | Outlet of Heating Appliance Room 1.85m |
| 4 (tie) | Upstairs Hallway Tree -X side 1.85m | 5 (tie) | Outlet of Heating Appliance Room 1.1m |
| 4 (tie) | Upstairs Hallway Tree +X Side 2.2m | 5 (tie) | Basement to floor 1 stairs |
| 4 (tie) | Upstairs Hallway Tree +X Side 1.85m | 7 | Outlet of Heating Appliance Room 0.35m |
| 4 (tie) | Bathroom 2 2.2m | 8 | Vent Outlet Bathroom 3 |
| 4 (tie) | Bathroom 2 1.85m | 9 | 2nd floor duct |
| 4 (tie) | Bathroom 2 1.15m | 10 | Vent Outlet Study |

This table was merely meant to show the very different style of dispersion that can result from the presence of the HVAC system.

**Table 17: First ten detector placement locations for 10kW, 6e-5 kg/s, closed door geometry from the basement.**

| 0 ACH | | 5 ACH | |
|---|---|---|---|
| **Activ. (s)** | **Description** | **Activ. (s)** | **Description** |
| 69 | Heat Appliances Room 2.2m | 57 | Heat Appliances Room 2.2m |
| 77 | Heat Appliances Room 1.85m | 67 | Heat Appliances Room 1.85m |
| 90 | Return Outlet Second Floor | 385 | Outlet of Heating Appl. Room 2.2m |
| 148 | Upstairs Hallway Tree -X side 2.2m | 395 | Outlet of Heating Appl. Room 1.85m |
| 148 | Upstairs Hallway Tree -X side 1.85m | 437 | Outlet of Heating Appl. Room 1.1m |
| 148 | Upstairs Hallway Tree +X Side 2.2m | 437 | Basement to floor 1 stairs |
| 148 | Upstairs Hallway Tree +X Side 1.85m | 530 | Outlet of Heating Appl. Room 0.35m |
| 148 | Bathroom 2 2.2m | 619 | Vent Outlet Bathroom 3 |
| 148 | Bathroom 2 1.85m | 640 | 2nd floor duct |
| 148 | Bathroom 2 1.1m | 643 | Vent Outlet Study |

Table 17 shows the time to detection rather than the rank. From this it is clear that the 0 ACH case has a much higher concentration plume than does the 5 ACH case. With the 0 ACH case, the CO migrates back up the HVAC inlet side and remains in very high concentrations triggering the alarm in a short period of time. When the HVAC system is operational, the flow path creates a high pressure area preventing CO from migrating backwards. This also dilutes the CO concentration and spreads it more evenly through the house. While it is not well mixed, it is certainly more diluted than the 0 ACH cases, which is also as expected.

Once interesting piece to take away from this table, is that while detector placement within the vent was an adequate third or fourth detector placement location, a placement over a vent outlet would yield in comparable alarm times, but without the hassle of placement within the duct work. This would allow for easier access for maintenance as well as benefit from being able to provide visual feedback.

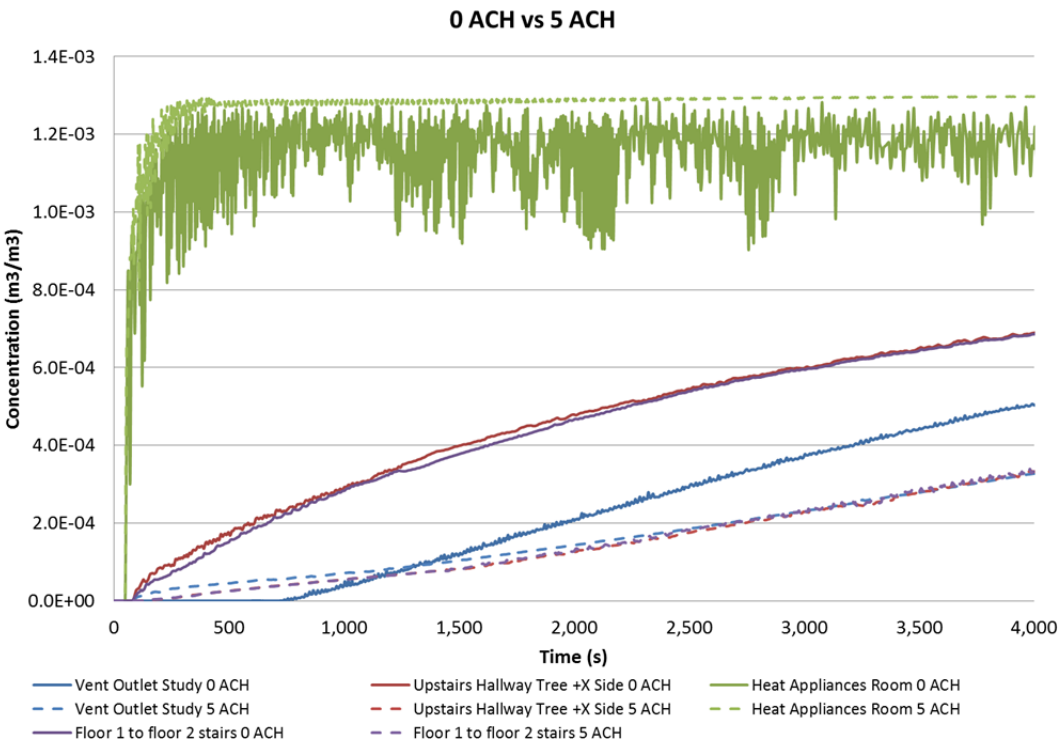


**Figure 53: Concentration at CO at various points through house, 0 ACH (solid lines) vs. 5 ACH (dotted lines).**

Figure 53 shows the time dependent CO profiles for two cases in which the CO source was located near the basement. Both of the cases are a 10kW source, with 6e-5 kg/s source and open doors. The solid lines are the 0 ACH condition and dotted lines are the 5 ACH condition. The concentration in the source room is the highest the fastest. With the 5 ACH ventilation condition, the other three points are nearly on top of each other, leading one to believe there is a lower dependency upon detector placement when the system is active, however there is still room to optimize detector placement to allow for early detection in all scenarios.

Figure 54 through Figure 56 present the time to detection data for some select cases of interest. The data in each of these scenarios is for the monitor points located near

the ceiling (except for the vent and stairwell locations). The scenario for each of the figures has been held constant so a fair assessment of detector location can be made.

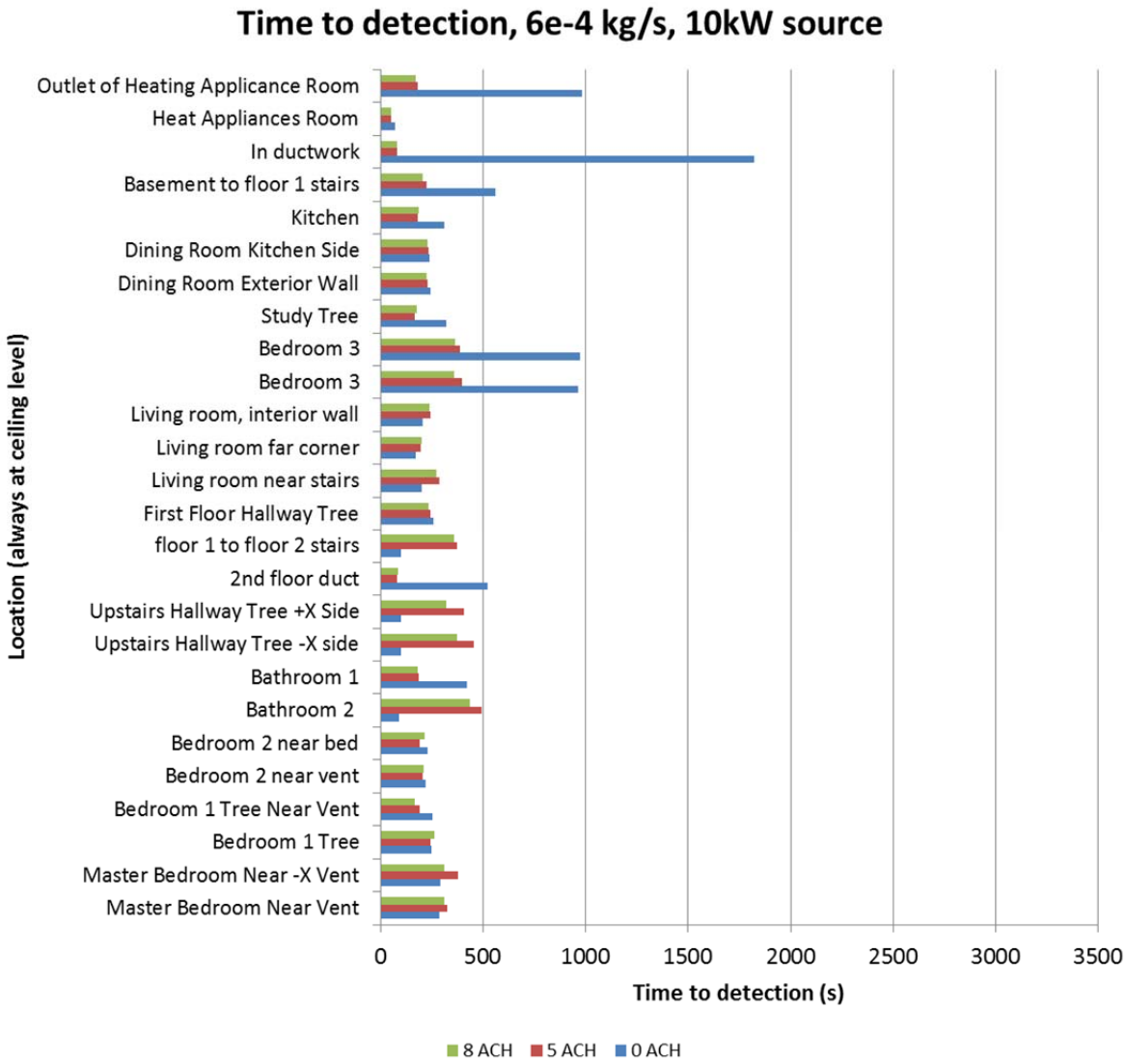


**Figure 54: Time to detection for each room placement point (near ceiling). Basement fire source, closed door geometry.**

Figure 54 shows that for this release location and source strength, there is a large dependence upon whether the HVAC system is on or off. From the data there is not a large dependence upon 5 or 8 ACH ventilation rates. The ductwork location alarmed the fastest for the case with ventilation. As CO does not generally use the ductwork as a migratory path, there was little exposure to CO with the zero ventilation

condition. There is no clear correlation between detector placement and detection time that can be made about all scenarios. There are some which are generally lower, such as in common spaces and spaces with high ventilation rates on the upper floors (such as bedroom 2).

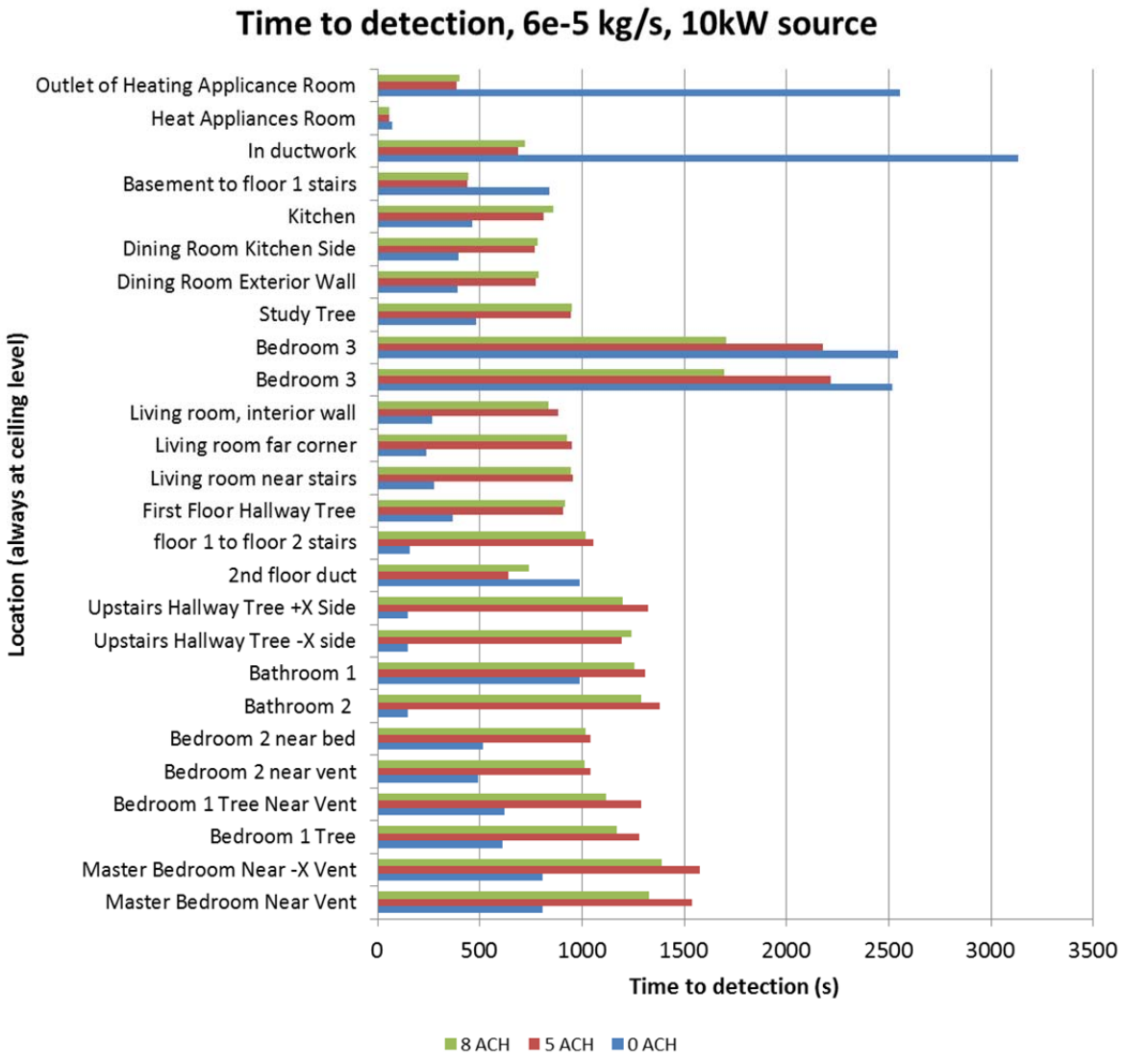


**Figure 55: Time to detection for each room placement point (near ceiling). Basement fire source, closed door geometry.**

Figure 55 shows some similar trends as Figure 54, but these are more exaggerated at the lower concentration releases. In fact a lower concentration release resulted in up to approximately 5 times longer detection delays.

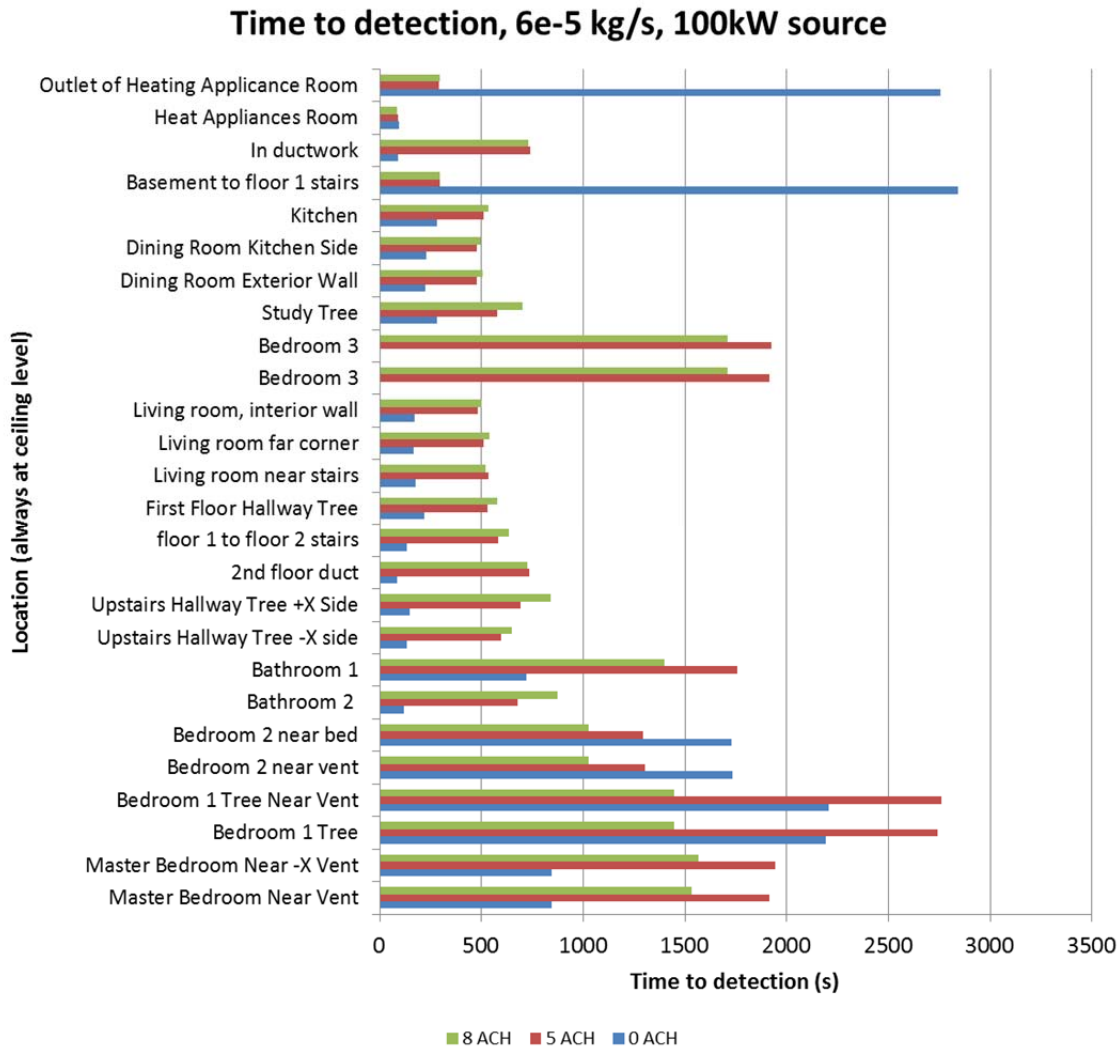


**Figure 56: Time to detection for each room placement point (near ceiling). Basement fire source, closed door geometry.**

Figure 56 illustrates some large differences in detection time between ventilated and non-ventilated conditions. Some of the lower detector placements failed to alarm (Bedroom 3) which alarmed in the lower heat release rate source.

In order to further analyze the mixing, a look at the temperature profiles within the living room area was conducted. Figure 57 and Figure 58 are 2d cut planes along the X axis of the geometry. These show that as expected, the 0 ACH case, has remained buoyant and is still well stratified throughout the house. With the 8 ACH case, there is some mixing, and again it can be seen that the most buildup of the CO is within the basement area. In this case there is less stratification across the levels of the house.

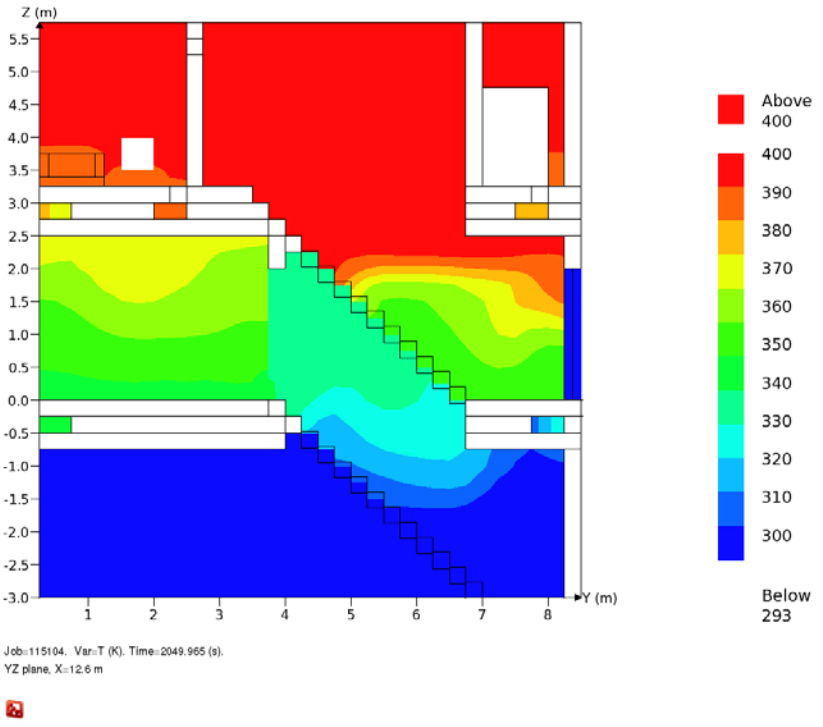


**Figure 57: 2d cut plane of temperature profile, 10kW source, 0 ACH, 6.6e-4 kg/s, 2000s after fire start.**

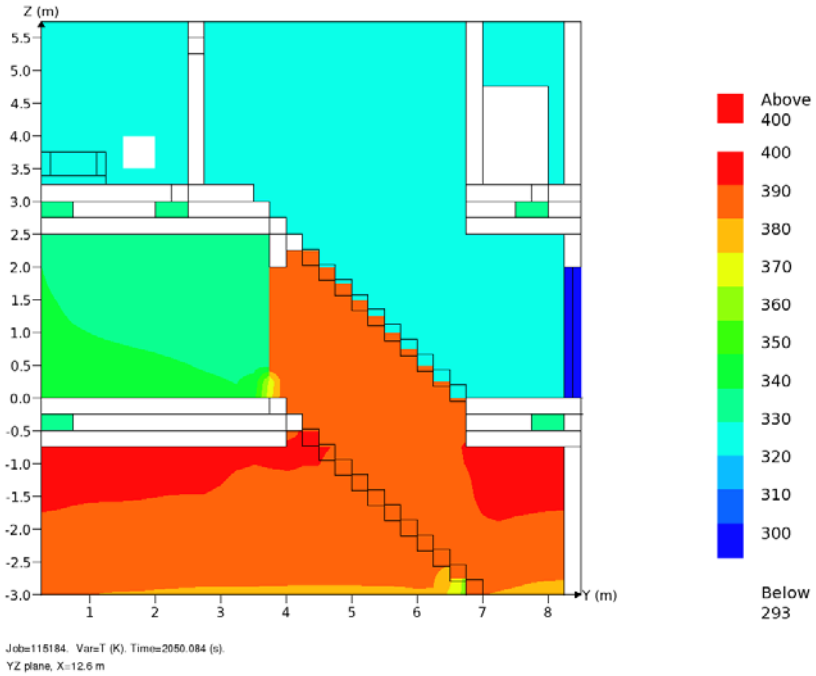


**Figure 58: 2d cut plane of temperature profile, 10kW source, 8 ACH, 6.6e-4 kg/s, 2000s after fire start.**

In order to more adequately assess the difference in temperature in the living room area, the range of plotted values was changed to allow for more detail seen in Figure 59. Comparatively, there is much more mixing and less stratification in the 8 ACH case.

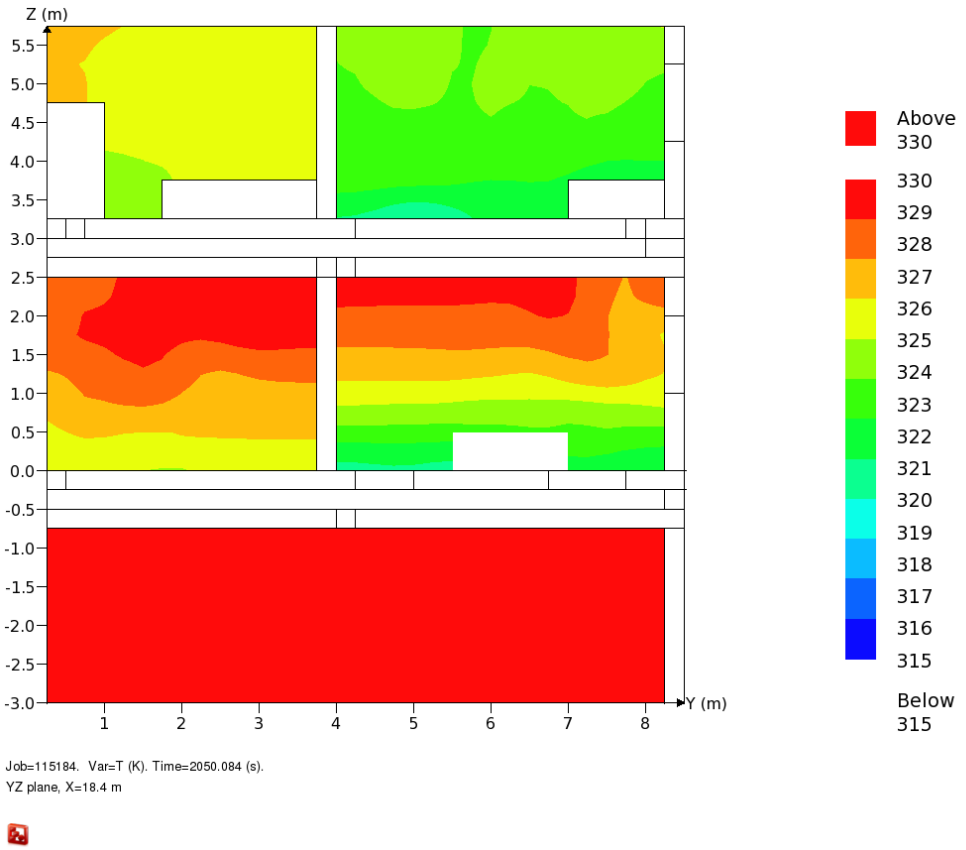


**Figure 59: 2d cut plane of temperature profile, 10kW source, 8 ACH, 6.6e-4 kg/s, 2800s after fire start.**

Figure 60 shows the temperature profiles recorded at the detector tree placed near the stairs in the living room. The solid lines are for the 0 ACH case, and the dotted lines are for the 8 ACH. From this it is observed that the temperature is generally hotter when there is minimal mixing. The stratification is also larger as the difference between the top (2.2m) and bottom (0.35m) detection points is almost consistently 20-25 °C. With the HVAC enabled, the temperature gradient drops to near 10 °C and

the temperature is generally lower than the 0 ACH case except for the initial development phase (time less than 1000s).

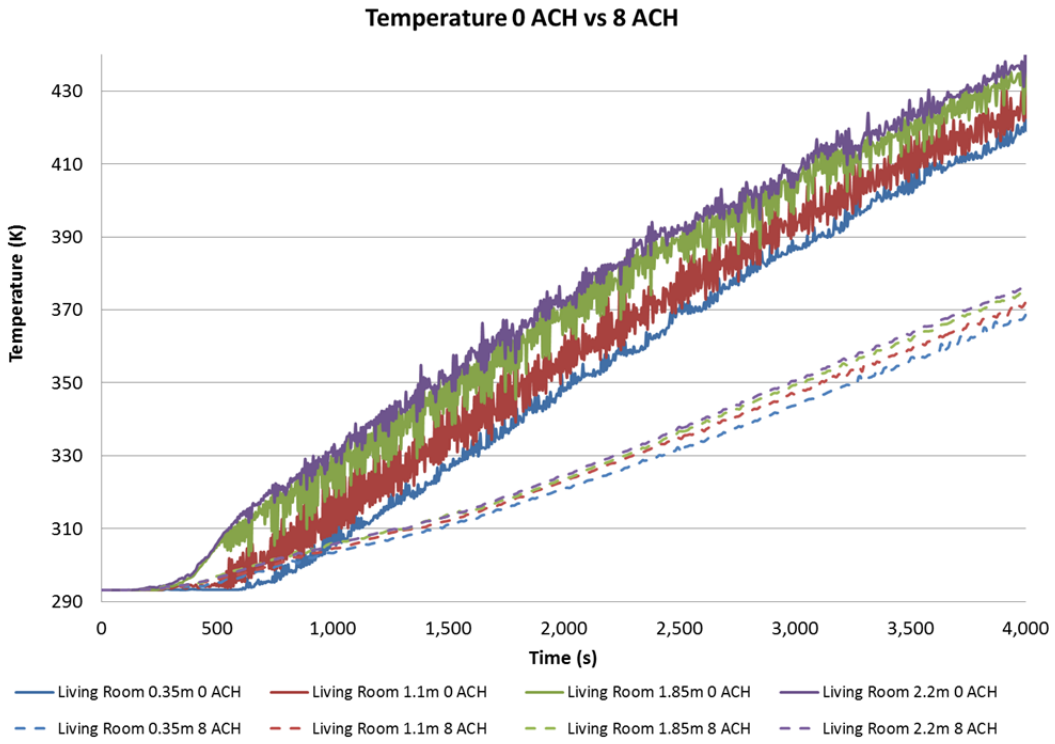


**Figure 60: Temperature profiles, at detector tree near the stairs in the living room.**

While these plots are useful to see relative temperature and temperature gradients, they do not accurately capture heat transfer between the fluid and the surrounding solids. Since FLACS was designed to predict explosion overpressure and model large scale outdoor gaseous releases, transient heat transfer is not included in the FLACS solver as it is generally insignificant over short time scales. For these simulations, the hot gases are allowed to interact with each other, but there was no heat transfer between the surrounding environment and the products of combustion. While this omission would have a large impact over long time scales and steady state temperature profiles, many of the alarm times presented here are on the order of a few hundred seconds and the neglected heat transfer will be minor.

#### 4.6.2.1. General Conclusions from the Basement Releases

These scenarios had much more variation than the ones previously. Since the release was generally dispersed through the HVAC ductwork, it made a large difference whether that was operational or not. In such cases in which the system was not operation, a buoyant plume was the result, however rather than infiltrate the basement and migrate up from there, it was able to fill the HVAC and followed the shortest path to the highest part of the structure. That path was the return air inlet of the HVAC system. This led to high concentrations of CO in the upper level of the structure first. When the HVAC system was operational, the prevailing path became the outlets of the ductwork. This would then spread CO evenly to the separate rooms of the house, while losing some of the buoyancy driven flow characteristics that were present in the case without an active ventilation system.

With respect to having the doors open or closed, this was a subject of interest. When the doors were closed in the no ventilation condition, a subject would be relatively protected. This was not the case when the ventilation system was on. In the 5 or 8 ACH conditions, the CO concentrations would be equally as high if not higher in the bedrooms and would result in CO exposure much sooner. In these cases the CO tended to be cooler which would result in less stratification.

# 5. Conclusions

This CFD study has analyzed CO dispersion from a representative "waste-basket" size fire source. A total of 128 simulation have been simulated using the CFD software FLACS, 80 simulations from a representative ventilated box and 48 in a realistic house geometry complete with a HVAC system. Since CO detector functionality is not inherently programmed into FLACS a MATLAB tool was developed to mimic detector functionality based upon the CFK equation. While the time to detection script was based on a 10% COHb exposure level for a healthy person, this may not represent the typical time to alarm as a commercially available detector would display.

From this study there are several things that can be concluded. CO migration is a worthwhile topic to investigate. Current literature assumes that CO dispersion is generally well mixed, while there may be CO present in all locations concentrations may vary and thus times to detection may vary. There are several ways to handle this problem, however if the well-mixed assumption is not valid, a full CFD analysis can be performed.

From the ventilated box, it was observed that a HVAC system can affect detector time and that horizontal stratification is possible. From the results it was evident that CO, when released, was generally buoyant and any detectors should be placed near the ceiling level. Also with the cross flow of the HVAC system, there was a

noticeably lower concentration of CO on the side opposite the source. For the shortest detection times, an alarm should be placed as close to the source as possible.

In the realistic house, there were several general flow patterns observed. When the CO source was a kitchen appliance, the CO generally migrated in a predicted manner. The CO would buoyantly rise to the ceiling of the first floor and fill from the top down any open rooms. If the doors were closed, they were well protected from any CO source. There was generally little variation among the different source and HVAC conditions making detector placement recommendations relatively easy. Since CO detectors have been shown to have a high failure rate, three locations recommendations are formed. For this style of CO release, there should be a detector placed in the kitchen (source room), one protecting any sleeping or ambient rooms on the first floor and one at the top of the stairwell leading to the second floor.

For a release in the basement, things become more complicated. Since the CO was allowed to infiltrate the HVAC system, CO was either dispersed through the system duct work or migrated out into the open basement area. When the HVAC system was not in operation, the dominate flow path was backwards through the furnace system inlet up directly to the second floor. When the HVAC system was operating, the CO was able to make it into bedrooms previously assumed to be safe. For these cases, the first alarm was again in the source room (appliance closet in basement). After that, the second fastest time to alarm was either on the second floor near the HVAC system

inlet (0 ACH condition) or at the top of the stairs from the basement to the first floor (5 and 8 ACH conditions). The third detector placement location then varied to detectors in open areas (0 ACH) or the dominant (or shortest) HVAC system flow path. The final recommendation for this style of housing would be one detector should be placed in the combustion appliance room, a second should be placed near the top of the stairwell from the basement to the first floor, and the third should be placed at the ceiling above the dominant flow path or shortest length HVAC supply or return duct.

# Appendices

## *Appendix A – MATLAB CO Detector Code*

```
% Written by:   Derek Engel
% Program to get the time to alarm for monitor points from FLACS output data
%
% Version 1.0
%
% Rev   Date        Text
% 1.0   03-10-2012  First version
% 2.0   03-25-2012  Second version with input from. Dr. Trouve
%
clear
clc
format longeng

CO_time_data = importdata('***FLACS FILE NAME HERE ***', ' '); %This imports the FLACS output
file
% NB: time is in units of minutes; CO is in units of ppm

array_size    = size(CO_time_data);  %Establishes a matrix dimensions for reference
array_columns = array_size(1,2);     %Number of columns in file as a reference
array_rows    = array_size(1,1);     %Number of rows in file as a reference

CO_time_data=CO_time_data*10^6;
CO_time_data(:,1)=CO_time_data(:,1)/10^6;

dCOdt      = zeros(array_rows,array_columns-1);
dCOdt(:,1) = CO_time_data(:,1); % time
for column_count = 2:array_columns
    for row_count = 2:array_rows
        dCOdt(row_count,column_count) = (CO_time_data(row_count,column_count) - CO_time_data(
        row_count-1,column_count)) ...
                                        /(CO_time_data(row_count,1)-CO_time_data(row_count-1,1));
    end
    dCOdt(1,column_count) = dCOdt(2,column_count);
end

COHB_0 = 0;  %Initial COHB concentration
alpha = 2398*0.0404; %Alpha shortcut for the formula to follow, this is from the UL 2034 standard

dfdt      = zeros(array_rows,array_columns-1);
dfdt(:,1) = CO_time_data(:,1); % time
for column_count = 2:array_columns
    for row_count = 2:array_rows
        time = CO_time_data(row_count,1);
        dfdt(row_count,column_count) = (-1*COHB_0*exp(-time/alpha)/(alpha)) ...
                                       +(218*(1-exp(-time/alpha))*dCOdt(row_count,column_count)/
                                       1316) ...
                                       +((0.0003 + CO_time_data(row_count,column_count)/1316)*(
                                       218*exp(-time/alpha)/alpha));
    end
    dfdt(1,column_count) = dfdt(2,column_count);
end

COHB_time_data = zeros(array_rows,array_columns);
COHB_time_data(:,1) = CO_time_data(:,1); %Copies the time data from the FLACS importfile to the
```

```
new COHB matrix

time_activation = zeros(array_columns-1,1);
CO_activation   = zeros(array_columns-1,1);

for column_count = 2:array_columns %This starts on column two, the first point data
    iflag = 0;
    for row_count = 2:array_rows %an interative approach for each row
        int = 0;
        CO_now = CO_time_data(row_count, column_count);

        for n = 2:row_count-1
            int = int + 0.5*(dfdt(n,column_count)+dfdt(n-1,column_count))*(CO_time_data(n,1)-
            CO_time_data(n-1,1));
        end
        COHB_time_data(row_count,column_count) = int;

        if ((COHB_time_data(row_count,column_count) > 10) & (iflag==0))
            fprintf(' detector activation at COHb = %g \n',COHB_time_data(row_count,column_count
            ));
            time_activation(column_count-1) = CO_time_data(row_count,1);
            CO_activation(column_count-1)   = CO_time_data(row_count,column_count);
            iflag = 1;
        end;

    end
    if(iflag==0)
        fprintf(' *** no detector activation, column_count = %g \n',column_count)
    end
end

concen_arra = CO_time_data(2,2:array_columns)';
time_activation
```

The N/A values for monitor points 10 and 20 are placeholders, as those numbered points did not exist

**Table 18: Time to activation various source rates, No ventilation, 10 kW source term (seconds).**

| Vent | Source Rate 6e-7 | | Source Rate 6e-6 | | Source Rate 6e-5 | | Source Rate 6e-4 | |
|---|---|---|---|---|---|---|---|---|
| | Low | High | Low | High | Low | High | Low | High |
| MP | Activation (s) | | | | | | | |
| 1 | 0 | 0 | 69 | 64 | 51 | 51 | 51 | 51 |
| 2 | 0 | 0 | 418 | 534 | 126 | 139 | 132 | 192 |
| 3 | 0 | 0 | 385 | 434 | 125 | 138 | 134 | 187 |
| 4 | 0 | 0 | 414 | 590 | 130 | 165 | 134 | 177 |
| 5 | 0 | 0 | 435 | 570 | 127 | 170 | 130 | 192 |
| 6 | 0 | 0 | 410 | 508 | 125 | 148 | 133 | 183 |
| 7 | 0 | 0 | 397 | 543 | 131 | 158 | 135 | 174 |
| 8 | 0 | 0 | 427 | 571 | 131 | 162 | 134 | 177 |
| 9 | 0 | 0 | 419 | 536 | 134 | 159 | 137 | 182 |
| 10 | n/a | n/a | n/a | n/a | n/a | n/a | n/a | n/a |
| 11 | 0 | 0 | 237 | 235 | 57 | 57 | 53 | 53 |
| 12 | 0 | 0 | 353 | 483 | 100 | 106 | 66 | 67 |
| 13 | 0 | 0 | 328 | 351 | 95 | 108 | 60 | 75 |
| 14 | 0 | 0 | 335 | 437 | 91 | 110 | 66 | 76 |
| 15 | 0 | 0 | 365 | 440 | 101 | 117 | 73 | 81 |
| 16 | 0 | 0 | 328 | 347 | 95 | 113 | 75 | 88 |
| 17 | 0 | 0 | 294 | 422 | 100 | 121 | 60 | 60 |
| 18 | 0 | 0 | 336 | 420 | 99 | 110 | 75 | 80 |
| 19 | 0 | 0 | 317 | 432 | 107 | 108 | 61 | 61 |
| 20 | n/a | n/a | n/a | n/a | n/a | n/a | n/a | n/a |
| 21 | 0 | 0 | 176 | 219 | 58 | 58 | 55 | 55 |
| 22 | 0 | 0 | 286 | 317 | 66 | 68 | 56 | 56 |
| 23 | 0 | 0 | 288 | 321 | 67 | 70 | 57 | 57 |
| 24 | 0 | 0 | 281 | 384 | 60 | 71 | 56 | 56 |
| 25 | 0 | 0 | 279 | 381 | 73 | 76 | 56 | 56 |
| 26 | 0 | 0 | 286 | 400 | 71 | 77 | 58 | 58 |
| 27 | 0 | 0 | 251 | 393 | 71 | 71 | 57 | 57 |
| 28 | 0 | 0 | 299 | 368 | 73 | 73 | 58 | 58 |
| 29 | 0 | 0 | 302 | 388 | 73 | 77 | 59 | 59 |

**Table 19: Time to activation various generation rates, No ventilation, 100 kW source term.**

| | Source Rate 6e-7 | | Source Rate 6e-6 | | Source Rate 6e-5 | | Source Rate 6e-4 | |
|---|---|---|---|---|---|---|---|---|
| Vent | Low | High | Low | High | Low | High | Low | High |
| MP | Activation (s) | | | | | | | |
| 1 | 0 | 0 | 0 | 0 | 66 | 66 | 51 | 51 |
| 2 | 0 | 0 | 0 | 0 | 101 | 114 | 63 | 91 |
| 3 | 0 | 0 | 0 | 0 | 102 | 109 | 62 | 91 |
| 4 | 0 | 0 | 0 | 0 | 101 | 113 | 67 | 88 |
| 5 | 0 | 0 | 0 | 0 | 101 | 113 | 68 | 89 |
| 6 | 0 | 0 | 0 | 0 | 101 | 109 | 57 | 57 |
| 7 | 0 | 0 | 0 | 0 | 97 | 111 | 66 | 78 |
| 8 | 0 | 0 | 0 | 0 | 98 | 113 | 58 | 85 |
| 9 | 0 | 0 | 0 | 0 | 100 | 108 | 56 | 56 |
| 10 | n/a | n/a | n/a | n/a | n/a | n/a | n/a | n/a |
| 11 | 0 | 0 | 0 | 0 | 66 | 68 | 52 | 52 |
| 12 | 0 | 0 | 0 | 0 | 104 | 116 | 61 | 60 |
| 13 | 0 | 0 | 0 | 0 | 98 | 114 | 56 | 61 |
| 14 | 0 | 0 | 0 | 0 | 102 | 115 | 59 | 60 |
| 15 | 0 | 0 | 0 | 0 | 105 | 120 | 60 | 64 |
| 16 | 0 | 0 | 0 | 0 | 101 | 119 | 55 | 57 |
| 17 | 0 | 0 | 0 | 0 | 102 | 112 | 56 | 56 |
| 18 | 0 | 0 | 0 | 0 | 100 | 115 | 55 | 55 |
| 19 | 0 | 0 | 0 | 0 | 99 | 108 | 55 | 55 |
| 20 | n/a | n/a | n/a | n/a | n/a | n/a | n/a | n/a |
| 21 | 0 | 0 | 0 | 0 | 62 | 62 | 53 | 53 |
| 22 | 0 | 0 | 0 | 0 | 96 | 109 | 53 | 53 |
| 23 | 0 | 0 | 0 | 0 | 96 | 113 | 55 | 55 |
| 24 | 0 | 0 | 0 | 0 | 95 | 110 | 53 | 53 |
| 25 | 0 | 0 | 0 | 0 | 99 | 107 | 54 | 54 |
| 26 | 0 | 0 | 0 | 0 | 99 | 112 | 54 | 55 |
| 27 | 0 | 0 | 0 | 0 | 96 | 111 | 55 | 55 |
| 28 | 0 | 0 | 0 | 0 | 98 | 107 | 54 | 54 |
| 29 | 0 | 0 | 0 | 0 | 100 | 107 | 55 | 55 |

**Table 20: 10kW Source with 5 ACH ventilation.**

| | Source Rate 6e-7 | | | | Source Rate 6e-6 | | | | Source Rate 6e-5 | | | | Source Rate 6e-4 | | | |
|---|---|---|---|---|---|---|---|---|---|---|---|---|---|---|---|---|
| Vent | Low | Low | High | High | Low | Low | High | High | Low | Low | High | High | Low | Low | High | High |
| Air Source | Low | High | Low | High | Low | High | Low | High | Low | High | Low | High | Low | High | Low | High |
| **MP** | **Activation (s)** | | | | | | | | | | | | | | | |
| 1 | 0 | 0 | 0 | 0 | 64 | 64 | 65 | 62 | 51 | 51 | 51 | 51 | 51 | 51 | 51 | 51 |
| 2 | 0 | 0 | 0 | 0 | 453 | 426 | 1250 | 1349 | 128 | 144 | 173 | 151 | 63 | 94 | 150 | 67 |
| 3 | 0 | 0 | 0 | 0 | 381 | 422 | 669 | 941 | 118 | 135 | 164 | 150 | 63 | 96 | 132 | 67 |
| 4 | 0 | 0 | 0 | 0 | 578 | 421 | 0 | 1271 | 146 | 142 | 210 | 171 | 63 | 97 | 136 | 68 |
| 5 | 0 | 0 | 0 | 0 | 449 | 422 | 754 | 1544 | 135 | 155 | 181 | 151 | 63 | 110 | 137 | 65 |
| 6 | 0 | 0 | 0 | 0 | 418 | 417 | 643 | 1292 | 128 | 141 | 195 | 158 | 62 | 111 | 144 | 64 |
| 7 | 0 | 0 | 0 | 0 | 0 | 407 | 0 | 0 | 135 | 129 | 256 | 149 | 64 | 92 | 137 | 66 |
| 8 | 0 | 0 | 0 | 0 | 406 | 407 | 1048 | 1247 | 134 | 140 | 195 | 158 | 62 | 101 | 146 | 64 |
| 9 | 0 | 0 | 0 | 0 | 367 | 412 | 0 | 1363 | 140 | 137 | 219 | 164 | 62 | 114 | 147 | 64 |
| 10 | n/a | n/a | n/a | n/a | n/a | n/a | n/a | n/a | n/a | n/a | n/a | n/a | n/a | n/a | n/a | n/a |
| 11 | 0 | 0 | 0 | 0 | 186 | 181 | 899 | 241 | 57 | 57 | 53 | 57 | 55 | 53 | 53 | 55 |
| 12 | 0 | 0 | 0 | 0 | 301 | 333 | 697 | 815 | 105 | 100 | 111 | 118 | 58 | 66 | 67 | 58 |
| 13 | 0 | 0 | 0 | 0 | 301 | 311 | 667 | 686 | 106 | 100 | 94 | 109 | 63 | 59 | 77 | 62 |
| 14 | 0 | 0 | 0 | 0 | 297 | 317 | 719 | 829 | 100 | 107 | 107 | 102 | 58 | 67 | 67 | 58 |
| 15 | 0 | 0 | 0 | 0 | 292 | 323 | 1185 | 937 | 111 | 108 | 124 | 119 | 62 | 72 | 71 | 64 |
| 16 | 0 | 0 | 0 | 0 | 267 | 312 | 626 | 635 | 106 | 86 | 121 | 115 | 63 | 60 | 78 | 63 |
| 17 | 0 | 0 | 0 | 0 | 262 | 365 | 545 | 1146 | 100 | 95 | 106 | 99 | 62 | 73 | 59 | 62 |
| 18 | 0 | 0 | 0 | 0 | 261 | 336 | 688 | 810 | 90 | 106 | 111 | 112 | 62 | 60 | 60 | 63 |
| 19 | 0 | 0 | 0 | 0 | 261 | 280 | 488 | 668 | 101 | 81 | 100 | 114 | 62 | 60 | 60 | 63 |
| 20 | n/a | n/a | n/a | n/a | n/a | n/a | n/a | n/a | n/a | n/a | n/a | n/a | n/a | n/a | n/a | n/a |
| 21 | 0 | 0 | 0 | 0 | 174 | 171 | 210 | 231 | 58 | 58 | 55 | 58 | 57 | 54 | 54 | 57 |
| 22 | 0 | 0 | 0 | 0 | 227 | 265 | 551 | 509 | 75 | 71 | 68 | 70 | 58 | 55 | 55 | 58 |
| 23 | 0 | 0 | 0 | 0 | 228 | 230 | 459 | 508 | 72 | 72 | 63 | 73 | 60 | 57 | 57 | 60 |
| 24 | 0 | 0 | 0 | 0 | 253 | 246 | 279 | 366 | 68 | 60 | 66 | 60 | 58 | 55 | 55 | 58 |
| 25 | 0 | 0 | 0 | 0 | 258 | 259 | 523 | 615 | 83 | 80 | 66 | 80 | 59 | 56 | 56 | 59 |
| 26 | 0 | 0 | 0 | 0 | 249 | 263 | 617 | 557 | 76 | 83 | 64 | 78 | 62 | 57 | 57 | 61 |
| 27 | 0 | 0 | 0 | 0 | 254 | 0 | 401 | 0 | 68 | 83 | 62 | 107 | 60 | 58 | 57 | 62 |
| 28 | 0 | 0 | 0 | 0 | 258 | 253 | 449 | 612 | 85 | 77 | 62 | 82 | 62 | 57 | 57 | 62 |
| 29 | 0 | 0 | 0 | 0 | 257 | 258 | 620 | 617 | 85 | 81 | 64 | 81 | 62 | 59 | 59 | 62 |

**Table 21: 10kW Source with 10 ACH ventilation.**

| | Source Rate 6e-7 | | | | Source Rate 6e-6 | | | | Source Rate 6e-5 | | | | Source Rate 6e-4 | | | |
|---|---|---|---|---|---|---|---|---|---|---|---|---|---|---|---|---|
| Vent | Low | Low | High | High | Low | Low | High | High | Low | Low | High | High | Low | Low | High | High |
| Air Source | Low | High | Low | High | Low | High | Low | High | Low | High | Low | High | Low | High | Low | High |
| **MP** | **Activation (s)** | | | | | | | | | | | | | | | |
| 1 | 0 | 0 | 0 | 0 | 62 | 64 | 63 | 63 | 51 | 51 | 51 | 51 | 51 | 51 | 51 | 51 |
| 2 | 0 | 0 | 0 | 0 | 483 | 0 | 1313 | 0 | 140 | 130 | 180 | 185 | 66 | 61 | 63 | 63 |
| 3 | 0 | 0 | 0 | 0 | 494 | 0 | 0 | 0 | 130 | 129 | 167 | 186 | 66 | 62 | 62 | 67 |
| 4 | 0 | 0 | 0 | 0 | 766 | 882 | 0 | 0 | 153 | 146 | 161 | 171 | 62 | 64 | 67 | 63 |
| 5 | 0 | 0 | 0 | 0 | 577 | 0 | 0 | 0 | 127 | 142 | 179 | 187 | 63 | 62 | 63 | 62 |
| 6 | 0 | 0 | 0 | 0 | 508 | 0 | 0 | 0 | 138 | 134 | 177 | 188 | 65 | 62 | 63 | 62 |
| 7 | 0 | 0 | 0 | 0 | 0 | 0 | 0 | 0 | 210 | 126 | 298 | 168 | 120 | 62 | 157 | 62 |
| 8 | 0 | 0 | 0 | 0 | 391 | 1044 | 0 | 0 | 138 | 138 | 199 | 180 | 66 | 62 | 62 | 62 |
| 9 | 0 | 0 | 0 | 0 | 594 | 0 | 0 | 0 | 139 | 146 | 193 | 184 | 66 | 62 | 64 | 61 |
| 10 | n/a | n/a | n/a | n/a | n/a | n/a | n/a | n/a | n/a | n/a | n/a | n/a | n/a | n/a | n/a | n/a |
| 11 | 0 | 0 | 0 | 0 | 220 | 225 | 924 | 247 | 54 | 54 | 54 | 54 | 54 | 54 | 54 | 54 |
| 12 | 0 | 0 | 0 | 0 | 437 | 571 | 0 | 0 | 98 | 106 | 97 | 126 | 56 | 56 | 56 | 56 |
| 13 | 0 | 0 | 0 | 0 | 378 | 394 | 0 | 0 | 97 | 110 | 119 | 115 | 60 | 60 | 60 | 61 |
| 14 | 0 | 0 | 0 | 0 | 387 | 620 | 0 | 0 | 101 | 102 | 102 | 118 | 56 | 56 | 56 | 56 |
| 15 | 0 | 0 | 0 | 0 | 591 | 619 | 0 | 0 | 103 | 107 | 119 | 119 | 62 | 63 | 66 | 61 |
| 16 | 0 | 0 | 0 | 0 | 496 | 437 | 0 | 0 | 107 | 84 | 108 | 125 | 61 | 61 | 61 | 60 |
| 17 | 0 | 0 | 0 | 0 | 350 | 666 | 0 | 0 | 102 | 102 | 113 | 101 | 60 | 62 | 60 | 61 |
| 18 | 0 | 0 | 0 | 0 | 381 | 591 | 0 | 0 | 107 | 104 | 113 | 132 | 62 | 61 | 61 | 61 |
| 19 | 0 | 0 | 0 | 0 | 381 | 448 | 0 | 0 | 103 | 72 | 113 | 116 | 63 | 61 | 62 | 61 |
| 20 | n/a | n/a | n/a | n/a | n/a | n/a | n/a | n/a | n/a | n/a | n/a | n/a | n/a | n/a | n/a | n/a |
| 21 | 0 | 0 | 0 | 0 | 177 | 178 | 262 | 197 | 56 | 56 | 56 | 56 | 55 | 55 | 55 | 55 |
| 22 | 0 | 0 | 0 | 0 | 330 | 280 | 619 | 1278 | 58 | 58 | 58 | 58 | 56 | 56 | 56 | 56 |
| 23 | 0 | 0 | 0 | 0 | 397 | 278 | 0 | 1466 | 67 | 82 | 65 | 74 | 59 | 59 | 58 | 58 |
| 24 | 0 | 0 | 0 | 0 | 297 | 294 | 488 | 617 | 58 | 58 | 58 | 58 | 56 | 56 | 56 | 56 |
| 25 | 0 | 0 | 0 | 0 | 354 | 388 | 743 | 1987 | 75 | 76 | 70 | 71 | 57 | 57 | 57 | 57 |
| 26 | 0 | 0 | 0 | 0 | 376 | 379 | 894 | 0 | 71 | 78 | 67 | 71 | 60 | 60 | 60 | 59 |
| 27 | 0 | 0 | 0 | 0 | 310 | 0 | 375 | 0 | 74 | 86 | 65 | 86 | 59 | 60 | 59 | 69 |
| 28 | 0 | 0 | 0 | 0 | 321 | 385 | 698 | 1188 | 75 | 71 | 65 | 65 | 60 | 60 | 60 | 60 |
| 29 | 0 | 0 | 0 | 0 | 349 | 377 | 0 | 0 | 75 | 77 | 67 | 66 | 61 | 60 | 61 | 60 |

**Table 22: 100kW source with 5 ACH ventilation.**

| | Source Rate 6e-7 | | | | Source Rate 6e-6 | | | | Source Rate 6e-5 | | | | Source Rate 6e-4 | | | |
|---|---|---|---|---|---|---|---|---|---|---|---|---|---|---|---|---|
| Vent | Low | Low | High | High | Low | Low | High | High | Low | Low | High | High | Low | Low | High | High |
| Air Source | Low | High | Low | High | Low | High | Low | High | Low | High | Low | High | Low | High | Low | High |
| **MP** | **Activation (s)** | | | | | | | | | | | | | | | |
| 1 | 0 | 0 | 0 | 0 | 0 | 0 | 0 | 0 | 66 | 66 | 66 | 66 | 51 | 51 | 51 | 51 |
| 2 | 0 | 0 | 0 | 0 | 0 | 0 | 0 | 0 | 102 | 103 | 119 | 115 | 63 | 63 | 92 | 91 |
| 3 | 0 | 0 | 0 | 0 | 0 | 0 | 0 | 0 | 104 | 103 | 115 | 115 | 61 | 62 | 91 | 90 |
| 4 | 0 | 0 | 0 | 0 | 0 | 0 | 0 | 0 | 115 | 103 | 150 | 121 | 72 | 71 | 95 | 85 |
| 5 | 0 | 0 | 0 | 0 | 0 | 0 | 0 | 0 | 101 | 102 | 114 | 117 | 68 | 66 | 91 | 89 |
| 6 | 0 | 0 | 0 | 0 | 0 | 0 | 0 | 0 | 102 | 102 | 114 | 115 | 57 | 57 | 57 | 57 |
| 7 | 0 | 0 | 0 | 0 | 0 | 0 | 0 | 0 | 150 | 110 | 165 | 119 | 67 | 67 | 78 | 85 |
| 8 | 0 | 0 | 0 | 0 | 0 | 0 | 0 | 0 | 99 | 101 | 116 | 116 | 57 | 57 | 91 | 87 |
| 9 | 0 | 0 | 0 | 0 | 0 | 0 | 0 | 0 | 101 | 101 | 111 | 113 | 56 | 56 | 56 | 56 |
| 10 | n/a | n/a | n/a | n/a | n/a | n/a | n/a | n/a | n/a | n/a | n/a | n/a | n/a | n/a | n/a | n/a |
| 11 | 0 | 0 | 0 | 0 | 0 | 0 | 0 | 0 | 66 | 65 | 68 | 68 | 52 | 52 | 52 | 52 |
| 12 | 0 | 0 | 0 | 0 | 0 | 0 | 0 | 0 | 105 | 105 | 118 | 120 | 61 | 60 | 60 | 61 |
| 13 | 0 | 0 | 0 | 0 | 0 | 0 | 0 | 0 | 105 | 99 | 118 | 120 | 56 | 56 | 61 | 60 |
| 14 | 0 | 0 | 0 | 0 | 0 | 0 | 0 | 0 | 105 | 106 | 123 | 123 | 59 | 60 | 64 | 62 |
| 15 | 0 | 0 | 0 | 0 | 0 | 0 | 0 | 0 | 108 | 107 | 124 | 125 | 61 | 60 | 63 | 63 |
| 16 | 0 | 0 | 0 | 0 | 0 | 0 | 0 | 0 | 102 | 104 | 123 | 124 | 55 | 55 | 57 | 57 |
| 17 | 0 | 0 | 0 | 0 | 0 | 0 | 0 | 0 | 111 | 110 | 114 | 121 | 56 | 56 | 56 | 56 |
| 18 | 0 | 0 | 0 | 0 | 0 | 0 | 0 | 0 | 103 | 104 | 118 | 117 | 55 | 56 | 55 | 55 |
| 19 | 0 | 0 | 0 | 0 | 0 | 0 | 0 | 0 | 101 | 101 | 111 | 113 | 55 | 55 | 55 | 55 |
| 20 | n/a | n/a | n/a | n/a | n/a | n/a | n/a | n/a | n/a | n/a | n/a | n/a | n/a | n/a | n/a | n/a |
| 21 | 0 | 0 | 0 | 0 | 0 | 0 | 0 | 0 | 62 | 62 | 62 | 62 | 53 | 53 | 53 | 53 |
| 22 | 0 | 0 | 0 | 0 | 0 | 0 | 0 | 0 | 97 | 97 | 111 | 112 | 53 | 53 | 53 | 53 |
| 23 | 0 | 0 | 0 | 0 | 0 | 0 | 0 | 0 | 98 | 98 | 117 | 112 | 55 | 55 | 55 | 55 |
| 24 | 0 | 0 | 0 | 0 | 0 | 0 | 0 | 0 | 97 | 92 | 112 | 106 | 53 | 53 | 53 | 53 |
| 25 | 0 | 0 | 0 | 0 | 0 | 0 | 0 | 0 | 101 | 101 | 110 | 112 | 54 | 54 | 54 | 54 |
| 26 | 0 | 0 | 0 | 0 | 0 | 0 | 0 | 0 | 100 | 95 | 115 | 114 | 54 | 54 | 55 | 55 |
| 27 | 0 | 0 | 0 | 0 | 0 | 0 | 0 | 0 | 98 | 0 | 112 | 188 | 55 | 54 | 55 | 54 |
| 28 | 0 | 0 | 0 | 0 | 0 | 0 | 0 | 0 | 99 | 98 | 112 | 114 | 54 | 54 | 54 | 54 |
| 29 | 0 | 0 | 0 | 0 | 0 | 0 | 0 | 0 | 101 | 101 | 110 | 114 | 55 | 55 | 55 | 55 |

**Table 23: 100kW source with 10 ACH ventilation.**

| | Source Rate 6e-7 | | | | Source Rate 6e-6 | | | | Source Rate 6e-5 | | | | Source Rate 6e-4 | | | |
|---|---|---|---|---|---|---|---|---|---|---|---|---|---|---|---|---|
| Vent | Low | Low | High | High | Low | Low | High | High | Low | Low | High | High | Low | Low | High | High |
| Air Source | Low | High | Low | High | Low | High | Low | High | Low | High | Low | High | Low | High | Low | High |
| **MP** | **Activation (s)** | | | | | | | | | | | | | | | |
| 1 | 0 | 0 | 0 | 0 | 0 | 0 | 0 | 0 | 66 | 66 | 66 | 66 | 51 | 51 | 51 | 51 |
| 2 | 0 | 0 | 0 | 0 | 0 | 0 | 0 | 0 | 103 | 103 | 121 | 119 | 62 | 65 | 95 | 91 |
| 3 | 0 | 0 | 0 | 0 | 0 | 0 | 0 | 0 | 105 | 105 | 119 | 118 | 61 | 63 | 94 | 91 |
| 4 | 0 | 0 | 0 | 0 | 0 | 0 | 0 | 0 | 144 | 107 | 0 | 132 | 69 | 63 | 98 | 88 |
| 5 | 0 | 0 | 0 | 0 | 0 | 0 | 0 | 0 | 103 | 104 | 121 | 119 | 69 | 66 | 97 | 90 |
| 6 | 0 | 0 | 0 | 0 | 0 | 0 | 0 | 0 | 103 | 103 | 119 | 118 | 58 | 57 | 57 | 57 |
| 7 | 0 | 0 | 0 | 0 | 0 | 0 | 0 | 0 | 216 | 122 | 245 | 132 | 71 | 68 | 82 | 87 |
| 8 | 0 | 0 | 0 | 0 | 0 | 0 | 0 | 0 | 103 | 101 | 120 | 122 | 57 | 57 | 91 | 89 |
| 9 | 0 | 0 | 0 | 0 | 0 | 0 | 0 | 0 | 101 | 102 | 115 | 115 | 56 | 56 | 56 | 56 |
| 10 | n/a | n/a | n/a | n/a | n/a | n/a | n/a | n/a | n/a | n/a | n/a | n/a | n/a | n/a | n/a | n/a |
| 11 | 0 | 0 | 0 | 0 | 0 | 0 | 0 | 0 | 66 | 65 | 68 | 67 | 52 | 52 | 52 | 52 |
| 12 | 0 | 0 | 0 | 0 | 0 | 0 | 0 | 0 | 106 | 107 | 124 | 127 | 59 | 59 | 60 | 61 |
| 13 | 0 | 0 | 0 | 0 | 0 | 0 | 0 | 0 | 102 | 102 | 122 | 121 | 56 | 56 | 62 | 64 |
| 14 | 0 | 0 | 0 | 0 | 0 | 0 | 0 | 0 | 111 | 110 | 129 | 135 | 59 | 60 | 60 | 62 |
| 15 | 0 | 0 | 0 | 0 | 0 | 0 | 0 | 0 | 111 | 112 | 129 | 130 | 57 | 60 | 64 | 63 |
| 16 | 0 | 0 | 0 | 0 | 0 | 0 | 0 | 0 | 104 | 103 | 127 | 128 | 56 | 55 | 57 | 57 |
| 17 | 0 | 0 | 0 | 0 | 0 | 0 | 0 | 0 | 115 | 125 | 121 | 132 | 56 | 56 | 56 | 56 |
| 18 | 0 | 0 | 0 | 0 | 0 | 0 | 0 | 0 | 104 | 112 | 121 | 120 | 55 | 56 | 55 | 56 |
| 19 | 0 | 0 | 0 | 0 | 0 | 0 | 0 | 0 | 101 | 101 | 117 | 116 | 55 | 55 | 55 | 55 |
| 20 | n/a | n/a | n/a | n/a | n/a | n/a | n/a | n/a | n/a | n/a | n/a | n/a | n/a | n/a | n/a | n/a |
| 21 | 0 | 0 | 0 | 0 | 0 | 0 | 0 | 0 | 62 | 63 | 63 | 62 | 53 | 53 | 53 | 53 |
| 22 | 0 | 0 | 0 | 0 | 0 | 0 | 0 | 0 | 97 | 101 | 110 | 111 | 53 | 53 | 53 | 53 |
| 23 | 0 | 0 | 0 | 0 | 0 | 0 | 0 | 0 | 97 | 101 | 115 | 117 | 55 | 55 | 55 | 55 |
| 24 | 0 | 0 | 0 | 0 | 0 | 0 | 0 | 0 | 97 | 91 | 114 | 109 | 53 | 53 | 53 | 53 |
| 25 | 0 | 0 | 0 | 0 | 0 | 0 | 0 | 0 | 102 | 104 | 117 | 115 | 54 | 54 | 54 | 54 |
| 26 | 0 | 0 | 0 | 0 | 0 | 0 | 0 | 0 | 100 | 101 | 117 | 117 | 54 | 54 | 55 | 55 |
| 27 | 0 | 0 | 0 | 0 | 0 | 0 | 0 | 0 | 103 | 0 | 114 | 368 | 55 | 54 | 55 | 54 |
| 28 | 0 | 0 | 0 | 0 | 0 | 0 | 0 | 0 | 100 | 98 | 118 | 117 | 54 | 54 | 54 | 54 |
| 29 | 0 | 0 | 0 | 0 | 0 | 0 | 0 | 0 | 101 | 102 | 118 | 116 | 55 | 55 | 55 | 55 |

*Appendix C – Computational Results of Real World Geometry*

The FLACS CFD package requires that simulations follow a naming convention of using six digits. This means that a text description of each scenario is not possible unless post processed. For simplicity the following Table 24 contains an over of the 6 digit numbering convention used for these real world geometry scenarios.

**Table 24: Scenario numbering key.**

| Digit 1 | | Digit 2 | | Digit 3 | |
|---|---|---|---|---|---|
| 1 | Open Doors | 1 | Basement Source | 5 | +Z Source Direction |
| 2 | Closed Doors | 5 | Kitchen Source | | |

| Digit 4 | | Digit 5 | | Digit 6 | |
|---|---|---|---|---|---|
| 1 | 10 kW Source | 0 | 0 ACH | 4 | 6.0e-4 kg/s CO release |
| 5 | 100 kW Source | 5 | 5 ACH | 5 | 6.0e-5 kg/s CO Release |
| | | 8 | 8 ACH | | |

**Table 25: Open doors geometry, fire source in basement.**

| Job | 115104 | 115105 | 115154 | 115155 | 115184 | 115185 | 115504 | 115505 | 115554 | 115555 | 115584 | 115585 |
|---|---|---|---|---|---|---|---|---|---|---|---|---|
| MP | Activation (s) | | | | | | | | | | | |
| 1 | 308 | 461 | 95 | 829 | 94 | 830 | 70 | 155 | 345 | 984 | 240 | 830 |
| 2 | 300 | 442 | 97 | 790 | 92 | 793 | 77 | 129 | 353 | 986 | 224 | 793 |
| 3 | 270 | 416 | 95 | 756 | 94 | 811 | 76 | 155 | 340 | 984 | 222 | 811 |
| 4 | 230 | 457 | 1297 | 2108 | 1342 | 2236 | 223 | 541 | 1144 | 2903 | 1128 | 2236 |
| 5 | 304 | 465 | 86 | 735 | 92 | 805 | 67 | 128 | 324 | 963 | 214 | 805 |
| 6 | 233 | 468 | 102 | 746 | 96 | 811 | 81 | 133 | 353 | 991 | 223 | 811 |
| 7 | 781 | 1112 | 166 | 843 | 137 | 877 | 339 | 664 | 190 | 916 | 192 | 877 |
| 8 | 748 | 1121 | 188 | 874 | 153 | 865 | 275 | 576 | 144 | 602 | 142 | 865 |
| 9 | 759 | 1145 | 104 | 809 | 102 | 830 | 341 | 705 | 313 | 960 | 207 | 830 |
| 10 | 796 | 1137 | 104 | 793 | 100 | 848 | 326 | 680 | 190 | 869 | 191 | 848 |
| 11 | 846 | 1185 | 121 | 944 | 110 | 869 | 331 | 720 | 186 | 778 | 181 | 869 |
| 12 | 762 | 1125 | 464 | 1263 | 145 | 867 | 361 | 714 | 163 | 671 | 167 | 867 |
| 13 | 77 | 90 | 360 | 1309 | 283 | 1145 | 56 | 88 | 416 | 1010 | 382 | 1145 |
| 14 | 96 | 1125 | 381 | 1276 | 325 | 1022 | 320 | 637 | 150 | 583 | 150 | 1022 |
| 15 | 781 | 1125 | 654 | 1362 | 588 | 1383 | 297 | 598 | 259 | 832 | 247 | 1383 |
| 16 | 781 | 1129 | 657 | 1360 | 588 | 1387 | 296 | 593 | 260 | 830 | 249 | 1387 |
| 17 | 226 | 405 | 308 | 1182 | 201 | 1022 | 131 | 323 | 384 | 997 | 360 | 1022 |
| 18 | 237 | 401 | 293 | 1182 | 195 | 1020 | 133 | 321 | 374 | 994 | 361 | 1020 |
| 19 | 230 | 390 | 344 | 1271 | 273 | 1097 | 122 | 334 | 354 | 1050 | 348 | 1097 |
| 20 | 107 | 249 | 285 | 1174 | 241 | 1055 | 67 | 269 | 220 | 780 | 251 | 1055 |
| 21 | 102 | 178 | 200 | 1040 | 175 | 995 | 67 | 241 | 212 | 764 | 225 | 995 |
| 22 | 102 | 178 | 212 | 1051 | 211 | 1014 | 67 | 241 | 209 | 758 | 226 | 1014 |
| 23 | 102 | 187 | 252 | 1107 | 227 | 1022 | 67 | 239 | 211 | 774 | 227 | 1022 |
| 24 | 102 | 187 | 242 | 1110 | 211 | 1024 | 68 | 248 | 214 | 774 | 233 | 1024 |
| 25 | 102 | 286 | 240 | 1161 | 215 | 1043 | 110 | 331 | 284 | 855 | 292 | 1043 |
| 26 | 270 | 431 | 360 | 1271 | 237 | 1112 | 166 | 415 | 409 | 1026 | 376 | 1112 |
| 27 | 762 | 1145 | 347 | 1354 | 351 | 1360 | 320 | 619 | 150 | 619 | 155 | 1360 |
| 28 | 630 | 936 | 347 | 1089 | 343 | 1112 | 234 | 487 | 154 | 619 | 162 | 1112 |
| 29 | 390 | 656 | 344 | 1043 | 347 | 1057 | 151 | 338 | 162 | 631 | 154 | 1057 |
| 30 | 386 | 626 | 347 | 1032 | 353 | 1018 | 151 | 334 | 162 | 626 | 163 | 1018 |
| 31 | 0 | 0 | 0 | 0 | 0 | 0 | 0 | 0 | 0 | 0 | 0 | 0 |
| 32 | 0 | 0 | 0 | 0 | 0 | 0 | 0 | 0 | 0 | 0 | 0 | 0 |
| 33 | 69 | 77 | 57 | 67 | 55 | 67 | 55 | 86 | 52 | 69 | 53 | 67 |
| 34 | 69 | 69 | 54 | 55 | 53 | 55 | 55 | 93 | 52 | 91 | 52 | 55 |
| 35 | 289 | 416 | 383 | 1346 | 341 | 1202 | 168 | 412 | 420 | 1035 | 392 | 1202 |
| 36 | 202 | 365 | 298 | 1241 | 275 | 1139 | 124 | 348 | 342 | 923 | 347 | 1139 |
| 37 | 162 | 286 | 270 | 1233 | 265 | 1145 | 106 | 320 | 300 | 880 | 315 | 1145 |
| 38 | 146 | 282 | 272 | 1201 | 261 | 1147 | 101 | 312 | 292 | 870 | 305 | 1147 |
| 39 | 132 | 275 | 190 | 1177 | 161 | 1059 | 103 | 307 | 283 | 857 | 320 | 1059 |
| 40 | 150 | 282 | 283 | 1228 | 205 | 1091 | 103 | 308 | 289 | 867 | 317 | 1091 |
| 41 | 222 | 350 | 339 | 1276 | 275 | 1166 | 129 | 359 | 348 | 935 | 343 | 1166 |
| 42 | 270 | 450 | 388 | 1341 | 337 | 1233 | 159 | 408 | 408 | 1019 | 390 | 1233 |
| 43 | 297 | 461 | 288 | 1164 | 265 | 1082 | 148 | 346 | 430 | 1042 | 400 | 1082 |
| 44 | 178 | 309 | 240 | 1115 | 243 | 1070 | 107 | 286 | 327 | 933 | 320 | 1070 |
| 45 | 154 | 279 | 232 | 1113 | 211 | 1043 | 97 | 271 | 289 | 863 | 319 | 1043 |
| 46 | 146 | 271 | 227 | 1094 | 203 | 1039 | 93 | 267 | 282 | 851 | 320 | 1039 |
| 47 | 132 | 238 | 190 | 1067 | 211 | 1030 | 80 | 267 | 248 | 805 | 290 | 1030 |
| 48 | 132 | 246 | 220 | 1081 | 219 | 1033 | 80 | 273 | 248 | 806 | 297 | 1033 |
| 49 | 202 | 350 | 235 | 1089 | 211 | 1028 | 110 | 293 | 328 | 925 | 321 | 1028 |
| 50 | 226 | 442 | 324 | 1233 | 265 | 1082 | 142 | 338 | 438 | 1058 | 356 | 1082 |
| 51 | 237 | 379 | 352 | 1309 | 219 | 1055 | 166 | 412 | 397 | 1022 | 373 | 1055 |
| 52 | 158 | 320 | 242 | 1206 | 215 | 1051 | 106 | 322 | 309 | 856 | 292 | 1051 |
| 53 | 132 | 249 | 240 | 1174 | 215 | 1053 | 90 | 297 | 269 | 838 | 288 | 1053 |
| 54 | 128 | 227 | 207 | 1142 | 195 | 1026 | 89 | 296 | 257 | 834 | 287 | 1026 |
| 55 | 128 | 238 | 215 | 1107 | 217 | 1041 | 89 | 292 | 260 | 819 | 271 | 1041 |
| 56 | 132 | 242 | 220 | 1107 | 215 | 1051 | 89 | 297 | 261 | 824 | 281 | 1051 |
| 57 | 174 | 290 | 237 | 1190 | 231 | 1070 | 111 | 327 | 308 | 885 | 305 | 1070 |
| 58 | 259 | 416 | 321 | 1265 | 261 | 1126 | 167 | 414 | 389 | 1017 | 351 | 1126 |
| 59 | 96 | 230 | 375 | 1311 | 327 | 1185 | 58 | 223 | 429 | 1029 | 388 | 1185 |
| 60 | 90 | 187 | 357 | 1268 | 287 | 1149 | 61 | 226 | 326 | 905 | 331 | 1149 |
| 61 | 90 | 158 | 306 | 1220 | 277 | 1099 | 59 | 223 | 267 | 834 | 277 | 1099 |
| 62 | 90 | 158 | 298 | 1193 | 253 | 1093 | 59 | 223 | 251 | 808 | 260 | 1093 |
| 63 | 218 | 365 | 147 | 989 | 135 | 883 | 89 | 261 | 345 | 933 | 310 | 883 |

| | | | | | | | | | | | | |
|---|---|---|---|---|---|---|---|---|---|---|---|---|
| **64** | 218 | 361 | 168 | 1038 | 137 | 887 | 92 | 262 | 345 | 935 | 323 | 887 |
| **65** | 274 | 420 | 237 | 1091 | 149 | 925 | 120 | 305 | 376 | 970 | 361 | 925 |
| **66** | 297 | 450 | 270 | 1188 | 173 | 950 | 141 | 343 | 408 | 1016 | 373 | 950 |
| **67** | 0 | 0 | 0 | 0 | 0 | 0 | 0 | 0 | 0 | 0 | 0 | 0 |
| **68** | 0 | 0 | 0 | 0 | 0 | 0 | 0 | 0 | 0 | 0 | 0 | 0 |
| **69** | 0 | 0 | 0 | 0 | 0 | 0 | 0 | 0 | 0 | 0 | 0 | 0 |
| **70** | 0 | 0 | 0 | 0 | 0 | 0 | 0 | 0 | 0 | 0 | 0 | 0 |
| **71** | 758 | 3049 | 166 | 381 | 171 | 390 | 234 | 2794 | 92 | 290 | 92 | 390 |
| **72** | 758 | 3097 | 166 | 381 | 171 | 408 | 258 | 2796 | 92 | 290 | 92 | 408 |
| **73** | 758 | 3290 | 168 | 423 | 173 | 452 | 331 | 2813 | 90 | 289 | 90 | 452 |
| **74** | 758 | 3514 | 156 | 517 | 157 | 562 | 531 | 2897 | 84 | 276 | 84 | 562 |
| **75** | 923 | 1292 | 88 | 798 | 86 | 768 | 489 | 504 | 325 | 958 | 203 | 768 |
| **76** | 541 | 873 | 381 | 1222 | 359 | 1206 | 201 | 424 | 238 | 823 | 236 | 1206 |
| **77** | 563 | 900 | 407 | 1198 | 418 | 1227 | 210 | 439 | 237 | 808 | 235 | 1227 |
| **78** | 699 | 1011 | 480 | 1244 | 464 | 1288 | 260 | 519 | 251 | 829 | 249 | 1288 |
| **79** | 800 | 1153 | 692 | 1397 | 649 | 1422 | 316 | 633 | 295 | 874 | 293 | 1422 |
| **80** | 537 | 885 | 375 | 1161 | 365 | 1181 | 205 | 429 | 221 | 780 | 227 | 1181 |
| **81** | 596 | 928 | 383 | 1225 | 375 | 1237 | 222 | 448 | 244 | 821 | 244 | 1237 |
| **82** | 666 | 1022 | 464 | 1252 | 484 | 1259 | 249 | 514 | 254 | 835 | 254 | 1259 |
| **83** | 807 | 1185 | 702 | 1419 | 649 | 1411 | 320 | 637 | 291 | 879 | 285 | 1411 |
| **84** | 500 | 839 | 270 | 1137 | 269 | 1187 | 187 | 411 | 159 | 625 | 160 | 1187 |
| **85** | 519 | 854 | 352 | 1134 | 303 | 1185 | 191 | 418 | 159 | 639 | 160 | 1185 |
| **86** | 626 | 889 | 363 | 1185 | 331 | 1210 | 231 | 478 | 164 | 639 | 170 | 1210 |
| **87** | 756 | 1133 | 472 | 1306 | 440 | 1294 | 296 | 622 | 167 | 654 | 178 | 1294 |
| **88** | 390 | 687 | 311 | 928 | 295 | 914 | 161 | 342 | 145 | 574 | 145 | 914 |
| **89** | 394 | 694 | 316 | 938 | 301 | 929 | 164 | 339 | 147 | 583 | 148 | 929 |
| **90** | 574 | 896 | 306 | 941 | 293 | 935 | 253 | 532 | 146 | 580 | 146 | 935 |
| **91** | 710 | 1100 | 265 | 930 | 275 | 933 | 277 | 609 | 145 | 580 | 146 | 933 |
| **92** | 382 | 705 | 308 | 922 | 297 | 912 | 161 | 356 | 144 | 574 | 144 | 912 |
| **93** | 404 | 668 | 308 | 922 | 297 | 910 | 162 | 357 | 144 | 574 | 143 | 910 |
| **94** | 559 | 748 | 306 | 920 | 293 | 908 | 187 | 511 | 143 | 572 | 143 | 908 |
| **95** | 725 | 1125 | 306 | 920 | 293 | 910 | 287 | 598 | 144 | 575 | 144 | 910 |
| **96** | 481 | 805 | 308 | 1046 | 267 | 1006 | 200 | 385 | 159 | 604 | 160 | 1006 |
| **97** | 500 | 832 | 311 | 1051 | 283 | 1012 | 206 | 410 | 160 | 605 | 161 | 1012 |
| **98** | 563 | 920 | 324 | 1054 | 305 | 1020 | 217 | 487 | 160 | 606 | 160 | 1020 |
| **99** | 752 | 1125 | 363 | 1107 | 341 | 1066 | 309 | 628 | 165 | 647 | 166 | 1066 |
| **100** | 634 | 1108 | 567 | 1392 | 464 | 1309 | 271 | 623 | 172 | 720 | 171 | 1309 |
| **101** | 493 | 675 | 488 | 1260 | 377 | 1197 | 144 | 390 | 170 | 700 | 174 | 1197 |
| **102** | 334 | 535 | 485 | 1222 | 375 | 1135 | 122 | 308 | 165 | 677 | 171 | 1135 |
| **103** | 297 | 522 | 449 | 1185 | 377 | 1133 | 112 | 280 | 158 | 688 | 164 | 1133 |
| **104** | 710 | 1087 | 456 | 1362 | 414 | 1261 | 131 | 614 | 164 | 673 | 168 | 1261 |
| **105** | 297 | 767 | 449 | 1239 | 369 | 1187 | 123 | 359 | 165 | 677 | 167 | 1187 |
| **106** | 293 | 490 | 454 | 1188 | 327 | 1147 | 123 | 309 | 161 | 670 | 165 | 1147 |
| **107** | 289 | 479 | 449 | 1185 | 317 | 1131 | 122 | 303 | 160 | 669 | 165 | 1131 |
| **108** | 663 | 1091 | 321 | 1222 | 309 | 991 | 288 | 601 | 144 | 575 | 145 | 991 |
| **109** | 341 | 801 | 365 | 1110 | 335 | 1039 | 180 | 411 | 146 | 585 | 147 | 1039 |
| **110** | 330 | 522 | 370 | 1107 | 347 | 1099 | 119 | 318 | 149 | 608 | 146 | 1099 |
| **111** | 326 | 515 | 355 | 1089 | 339 | 1057 | 118 | 309 | 149 | 620 | 146 | 1057 |
| **112** | 892 | 1326 | 197 | 449 | 203 | 456 | 363 | 2859 | 98 | 297 | 93 | 456 |
| **113** | 102 | 246 | 240 | 1094 | 201 | 1014 | 67 | 236 | 204 | 740 | 202 | 1014 |
| **114** | 323 | 508 | 83 | 722 | 88 | 799 | 63 | 108 | 315 | 968 | 202 | 799 |

**Table 26: Open doors geometry, fire source in kitchen.**

| Job | 155104 | 155105 | 155154 | 155155 | 155184 | 155185 | 155504 | 155505 | 155554 | 155555 | 155584 | 155585 |
|---|---|---|---|---|---|---|---|---|---|---|---|---|
| MP | Activation (s) | | | | | | | | | | | |
| 1 | 398 | 691 | 264 | 668 | 286 | 650 | 253 | 544 | 240 | 583 | 218 | 548 |
| 2 | 405 | 670 | 261 | 665 | 288 | 652 | 241 | 533 | 240 | 585 | 218 | 552 |
| 3 | 345 | 649 | 251 | 659 | 288 | 645 | 268 | 556 | 237 | 580 | 215 | 550 |
| 4 | 560 | 831 | 747 | 1056 | 954 | 1345 | 406 | 1070 | 426 | 1194 | 471 | 1245 |
| 5 | 392 | 698 | 241 | 646 | 282 | 645 | 225 | 504 | 224 | 567 | 211 | 548 |
| 6 | 373 | 677 | 264 | 668 | 290 | 652 | 253 | 544 | 242 | 587 | 220 | 550 |
| 7 | 170 | 725 | 314 | 712 | 327 | 685 | 58 | 286 | 59 | 389 | 66 | 437 |
| 8 | 359 | 677 | 251 | 653 | 286 | 650 | 268 | 611 | 227 | 568 | 211 | 538 |
| 9 | 306 | 698 | 264 | 665 | 292 | 650 | 298 | 630 | 235 | 577 | 221 | 550 |
| 10 | 249 | 725 | 261 | 662 | 292 | 647 | 324 | 628 | 222 | 562 | 218 | 550 |
| 11 | 249 | 738 | 297 | 678 | 313 | 666 | 251 | 532 | 255 | 619 | 234 | 563 |
| 12 | 287 | 725 | 314 | 725 | 321 | 683 | 331 | 628 | 262 | 609 | 239 | 570 |
| 13 | 325 | 649 | 357 | 719 | 313 | 678 | 210 | 487 | 262 | 604 | 251 | 598 |
| 14 | 353 | 738 | 215 | 583 | 268 | 602 | 225 | 506 | 201 | 543 | 206 | 538 |
| 15 | 221 | 432 | 231 | 431 | 250 | 465 | 154 | 436 | 153 | 395 | 152 | 385 |
| 16 | 215 | 426 | 218 | 399 | 247 | 465 | 153 | 429 | 150 | 393 | 150 | 379 |
| 17 | 300 | 609 | 350 | 706 | 288 | 710 | 196 | 445 | 229 | 562 | 233 | 580 |
| 18 | 313 | 603 | 347 | 703 | 278 | 707 | 194 | 436 | 229 | 558 | 231 | 574 |
| 19 | 313 | 596 | 314 | 643 | 309 | 670 | 230 | 494 | 212 | 607 | 197 | 553 |
| 20 | 164 | 398 | 158 | 431 | 164 | 447 | 108 | 377 | 115 | 380 | 141 | 332 |
| 21 | 151 | 319 | 151 | 324 | 155 | 288 | 96 | 288 | 97 | 335 | 97 | 378 |
| 22 | 151 | 313 | 151 | 324 | 155 | 288 | 96 | 298 | 97 | 334 | 97 | 360 |
| 23 | 170 | 360 | 161 | 327 | 164 | 294 | 107 | 278 | 104 | 337 | 99 | 339 |
| 24 | 170 | 366 | 161 | 353 | 164 | 296 | 107 | 298 | 106 | 334 | 99 | 339 |
| 25 | 228 | 537 | 165 | 583 | 168 | 568 | 151 | 365 | 166 | 417 | 160 | 473 |
| 26 | 366 | 670 | 357 | 722 | 339 | 676 | 220 | 489 | 253 | 577 | 249 | 592 |
| 27 | 228 | 492 | 235 | 461 | 268 | 523 | 202 | 522 | 170 | 409 | 176 | 597 |
| 28 | 94 | 353 | 92 | 284 | 88 | 315 | 101 | 368 | 66 | 323 | 66 | 242 |
| 29 | 94 | 113 | 88 | 108 | 86 | 104 | 65 | 175 | 64 | 161 | 65 | 155 |
| 30 | 94 | 113 | 88 | 105 | 86 | 104 | 65 | 175 | 64 | 155 | 65 | 154 |
| 31 | 0 | 0 | 0 | 0 | 0 | 0 | 0 | 0 | 0 | 0 | 0 | 0 |
| 32 | 0 | 0 | 0 | 0 | 0 | 0 | 0 | 0 | 0 | 0 | 0 | 0 |
| 33 | 739 | 3900 | 602 | 1962 | 563 | 1245 | 6163 | 0 | 462 | 1753 | 474 | 1998 |
| 34 | 685 | 3830 | 561 | 1916 | 545 | 1184 | 5652 | 0 | 439 | 1672 | 445 | 1925 |
| 35 | 412 | 663 | 383 | 712 | 365 | 709 | 223 | 498 | 252 | 592 | 246 | 600 |
| 36 | 300 | 603 | 307 | 615 | 331 | 635 | 180 | 411 | 193 | 455 | 192 | 503 |
| 37 | 249 | 524 | 254 | 525 | 241 | 529 | 153 | 385 | 155 | 405 | 160 | 433 |
| 38 | 235 | 512 | 225 | 506 | 235 | 491 | 146 | 377 | 147 | 399 | 150 | 425 |
| 39 | 228 | 479 | 245 | 470 | 307 | 588 | 140 | 368 | 139 | 385 | 152 | 416 |
| 40 | 249 | 473 | 311 | 499 | 298 | 685 | 142 | 372 | 150 | 394 | 166 | 408 |
| 41 | 325 | 603 | 353 | 697 | 311 | 666 | 183 | 421 | 193 | 454 | 215 | 577 |
| 42 | 386 | 691 | 376 | 731 | 321 | 712 | 230 | 489 | 247 | 587 | 231 | 575 |
| 43 | 380 | 629 | 281 | 715 | 302 | 623 | 223 | 496 | 248 | 592 | 248 | 592 |
| 44 | 242 | 524 | 278 | 560 | 300 | 602 | 143 | 379 | 180 | 448 | 161 | 506 |
| 45 | 215 | 479 | 278 | 512 | 307 | 537 | 129 | 365 | 145 | 385 | 155 | 428 |
| 46 | 215 | 479 | 278 | 480 | 298 | 521 | 126 | 358 | 134 | 378 | 144 | 401 |
| 47 | 190 | 380 | 231 | 435 | 268 | 461 | 112 | 331 | 114 | 342 | 131 | 366 |
| 48 | 190 | 392 | 228 | 448 | 268 | 555 | 113 | 332 | 115 | 342 | 134 | 383 |
| 49 | 274 | 550 | 258 | 538 | 282 | 643 | 156 | 401 | 172 | 443 | 152 | 482 |
| 50 | 306 | 649 | 337 | 725 | 363 | 714 | 226 | 486 | 255 | 572 | 253 | 593 |
| 51 | 306 | 622 | 258 | 690 | 274 | 584 | 231 | 506 | 255 | 592 | 228 | 560 |
| 52 | 249 | 499 | 241 | 551 | 268 | 555 | 145 | 382 | 161 | 399 | 160 | 487 |
| 53 | 209 | 432 | 238 | 441 | 274 | 521 | 126 | 349 | 136 | 373 | 142 | 394 |
| 54 | 203 | 432 | 238 | 425 | 282 | 429 | 121 | 346 | 128 | 365 | 135 | 387 |
| 55 | 203 | 412 | 211 | 402 | 225 | 401 | 121 | 341 | 128 | 354 | 130 | 377 |
| 56 | 203 | 419 | 211 | 435 | 223 | 453 | 126 | 342 | 132 | 368 | 134 | 387 |
| 57 | 249 | 473 | 271 | 554 | 270 | 596 | 153 | 389 | 164 | 409 | 168 | 483 |
| 58 | 325 | 657 | 314 | 700 | 329 | 635 | 228 | 511 | 250 | 585 | 231 | 573 |
| 59 | 359 | 629 | 399 | 731 | 403 | 735 | 215 | 492 | 254 | 605 | 246 | 605 |
| 60 | 249 | 556 | 278 | 586 | 307 | 619 | 153 | 411 | 177 | 445 | 187 | 515 |
| 61 | 203 | 452 | 201 | 428 | 200 | 417 | 126 | 367 | 128 | 370 | 128 | 394 |
| 62 | 183 | 419 | 181 | 405 | 176 | 379 | 112 | 358 | 114 | 361 | 117 | 383 |
| 63 | 293 | 562 | 314 | 678 | 315 | 699 | 161 | 411 | 177 | 431 | 216 | 552 |

| | | | | | | | | | | | | |
|---|---|---|---|---|---|---|---|---|---|---|---|---|
| **64** | 293 | 562 | 320 | 672 | 319 | 710 | 162 | 411 | 177 | 436 | 211 | 542 |
| **65** | 359 | 643 | 340 | 678 | 333 | 722 | 194 | 455 | 206 | 521 | 215 | 553 |
| **66** | 386 | 684 | 383 | 687 | 351 | 735 | 208 | 472 | 232 | 556 | 218 | 552 |
| **67** | 0 | 0 | 0 | 0 | 0 | 0 | 0 | 0 | 0 | 0 | 0 | 0 |
| **68** | 0 | 0 | 0 | 0 | 0 | 0 | 0 | 0 | 0 | 0 | 0 | 0 |
| **69** | 0 | 0 | 0 | 0 | 0 | 0 | 0 | 0 | 0 | 0 | 0 | 0 |
| **70** | 0 | 0 | 0 | 0 | 0 | 0 | 0 | 0 | 0 | 0 | 0 | 0 |
| **71** | 1734 | 4634 | 4783 | 0 | 8950 | 0 | 1691 | 0 | 0 | 0 | 0 | 0 |
| **72** | 1816 | 4726 | 5233 | 0 | 9879 | 0 | 1987 | 0 | 0 | 0 | 0 | 0 |
| **73** | 2125 | 4986 | 6535 | 0 | 0 | 0 | 4064 | 0 | 0 | 0 | 0 | 0 |
| **74** | 2494 | 5382 | 9227 | 0 | 0 | 0 | 7453 | 0 | 0 | 0 | 0 | 0 |
| **75** | 466 | 771 | 251 | 649 | 282 | 645 | 284 | 587 | 225 | 577 | 210 | 547 |
| **76** | 126 | 249 | 118 | 208 | 117 | 194 | 90 | 233 | 89 | 219 | 89 | 215 |
| **77** | 126 | 274 | 122 | 211 | 119 | 207 | 98 | 245 | 98 | 234 | 97 | 225 |
| **78** | 190 | 366 | 198 | 317 | 207 | 292 | 129 | 283 | 128 | 304 | 127 | 279 |
| **79** | 235 | 486 | 241 | 483 | 280 | 535 | 188 | 450 | 169 | 477 | 168 | 483 |
| **80** | 107 | 228 | 102 | 195 | 98 | 190 | 90 | 233 | 89 | 230 | 89 | 225 |
| **81** | 151 | 287 | 145 | 241 | 139 | 231 | 107 | 256 | 106 | 248 | 105 | 235 |
| **82** | 164 | 373 | 158 | 310 | 158 | 290 | 118 | 344 | 117 | 291 | 116 | 267 |
| **83** | 235 | 466 | 254 | 474 | 268 | 511 | 196 | 431 | 178 | 399 | 187 | 573 |
| **84** | 113 | 228 | 112 | 178 | 113 | 170 | 77 | 212 | 75 | 193 | 77 | 195 |
| **85** | 120 | 235 | 115 | 181 | 117 | 176 | 79 | 200 | 83 | 194 | 77 | 195 |
| **86** | 145 | 313 | 122 | 234 | 119 | 254 | 99 | 360 | 98 | 279 | 99 | 240 |
| **87** | 196 | 452 | 231 | 451 | 235 | 479 | 183 | 811 | 166 | 599 | 166 | 508 |
| **88** | 77 | 107 | 75 | 98 | 72 | 94 | 61 | 178 | 63 | 182 | 63 | 176 |
| **89** | 82 | 138 | 78 | 121 | 76 | 104 | 64 | 194 | 66 | 201 | 65 | 197 |
| **90** | 107 | 255 | 128 | 221 | 155 | 325 | 73 | 266 | 75 | 252 | 74 | 253 |
| **91** | 177 | 556 | 231 | 637 | 282 | 654 | 236 | 523 | 212 | 540 | 205 | 520 |
| **92** | 77 | 101 | 75 | 95 | 72 | 92 | 61 | 176 | 60 | 182 | 61 | 168 |
| **93** | 77 | 126 | 75 | 125 | 74 | 121 | 63 | 175 | 60 | 185 | 61 | 166 |
| **94** | 101 | 209 | 102 | 191 | 98 | 217 | 70 | 325 | 62 | 240 | 61 | 250 |
| **95** | 177 | 326 | 191 | 483 | 250 | 600 | 202 | 494 | 62 | 519 | 61 | 489 |
| **96** | 62 | 77 | 62 | 68 | 59 | 65 | 55 | 143 | 56 | 145 | 55 | 135 |
| **97** | 67 | 82 | 62 | 75 | 59 | 72 | 55 | 145 | 56 | 147 | 55 | 135 |
| **98** | 67 | 120 | 65 | 121 | 63 | 135 | 55 | 143 | 56 | 136 | 55 | 135 |
| **99** | 132 | 426 | 215 | 637 | 304 | 666 | 60 | 241 | 62 | 257 | 63 | 255 |
| **100** | 228 | 569 | 235 | 573 | 241 | 647 | 191 | 489 | 158 | 443 | 164 | 454 |
| **101** | 151 | 385 | 151 | 405 | 147 | 447 | 101 | 360 | 100 | 370 | 99 | 347 |
| **102** | 132 | 249 | 125 | 261 | 102 | 233 | 87 | 281 | 86 | 298 | 85 | 287 |
| **103** | 107 | 203 | 102 | 181 | 100 | 172 | 71 | 207 | 72 | 206 | 72 | 218 |
| **104** | 132 | 589 | 132 | 649 | 129 | 647 | 197 | 504 | 155 | 526 | 158 | 483 |
| **105** | 132 | 439 | 125 | 418 | 123 | 483 | 93 | 356 | 92 | 368 | 117 | 356 |
| **106** | 126 | 255 | 125 | 231 | 121 | 213 | 79 | 248 | 83 | 257 | 82 | 236 |
| **107** | 126 | 228 | 125 | 195 | 121 | 186 | 82 | 251 | 83 | 252 | 80 | 235 |
| **108** | 164 | 531 | 238 | 583 | 247 | 617 | 197 | 515 | 185 | 502 | 179 | 483 |
| **109** | 158 | 426 | 151 | 392 | 149 | 409 | 101 | 406 | 98 | 409 | 99 | 373 |
| **110** | 120 | 228 | 115 | 251 | 110 | 239 | 67 | 202 | 86 | 214 | 74 | 210 |
| **111** | 101 | 190 | 95 | 171 | 94 | 168 | 67 | 199 | 66 | 196 | 66 | 184 |
| **112** | 832 | 1286 | 1056 | 3698 | 2291 | 5273 | 418 | 1172 | 830 | 0 | 1650 | 0 |
| **113** | 145 | 287 | 145 | 317 | 143 | 266 | 91 | 286 | 93 | 274 | 94 | 332 |
| **114** | 405 | 731 | 238 | 643 | 280 | 635 | 240 | 540 | 220 | 563 | 206 | 538 |

**Table 27: Closed door geometry, fire source in basement.**

| Job | 215104 | 215105 | 215154 | 215155 | 215184 | 215185 | 215504 | 215505 | 215554 | 215555 | 215584 | 215585 |
|---|---|---|---|---|---|---|---|---|---|---|---|---|
| MP | Activation (s) | | | | | | | | | | | |
| 1 | 496 | 863 | 94 | 735 | 94 | 771 | 81 | 1184 | 229 | 1976 | 198 | 1027 |
| 2 | 694 | 1214 | 195 | 1287 | 159 | 1032 | 454 | 1242 | 872 | 2371 | 765 | 1954 |
| 3 | 374 | 650 | 96 | 672 | 96 | 758 | 89 | 1199 | 228 | 882 | 198 | 788 |
| 4 | 202 | 265 | 1846 | 2214 | 1251 | 2279 | 198 | 362 | 1226 | 3381 | 1214 | 3480 |
| 5 | 595 | 1152 | 88 | 717 | 92 | 783 | 76 | 104 | 215 | 957 | 195 | 900 |
| 6 | 623 | 1148 | 164 | 951 | 138 | 870 | 449 | 1243 | 360 | 1134 | 250 | 1094 |
| 7 | 484 | 675 | 107 | 646 | 106 | 777 | 115 | 188 | 190 | 663 | 176 | 733 |
| 8 | 443 | 650 | 89 | 653 | 94 | 762 | 72 | 175 | 138 | 495 | 140 | 523 |
| 9 | 488 | 679 | 88 | 619 | 94 | 756 | 78 | 159 | 202 | 740 | 191 | 728 |
| 10 | 475 | 662 | 87 | 643 | 94 | 764 | 77 | 132 | 202 | 740 | 190 | 729 |
| 11 | 1684 | 2952 | 115 | 1069 | 108 | 841 | 1280 | 0 | 227 | 990 | 200 | 907 |
| 12 | 456 | 666 | 97 | 735 | 94 | 746 | 91 | 189 | 158 | 613 | 177 | 715 |
| 13 | 77 | 90 | 440 | 1258 | 388 | 1212 | 55 | 83 | 242 | 745 | 224 | 870 |
| 14 | 415 | 476 | 233 | 862 | 235 | 870 | 169 | 367 | 141 | 500 | 143 | 510 |
| 15 | 1462 | 2933 | 726 | 2398 | 715 | 2049 | 1129 | 0 | 670 | 2139 | 607 | 1899 |
| 16 | 1466 | 2933 | 730 | 2398 | 703 | 2042 | 1129 | 0 | 665 | 2131 | 604 | 1901 |
| 17 | 545 | 1089 | 620 | 1864 | 519 | 1581 | 348 | 1133 | 725 | 2158 | 625 | 1772 |
| 18 | 558 | 1102 | 629 | 1867 | 548 | 1596 | 347 | 1118 | 722 | 2155 | 628 | 1769 |
| 19 | 107 | 189 | 456 | 1220 | 376 | 1227 | 68 | 140 | 202 | 648 | 213 | 720 |
| 20 | 107 | 152 | 456 | 1217 | 374 | 1227 | 67 | 133 | 197 | 606 | 204 | 701 |
| 21 | 102 | 148 | 457 | 1194 | 374 | 1240 | 67 | 132 | 196 | 595 | 202 | 651 |
| 22 | 102 | 148 | 457 | 1194 | 374 | 1240 | 67 | 132 | 196 | 596 | 202 | 651 |
| 23 | 102 | 148 | 409 | 1323 | 323 | 1200 | 65 | 147 | 216 | 693 | 282 | 841 |
| 24 | 102 | 148 | 410 | 1323 | 323 | 1202 | 68 | 150 | 216 | 693 | 281 | 860 |
| 25 | 102 | 152 | 417 | 1326 | 335 | 1208 | 70 | 164 | 217 | 684 | 281 | 964 |
| 26 | 107 | 161 | 422 | 1331 | 337 | 1216 | 72 | 165 | 218 | 683 | 280 | 964 |
| 27 | 456 | 658 | 239 | 977 | 221 | 990 | 164 | 332 | 148 | 585 | 159 | 566 |
| 28 | 362 | 535 | 238 | 922 | 225 | 936 | 123 | 301 | 157 | 551 | 159 | 631 |
| 29 | 270 | 373 | 211 | 909 | 233 | 919 | 122 | 224 | 162 | 541 | 154 | 571 |
| 30 | 258 | 365 | 244 | 909 | 235 | 919 | 122 | 217 | 150 | 529 | 151 | 577 |
| 31 | 0 | 0 | 0 | 0 | 0 | 0 | 0 | 0 | 0 | 0 | 0 | 0 |
| 32 | 0 | 0 | 0 | 0 | 0 | 0 | 0 | 0 | 0 | 0 | 0 | 0 |
| 33 | 69 | 77 | 55 | 67 | 55 | 67 | 52 | 85 | 52 | 73 | 53 | 67 |
| 34 | 69 | 69 | 53 | 57 | 53 | 55 | 52 | 93 | 52 | 88 | 51 | 85 |
| 35 | 463 | 839 | 432 | 1487 | 325 | 1261 | 1072 | 2476 | 966 | 3013 | 482 | 1576 |
| 36 | 358 | 723 | 280 | 1326 | 273 | 1189 | 880 | 2295 | 777 | 2846 | 386 | 1482 |
| 37 | 258 | 622 | 244 | 1310 | 267 | 1172 | 790 | 2213 | 643 | 2767 | 374 | 1453 |
| 38 | 247 | 609 | 243 | 1279 | 261 | 1172 | 772 | 2193 | 601 | 2741 | 360 | 1447 |
| 39 | 254 | 622 | 190 | 1287 | 167 | 1119 | 785 | 2206 | 687 | 2761 | 366 | 1447 |
| 40 | 258 | 626 | 282 | 1326 | 181 | 1170 | 821 | 2249 | 713 | 2795 | 385 | 1473 |
| 41 | 362 | 714 | 308 | 1362 | 289 | 1219 | 868 | 2297 | 799 | 2842 | 404 | 1501 |
| 42 | 463 | 821 | 412 | 1476 | 357 | 1292 | 1067 | 2495 | 976 | 3026 | 473 | 1565 |
| 43 | 574 | 1134 | 704 | 1963 | 582 | 1618 | 402 | 1193 | 789 | 2251 | 696 | 1838 |
| 44 | 423 | 949 | 491 | 1719 | 384 | 1457 | 247 | 980 | 624 | 2039 | 532 | 1660 |
| 45 | 318 | 826 | 342 | 1585 | 315 | 1341 | 158 | 864 | 542 | 1931 | 450 | 1567 |
| 46 | 286 | 808 | 325 | 1539 | 311 | 1326 | 146 | 843 | 516 | 1913 | 434 | 1535 |
| 47 | 290 | 808 | 377 | 1575 | 313 | 1390 | 146 | 847 | 542 | 1944 | 456 | 1568 |
| 48 | 294 | 821 | 385 | 1601 | 337 | 1392 | 156 | 865 | 553 | 1955 | 463 | 1578 |
| 49 | 431 | 936 | 506 | 1693 | 424 | 1469 | 241 | 961 | 629 | 2045 | 538 | 1658 |
| 50 | 578 | 1134 | 736 | 1966 | 578 | 1625 | 404 | 1144 | 790 | 2249 | 696 | 1843 |
| 51 | 366 | 609 | 304 | 1142 | 293 | 1059 | 911 | 1891 | 546 | 1470 | 389 | 1096 |
| 52 | 302 | 564 | 231 | 1058 | 231 | 1034 | 801 | 1783 | 445 | 1354 | 340 | 1059 |
| 53 | 218 | 492 | 217 | 1056 | 233 | 1034 | 770 | 1754 | 417 | 1326 | 321 | 1038 |
| 54 | 218 | 492 | 206 | 1043 | 209 | 1013 | 745 | 1731 | 396 | 1302 | 316 | 1027 |
| 55 | 230 | 516 | 192 | 1043 | 217 | 1019 | 740 | 1729 | 395 | 1294 | 306 | 1025 |
| 56 | 238 | 513 | 221 | 1045 | 219 | 1023 | 752 | 1738 | 404 | 1306 | 329 | 1032 |
| 57 | 274 | 543 | 237 | 1085 | 241 | 1050 | 804 | 1782 | 447 | 1351 | 344 | 1050 |
| 58 | 358 | 626 | 284 | 1124 | 277 | 1082 | 908 | 1887 | 541 | 1458 | 373 | 1084 |
| 59 | 96 | 152 | 561 | 1404 | 418 | 1312 | 60 | 109 | 270 | 797 | 289 | 929 |
| 60 | 90 | 148 | 547 | 1396 | 438 | 1310 | 61 | 121 | 266 | 738 | 274 | 894 |
| 61 | 90 | 148 | 496 | 1383 | 434 | 1292 | 61 | 120 | 251 | 694 | 251 | 870 |
| 62 | 90 | 148 | 494 | 1380 | 434 | 1288 | 61 | 117 | 246 | 677 | 251 | 872 |
| 63 | 423 | 986 | 185 | 1308 | 181 | 1256 | 99 | 721 | 395 | 1755 | 321 | 1400 |

| | | | | | | | | | | | | |
|---|---|---|---|---|---|---|---|---|---|---|---|---|
| **64** | 427 | 990 | 184 | 1305 | 211 | 1282 | 103 | 716 | 403 | 1774 | 328 | 1400 |
| **65** | 512 | 1072 | 579 | 1807 | 452 | 1470 | 297 | 1093 | 687 | 2113 | 596 | 1724 |
| **66** | 570 | 1130 | 717 | 1947 | 576 | 1627 | 394 | 1227 | 787 | 2240 | 688 | 1832 |
| **67** | 0 | 0 | 0 | 0 | 0 | 0 | 0 | 0 | 0 | 0 | 0 | 0 |
| **68** | 0 | 0 | 0 | 0 | 0 | 0 | 0 | 0 | 0 | 0 | 0 | 0 |
| **69** | 0 | 0 | 0 | 0 | 0 | 0 | 0 | 0 | 0 | 0 | 0 | 0 |
| **70** | 0 | 0 | 0 | 0 | 0 | 0 | 0 | 0 | 0 | 0 | 0 | 0 |
| **71** | 984 | 2556 | 183 | 385 | 171 | 402 | 238 | 2756 | 92 | 291 | 93 | 295 |
| **72** | 1042 | 2626 | 185 | 395 | 171 | 402 | 258 | 2757 | 92 | 291 | 93 | 295 |
| **73** | 1341 | 2815 | 189 | 437 | 173 | 459 | 343 | 2788 | 89 | 290 | 91 | 294 |
| **74** | 1560 | 2938 | 179 | 530 | 157 | 542 | 580 | 2840 | 85 | 274 | 85 | 286 |
| **75** | 1823 | 3131 | 79 | 688 | 82 | 719 | 65 | 88 | 205 | 738 | 177 | 728 |
| **76** | 962 | 2516 | 399 | 2216 | 361 | 1694 | 851 | 0 | 468 | 1916 | 413 | 1710 |
| **77** | 976 | 2562 | 479 | 2250 | 414 | 1751 | 859 | 0 | 503 | 1952 | 442 | 1731 |
| **78** | 1264 | 2732 | 565 | 2281 | 479 | 1854 | 1006 | 0 | 551 | 2020 | 504 | 1787 |
| **79** | 1612 | 2920 | 751 | 2432 | 797 | 2143 | 1196 | 0 | 720 | 2213 | 648 | 1964 |
| **80** | 971 | 2545 | 390 | 2179 | 362 | 1703 | 867 | 0 | 477 | 1924 | 421 | 1708 |
| **81** | 1051 | 2622 | 413 | 2182 | 374 | 1709 | 904 | 0 | 483 | 1930 | 424 | 1711 |
| **82** | 1251 | 2766 | 585 | 2328 | 495 | 1896 | 964 | 0 | 563 | 2037 | 515 | 1811 |
| **83** | 1612 | 2903 | 799 | 2455 | 809 | 2159 | 1197 | 0 | 715 | 2209 | 663 | 1962 |
| **84** | 322 | 484 | 166 | 943 | 177 | 948 | 116 | 282 | 185 | 579 | 195 | 702 |
| **85** | 334 | 492 | 183 | 972 | 211 | 982 | 127 | 287 | 186 | 583 | 198 | 696 |
| **86** | 390 | 559 | 209 | 993 | 217 | 998 | 135 | 296 | 204 | 636 | 201 | 660 |
| **87** | 452 | 650 | 248 | 1040 | 221 | 1004 | 172 | 355 | 202 | 635 | 203 | 663 |
| **88** | 242 | 390 | 229 | 772 | 225 | 789 | 125 | 222 | 138 | 477 | 140 | 505 |
| **89** | 251 | 390 | 219 | 780 | 219 | 799 | 125 | 227 | 139 | 482 | 142 | 511 |
| **90** | 318 | 516 | 218 | 788 | 207 | 795 | 148 | 333 | 139 | 483 | 141 | 505 |
| **91** | 439 | 600 | 193 | 767 | 209 | 777 | 163 | 333 | 139 | 478 | 141 | 505 |
| **92** | 238 | 398 | 233 | 770 | 229 | 783 | 122 | 229 | 137 | 477 | 138 | 496 |
| **93** | 251 | 419 | 233 | 770 | 227 | 781 | 118 | 248 | 137 | 476 | 137 | 497 |
| **94** | 306 | 492 | 231 | 767 | 219 | 781 | 120 | 312 | 137 | 476 | 137 | 496 |
| **95** | 415 | 613 | 224 | 767 | 213 | 781 | 136 | 335 | 138 | 480 | 138 | 496 |
| **96** | 310 | 463 | 180 | 812 | 187 | 861 | 139 | 282 | 154 | 508 | 157 | 535 |
| **97** | 330 | 488 | 188 | 825 | 195 | 868 | 139 | 299 | 155 | 509 | 157 | 535 |
| **98** | 342 | 524 | 198 | 841 | 197 | 880 | 144 | 322 | 154 | 508 | 156 | 535 |
| **99** | 459 | 642 | 254 | 894 | 269 | 940 | 166 | 348 | 157 | 545 | 161 | 583 |
| **100** | 346 | 596 | 328 | 1137 | 299 | 1032 | 162 | 359 | 162 | 601 | 170 | 630 |
| **101** | 222 | 447 | 313 | 998 | 261 | 963 | 107 | 271 | 163 | 524 | 168 | 571 |
| **102** | 218 | 316 | 305 | 988 | 269 | 967 | 104 | 180 | 164 | 536 | 165 | 559 |
| **103** | 202 | 277 | 287 | 954 | 271 | 946 | 98 | 175 | 152 | 533 | 159 | 519 |
| **104** | 415 | 629 | 315 | 1090 | 311 | 1025 | 157 | 348 | 158 | 521 | 159 | 568 |
| **105** | 182 | 414 | 281 | 1001 | 285 | 942 | 110 | 262 | 159 | 516 | 161 | 568 |
| **106** | 182 | 284 | 198 | 951 | 201 | 928 | 91 | 170 | 157 | 511 | 156 | 540 |
| **107** | 174 | 237 | 196 | 949 | 201 | 925 | 90 | 166 | 157 | 511 | 157 | 539 |
| **108** | 427 | 662 | 237 | 822 | 229 | 812 | 171 | 334 | 138 | 482 | 140 | 504 |
| **109** | 210 | 509 | 245 | 870 | 241 | 832 | 106 | 327 | 139 | 487 | 143 | 505 |
| **110** | 206 | 277 | 251 | 894 | 241 | 837 | 102 | 175 | 142 | 485 | 144 | 507 |
| **111** | 206 | 269 | 245 | 883 | 241 | 834 | 100 | 173 | 142 | 481 | 145 | 499 |
| **112** | 562 | 839 | 224 | 437 | 205 | 444 | 387 | 2841 | 94 | 294 | 95 | 294 |
| **113** | 102 | 156 | 373 | 1053 | 359 | 1017 | 65 | 131 | 187 | 581 | 197 | 637 |
| **114** | 521 | 990 | 80 | 640 | 88 | 738 | 66 | 87 | 204 | 737 | 178 | 727 |

**Table 28: Closed door geometry, fire source in kitchen.**

| Job | 255104 | 255105 | 255154 | 255155 | 255184 | 255185 | 255504 | 255505 | 255554 | 255555 | 255584 | 255585 |
|---|---|---|---|---|---|---|---|---|---|---|---|---|
| MP | Activation (s) | | | | | | | | | | | |
| 1 | 662 | 1229 | 187 | 394 | 166 | 375 | 161 | 1470 | 148 | 910 | 131 | 642 |
| 2 | 914 | 1562 | 323 | 1463 | 243 | 567 | 329 | 1752 | 680 | 1968 | 553 | 1558 |
| 3 | 527 | 959 | 191 | 394 | 166 | 375 | 239 | 899 | 153 | 836 | 134 | 361 |
| 4 | 347 | 508 | 556 | 1055 | 528 | 1115 | 206 | 735 | 326 | 1654 | 390 | 2861 |
| 5 | 788 | 1528 | 184 | 386 | 160 | 369 | 157 | 2342 | 143 | 368 | 129 | 407 |
| 6 | 828 | 1522 | 262 | 507 | 191 | 439 | 174 | 2437 | 682 | 1985 | 180 | 611 |
| 7 | 164 | 428 | 201 | 395 | 175 | 373 | 64 | 191 | 158 | 287 | 134 | 295 |
| 8 | 183 | 535 | 181 | 381 | 165 | 366 | 151 | 1548 | 138 | 310 | 126 | 310 |
| 9 | 222 | 481 | 181 | 365 | 160 | 356 | 118 | 1533 | 140 | 314 | 126 | 327 |
| 10 | 202 | 474 | 181 | 365 | 160 | 356 | 123 | 2852 | 140 | 313 | 126 | 327 |
| 11 | 1640 | 3278 | 214 | 451 | 175 | 410 | 170 | 6953 | 170 | 2697 | 144 | 1283 |
| 12 | 228 | 508 | 191 | 375 | 181 | 371 | 141 | 2112 | 146 | 321 | 131 | 335 |
| 13 | 215 | 334 | 171 | 299 | 175 | 383 | 132 | 248 | 129 | 287 | 121 | 333 |
| 14 | 222 | 361 | 168 | 399 | 146 | 340 | 102 | 1178 | 129 | 303 | 118 | 296 |
| 15 | 1507 | 3138 | 671 | 1586 | 454 | 1278 | 319 | 6677 | 679 | 3916 | 501 | 2520 |
| 16 | 1507 | 3164 | 671 | 1578 | 443 | 1290 | 319 | 6677 | 680 | 3916 | 500 | 2516 |
| 17 | 708 | 1502 | 644 | 1204 | 473 | 1005 | 319 | 2284 | 562 | 1731 | 430 | 1367 |
| 18 | 715 | 1502 | 647 | 1207 | 404 | 1014 | 324 | 2282 | 562 | 1731 | 432 | 1361 |
| 19 | 164 | 314 | 187 | 257 | 210 | 379 | 121 | 216 | 108 | 241 | 113 | 257 |
| 20 | 158 | 261 | 184 | 239 | 210 | 377 | 105 | 206 | 102 | 207 | 108 | 236 |
| 21 | 151 | 254 | 184 | 237 | 210 | 377 | 102 | 201 | 100 | 200 | 105 | 231 |
| 22 | 151 | 254 | 184 | 236 | 210 | 377 | 102 | 201 | 100 | 202 | 105 | 231 |
| 23 | 170 | 275 | 227 | 365 | 210 | 534 | 105 | 213 | 109 | 224 | 131 | 297 |
| 24 | 170 | 275 | 227 | 366 | 210 | 532 | 105 | 213 | 114 | 231 | 131 | 297 |
| 25 | 170 | 281 | 224 | 389 | 210 | 528 | 118 | 214 | 116 | 254 | 131 | 335 |
| 26 | 177 | 288 | 224 | 387 | 231 | 528 | 120 | 215 | 119 | 283 | 132 | 376 |
| 27 | 158 | 334 | 181 | 412 | 95 | 311 | 102 | 437 | 127 | 291 | 121 | 285 |
| 28 | 94 | 241 | 91 | 241 | 91 | 234 | 73 | 187 | 65 | 176 | 65 | 181 |
| 29 | 94 | 113 | 91 | 104 | 91 | 104 | 68 | 152 | 65 | 140 | 65 | 145 |
| 30 | 94 | 113 | 88 | 102 | 85 | 104 | 68 | 147 | 65 | 138 | 65 | 144 |
| 31 | 0 | 0 | 0 | 0 | 0 | 0 | 0 | 0 | 0 | 0 | 0 | 0 |
| 32 | 0 | 0 | 0 | 0 | 0 | 0 | 0 | 0 | 0 | 0 | 0 | 0 |
| 33 | 1210 | 3786 | 346 | 1302 | 372 | 952 | 159 | 0 | 269 | 2096 | 281 | 2306 |
| 34 | 1085 | 3707 | 304 | 1217 | 345 | 887 | 165 | 0 | 245 | 1998 | 259 | 2179 |
| 35 | 622 | 1195 | 517 | 977 | 302 | 801 | 350 | 1435 | 516 | 1713 | 352 | 1207 |
| 36 | 454 | 1104 | 358 | 848 | 295 | 708 | 279 | 1338 | 368 | 1598 | 264 | 1114 |
| 37 | 447 | 991 | 333 | 800 | 291 | 686 | 272 | 1239 | 301 | 1534 | 230 | 1094 |
| 38 | 447 | 985 | 336 | 770 | 291 | 680 | 268 | 1228 | 271 | 1505 | 226 | 1083 |
| 39 | 467 | 1025 | 259 | 793 | 221 | 657 | 255 | 1255 | 306 | 1519 | 227 | 1086 |
| 40 | 467 | 1025 | 355 | 825 | 279 | 695 | 267 | 1259 | 316 | 1534 | 252 | 1114 |
| 41 | 487 | 1071 | 380 | 869 | 281 | 725 | 276 | 1336 | 363 | 1595 | 271 | 1134 |
| 42 | 648 | 1195 | 495 | 975 | 421 | 779 | 333 | 1428 | 526 | 1711 | 340 | 1194 |
| 43 | 768 | 1528 | 745 | 1316 | 528 | 1054 | 329 | 2357 | 629 | 1875 | 485 | 1439 |
| 44 | 602 | 1369 | 538 | 1077 | 365 | 914 | 282 | 2169 | 439 | 1557 | 352 | 1254 |
| 45 | 481 | 1276 | 424 | 964 | 363 | 819 | 272 | 2080 | 329 | 1413 | 276 | 1161 |
| 46 | 467 | 1255 | 393 | 932 | 339 | 787 | 263 | 2064 | 308 | 1390 | 266 | 1141 |
| 47 | 494 | 1269 | 424 | 968 | 363 | 834 | 251 | 2082 | 303 | 1388 | 286 | 1175 |
| 48 | 501 | 1269 | 436 | 978 | 372 | 841 | 267 | 2080 | 326 | 1410 | 293 | 1176 |
| 49 | 595 | 1336 | 541 | 1087 | 387 | 914 | 301 | 2172 | 434 | 1545 | 353 | 1258 |
| 50 | 741 | 1496 | 739 | 1318 | 473 | 1051 | 319 | 2345 | 623 | 1832 | 488 | 1442 |
| 51 | 494 | 885 | 383 | 756 | 277 | 638 | 299 | 882 | 358 | 1276 | 259 | 674 |
| 52 | 393 | 878 | 311 | 686 | 277 | 580 | 246 | 814 | 274 | 1205 | 225 | 628 |
| 53 | 387 | 878 | 320 | 671 | 277 | 580 | 244 | 807 | 250 | 1185 | 215 | 614 |
| 54 | 374 | 871 | 298 | 642 | 243 | 565 | 242 | 800 | 233 | 1161 | 201 | 605 |
| 55 | 414 | 865 | 285 | 651 | 265 | 564 | 240 | 825 | 233 | 1147 | 192 | 588 |
| 56 | 420 | 865 | 301 | 654 | 277 | 571 | 236 | 827 | 245 | 1156 | 203 | 607 |
| 57 | 407 | 885 | 333 | 694 | 277 | 592 | 247 | 834 | 279 | 1200 | 225 | 627 |
| 58 | 501 | 899 | 361 | 739 | 279 | 620 | 291 | 887 | 353 | 1273 | 262 | 664 |
| 59 | 215 | 327 | 259 | 407 | 263 | 500 | 137 | 240 | 146 | 368 | 157 | 465 |
| 60 | 209 | 320 | 256 | 396 | 255 | 492 | 132 | 238 | 132 | 323 | 154 | 401 |
| 61 | 183 | 301 | 227 | 365 | 243 | 488 | 121 | 226 | 119 | 261 | 131 | 374 |
| 62 | 177 | 281 | 227 | 363 | 243 | 488 | 120 | 216 | 119 | 249 | 129 | 361 |
| 63 | 588 | 1362 | 262 | 753 | 233 | 708 | 247 | 2187 | 221 | 1311 | 197 | 1003 |

| | | | | | | | | | | | | |
|---|---|---|---|---|---|---|---|---|---|---|---|---|
| **64** | 575 | 1362 | 291 | 759 | 243 | 708 | 255 | 2187 | 229 | 1240 | 209 | 1002 |
| **65** | 695 | 1449 | 611 | 1162 | 244 | 971 | 303 | 2257 | 514 | 1691 | 401 | 1327 |
| **66** | 761 | 1516 | 733 | 1302 | 244 | 1056 | 322 | 2314 | 618 | 1847 | 480 | 1431 |
| **67** | 0 | 0 | 0 | 0 | 0 | 0 | 0 | 0 | 0 | 0 | 0 | 0 |
| **68** | 0 | 0 | 0 | 0 | 0 | 0 | 0 | 0 | 0 | 0 | 0 | 0 |
| **69** | 0 | 0 | 0 | 0 | 0 | 0 | 0 | 0 | 0 | 0 | 0 | 0 |
| **70** | 0 | 0 | 0 | 0 | 0 | 0 | 0 | 0 | 0 | 0 | 0 | 0 |
| **71** | 1829 | 4342 | 3903 | 0 | 619 | 0 | 280 | 0 | 0 | 0 | 0 | 0 |
| **72** | 1877 | 4487 | 4209 | 0 | 619 | 0 | 280 | 0 | 0 | 0 | 0 | 0 |
| **73** | 2200 | 4772 | 5519 | 0 | 868 | 0 | 289 | 0 | 0 | 0 | 0 | 0 |
| **74** | 2613 | 5183 | 8492 | 0 | 1064 | 0 | 289 | 0 | 0 | 0 | 0 | 0 |
| **75** | 688 | 1249 | 174 | 357 | 156 | 354 | 167 | 1855 | 133 | 310 | 123 | 327 |
| **76** | 1033 | 2825 | 427 | 1418 | 410 | 1154 | 265 | 6253 | 534 | 3754 | 385 | 2398 |
| **77** | 1040 | 2865 | 474 | 1450 | 417 | 1180 | 280 | 6275 | 572 | 3791 | 411 | 2422 |
| **78** | 1263 | 2995 | 559 | 1485 | 387 | 1200 | 284 | 6514 | 600 | 3830 | 437 | 2446 |
| **79** | 1560 | 3236 | 688 | 1612 | 504 | 1319 | 325 | 6788 | 697 | 3936 | 516 | 2544 |
| **80** | 1079 | 2811 | 424 | 1395 | 417 | 1131 | 279 | 6251 | 521 | 3739 | 375 | 2378 |
| **81** | 1131 | 2900 | 430 | 1397 | 383 | 1128 | 284 | 6329 | 526 | 3746 | 377 | 2380 |
| **82** | 1249 | 3070 | 550 | 1524 | 339 | 1231 | 249 | 6504 | 618 | 3847 | 450 | 2478 |
| **83** | 1600 | 3203 | 745 | 1642 | 565 | 1343 | 339 | 6772 | 722 | 3961 | 530 | 2559 |
| **84** | 113 | 203 | 121 | 143 | 130 | 167 | 80 | 175 | 77 | 173 | 78 | 173 |
| **85** | 113 | 215 | 121 | 153 | 133 | 220 | 80 | 172 | 77 | 170 | 80 | 172 |
| **86** | 120 | 261 | 161 | 263 | 130 | 287 | 83 | 184 | 95 | 197 | 96 | 231 |
| **87** | 170 | 281 | 168 | 380 | 133 | 297 | 114 | 276 | 127 | 296 | 113 | 282 |
| **88** | 77 | 107 | 74 | 94 | 80 | 96 | 66 | 152 | 63 | 153 | 65 | 151 |
| **89** | 82 | 132 | 78 | 110 | 80 | 110 | 70 | 158 | 65 | 158 | 64 | 161 |
| **90** | 107 | 203 | 108 | 272 | 100 | 248 | 90 | 189 | 74 | 185 | 75 | 194 |
| **91** | 164 | 320 | 204 | 421 | 166 | 391 | 138 | 317 | 148 | 308 | 134 | 303 |
| **92** | 77 | 101 | 74 | 90 | 76 | 92 | 64 | 155 | 60 | 148 | 61 | 150 |
| **93** | 77 | 126 | 78 | 118 | 76 | 120 | 68 | 160 | 60 | 151 | 61 | 157 |
| **94** | 101 | 209 | 101 | 268 | 80 | 258 | 75 | 187 | 62 | 183 | 61 | 190 |
| **95** | 158 | 314 | 204 | 444 | 203 | 412 | 105 | 503 | 62 | 299 | 61 | 316 |
| **96** | 62 | 77 | 61 | 64 | 62 | 65 | 59 | 131 | 55 | 130 | 55 | 129 |
| **97** | 67 | 82 | 61 | 69 | 62 | 71 | 59 | 131 | 55 | 132 | 55 | 130 |
| **98** | 67 | 120 | 64 | 117 | 62 | 110 | 63 | 131 | 55 | 127 | 55 | 130 |
| **99** | 126 | 314 | 201 | 452 | 181 | 418 | 63 | 170 | 62 | 202 | 64 | 194 |
| **100** | 215 | 340 | 227 | 424 | 210 | 408 | 132 | 310 | 128 | 308 | 134 | 328 |
| **101** | 151 | 275 | 154 | 308 | 141 | 307 | 101 | 209 | 98 | 216 | 99 | 225 |
| **102** | 132 | 241 | 104 | 211 | 105 | 222 | 90 | 199 | 86 | 203 | 85 | 207 |
| **103** | 107 | 203 | 104 | 165 | 105 | 171 | 76 | 178 | 71 | 173 | 71 | 178 |
| **104** | 132 | 340 | 134 | 394 | 137 | 368 | 130 | 319 | 132 | 299 | 126 | 299 |
| **105** | 132 | 307 | 131 | 314 | 130 | 279 | 96 | 218 | 94 | 236 | 94 | 236 |
| **106** | 126 | 235 | 131 | 181 | 126 | 192 | 86 | 180 | 81 | 185 | 82 | 191 |
| **107** | 126 | 228 | 128 | 174 | 126 | 188 | 84 | 182 | 81 | 186 | 82 | 191 |
| **108** | 164 | 327 | 214 | 417 | 193 | 393 | 120 | 331 | 140 | 308 | 136 | 319 |
| **109** | 158 | 281 | 154 | 312 | 150 | 309 | 101 | 214 | 98 | 228 | 99 | 263 |
| **110** | 120 | 203 | 91 | 211 | 95 | 222 | 68 | 172 | 74 | 175 | 74 | 177 |
| **111** | 101 | 158 | 94 | 167 | 100 | 175 | 70 | 160 | 66 | 156 | 66 | 157 |
| **112** | 1020 | 1356 | 685 | 2328 | 276 | 2984 | 154 | 9656 | 796 | 0 | 1165 | 0 |
| **113** | 145 | 241 | 141 | 214 | 175 | 240 | 99 | 202 | 97 | 211 | 102 | 229 |
| **114** | 701 | 1349 | 174 | 357 | 156 | 352 | 146 | 2172 | 135 | 311 | 123 | 325 |

# Works Cited


[1] NFPA 720. (2012). Standard for the Installation of Carbon Monoxide (CO) Detection and Warning Equipment. Quincy, MA: NFPA.

[2] Clifford, P. (1996). *Test Protocols for Residential Carbon Monoxide Alarms Phase 1.* Chicago, IL: The Gas Research Institute.

[3] Hnatov, M. V. (2011). Non-Fire Carbon Monoxide Deaths Associated with the Use of Consumer Products, 2007 Annual Estimates. Bethesda, MD: U.S. Consumer Product Safety Commission.

[4] S.E. Grant, A. K. (2006). Factors influencing the indoor transport or contaminants and modelling implications. Derbyshire, UK: Health & Safety Laboratory.

[5] Building Research Establishment Ltd. (1999). Evaluation of Carbon Monoxide Detectors in Domestic Premises. Garston, Watford, UK: Health and Safety Executive.

[6] Bukowski, R. (1979). Investigation of the Effects of Heating and Air Conditioning on the Performance of Smoke Detectors in Mobile Homes. Washington, D.C.: Division of Energy, U.S. Dept. of Housing and Urban Development.

[7] B. Jayaraman, e. a. (2004). *Coupled Model for Simulation of Indoor Airflow and Pollutant Transport.* Berkeley, CA: Indoor Enviornment Division, Lawrence Berkeley National Laboratory.

[8] Pitts, W. (1997). *An Algorithm for Estimating Carbon Monoxide Formation in Enclosure Fires.* Fire Safety Science - Proceedings of the Fifth International Symposium.

[9] Mora, L. (2003). Comparing zonal and CFD model predicitions of isothermal indoor airflows to experimental data. *Indoor Air*, Vol. 23, 77-85.

[10] Beyler, C. (2007). Development of a Technical Basis for Carbon Monoxide Detector Siting. *The Fire Protection Research Foundation*.

[11] Ryan, T. (2011). Residential Carbon Monoxide Failure Rates in the United States. *American Journal of Public Health*, Vol 101, No. 10, 15-17.

[12] Yoon, S. (1998). Deaths From Unintentional Carbon Monoxide Poisoning and Potential for Prevention with Carbon Monoxide Detectors. *The Journal of the American Medical Association*, Vol. 279, No. 9, 685-687.

[13] Chow, W. (1996). Simulation of Carbon Monoxide Level in Enclosed Car Parks Using an Air Flow Network Program. *Tunnelling and Underground Space Technology*, Vol. 11, No. 2, pp237-240.

[14] Duci, A. (2004). Numerical Approach of Carbon Monoxide Concentration Dispersion in an Enclosed Garage. *Building and Enviorment*, Vol 39, pp1043-1048.

[15] Peterson, J. (1975). Predicting the Carboxyhemoglobin Levels Resulting from Carbon Monoxide Exposures. *Journal of Applied Physiology*, Vol. 49, No. 4, pp633-638.

[16] Pitts, W. (1995). The Global Equivalence Ratio Concept and the Formation Mechanisms of Carbon Monoxide in Enclosure Fires. *Progress in Energy Combustion Science*, Vol. 21, pp. 197-237.

[17] American Housing Survey. (2001). American Housing Survey. Retrieved October 20, 2012, from www.census.gov: http://www.census.gov/housing/ahs/

[18] SFPE. (2008 (Version 4)). *The SFPE Handbook of Fire Protection Engineering.* Bethesda, MD: SFPE. Chapter 2-5, Gottuk.

[19] SFPE. (2008 (Version 4)). *The SFPE Handbook of Fire Protection Engineering.* Bethesda, MD: SFPE. Chapter 2-1, Heskestad.

[20] SFPE. (2008 (Version 4)). *The SFPE Handbook of Fire Protection Engineering.* Bethesda, MD: SFPE. Chapter 2-1, Heskestad.

[21] Quintiere, J. (2006). Fundamentals of Fire Phenomena. West Sussex, England: John Wiley & Sons

[22] GexCon. (2010). *FLACS v9.1 User Manual.* Bergen, Norway.

[23] McGrattan, K. (2010). *Fire Dynamics Simulator (Version 5).* Gaithersburd, MD.

[24] GexCon US. (2009). *CFD Valadation*. Retrieved October 20, 2012, from www.gexconus.com: http://gexconus.com/index.cfm?id=230350

[25] GexCon US. (2009). *CFD Blind Benchmarking*. Retrieved October 20, 2012, from www.gexconus.com: http://gexconus.com/index.cfm?id=230346

[26] Coburn, R.F. (1965). *Considerations of the Physiological Variables that Determine the Blood Carboxyhemoglobin Concentration in Man*, Journal of Clinical Investigation, Vol. 44, No. 11 pp1899-1910

[27] Underwriters Laboratories. (2005). UL 2034 Single and Multiple Station Carbon Monoxide Alarms. Northbrook, IL: Underwriters Laboratories Inc.

[28] Clifford, P. (2002). *Evaluating the Performance of Residential CO Alarms.* Des Plaines, IL: The Gas Research Institue.

[29] A.D. Putorti, J. M. (1998). *Full-Scale House Fire Experiment for InterFIRE VR.* Gaithersburg, MD: NIST - Building Fire Research Laboratory.

[30] Klote, J., Milke, J., (2002). Principles of Smoke Management. Atlanta, GA: American Society of Heating, Refrigerating and Air-Conditioning Engineers, Inc.

[31] American Society of Heating, Refrigerating and Air-Conditioning Engineers, Inc. (ASHRAE). (2001). ASHRAE Handbook - Fundamentals. Atlanta, GA: ASHRAE.